Transmembrane Channel-like (*Tmc)* Gene Therapy Restores Auditory Function in Deaf Mice

Charles Hicks Askew
Hailey, Idaho

B.A., University of Pennsylvania, 2004

A Dissertation presented to the Graduate Faculty
of the University of Virginia in Candidacy for the Degree of
Doctor of Philosophy

Department of Neuroscience

University of Virginia
August, 2015

Abstract:

Genetic hearing loss accounts for up to 50% of prelingual deafness worldwide, yet there are no biologic treatments currently available. To investigate gene therapy as a potential biologic strategy for restoration of auditory function in patients with genetic hearing loss, we tested a gene augmentation approach in mouse models of genetic deafness. We focused on DFNB7/11 and DFNA36, which are autosomal recessive and dominant deafnesses, respectively, caused by mutations in Transmembrane channel-like 1 (*TMC1*). Thirty-nine recessive mutations and five dominant mutations have been identified in human *TMC1*. Mice that carry targeted deletion of *Tmc1*, or a dominant point mutation, known as *Beethoven*, are good models for human DFNB7/11 and DFNA36. We screened several adeno-associated viral (AAV) serotypes and promoters and identified AAV2/1 and the chicken beta-actin promoter as an efficient combination for driving expression of exogenous *Tmc1* in inner hair cells *in vivo*. We find that exogenous *Tmc1* or its closely related ortholog, *Tmc2*, are capable of restoring sensory transduction, auditory brainstem responses and acoustic startle reflexes in otherwise deaf mice, suggesting that gene augmentation with *Tmc1* or *Tmc2* is well-suited for further development as a strategy for restoration of auditory function in deaf patients who carry *TMC1* mutations.

Table of Contents

Dedication

I would first like to thank my parents, Lynn and Janet, for supporting me in everything I do. Whenever I've hit a rough patch, you've never told me I can't make it or pulled the plug on my dreams. It is your unwavering optimism that gives me the courage to keep trying and the confidence to pull it off. I'd like to thank my wife, Amy, who has built me up every step of this intellectual, emotional, and physical journey. You've been my strategic guru and life support. Thank you for being my sounding board for every presentation and interview. Even when we made difficult choices to further our careers, our love and relationship was strengthened by our ability to overcome the odds. To my daughter Isabel, you are a most incredible gift and the easiest child new parents could hope for. Watching you discover the world has inspired me to continue doing the same. This document is proof that opportunities will be presented to you, but you choose the way, and you set your own limits in life.

To my mentor Jeff, you are someone I will always respect for good science. I joined your lab because of your ability to communicate complex biology with simplicity, your attention to students, and my obsession with the inner ear. You have given me space to discover my independence, while providing the structure to build success upon. I aspire to your level of discipline and productivity, and I hope I've reminded you what a huge benefit your students derive from one-on-one participation in the lab. Now that I'm moving on, I hope we can be friends and maintain a mentorship connection. To my lab mates, I've been honored to share my journey with you and hope that I've provided you with as much knowledge, support, and entertainment as you have imparted upon me. Gwen, thank you for listening to me and sharing your advice. You helped me pave over the cracks in the path. Thank you to Jeff, Gwen, and my committee for sticking with me and supporting my development.

Chapter I: Introduction and Background

A Case for Gene Therapy to Treat Genetic Deafness

An estimated 278 million people suffer from hearing loss worldwide making it the most common sensory deficit, with approximately 50% of cases attributed to genetic origins and the other 50% to environmental factors (Tucci et al., 2010). In developed countries, 1 in 1000 live births are afflicted by genetic causes of hearing loss (Dillon et al. 2010; Alford et al., 2014), and congenitally deaf patients find themselves with limited therapeutic options. Many are candidates for cochlear implants, which approximate hearing through direct electrical stimulation of the surviving auditory nerve. The portion of patients with residual hearing may benefit from sound amplification provided by hearing aids. However, many causes of hearing loss are progressive, as the sensory cells in the inner ear do not regenerate and damage accumulates throughout one's lifetime. Hearing aids benefit most those with a conductive hearing loss, and are of limited help to those who lack the ability to receive sound stimulus due to dysfunction or death of the sensory cells inside the inner ear. Although cochlear implants bypass dysfunctional sensory cells, they are expensive, they provide only coarse frequency discrimination insufficient for appreciation of many things apart from the human voice, and they require invasive surgery with the sacrifice of hosting an indwelling biomechanical apparatus in the skull of the patient.

A potential solution to these issues is to genetically repair the cells of the inner ear themselves, which could restore the whole range and sensitivity of the intact auditory system (Kohrman and Raphael 2013; Géléoc and Holt 2014).

However, few studies have provided proof-of-principle evidence supporting gene therapy as a viable strategy for restoration of auditory function in mouse models of genetic hearing loss. Since there are over 70 different identified deafness genes (and nearly 230 deafness loci containing unidentified genes), it will require the work of many scientists to examine their function and design strategies to compensate for mutations in these genes at the molecular level (Géléoc and Holt 2014). To date no biological therapeutics exist for those born with genetic defects of the inner ear, and any developed in the future will need to offer equal or greater benefit and fewer risks than the cochlear implant. Furthermore, the use of biologic treatments will have to be proven safe for administration in early childhood, as this is the optimal time point for intervention before the sensory structures begin to degenerate. Once a biologic treatment is identified, it will take many years to prove its effectiveness and to address the regulatory minefield that accompanies its transition from the bench to the clinic. Fortunately, there is hope that genetic treatment is becoming a reality in the form of gene therapy.

Gene therapy offers the chance to target dysfunctional cells and to deliver restorative genetic code. Basic science studies as well as clinical trials over the last decade have demonstrated some success in treating rare genetic disorders like hemophilia, inherited forms of blindness, lymphoblastic leukemia, canavan disease, and muscular dystrophy (Manno et al., 2006; Boye et al.,2013; Kalos et al., 2011; Leone et al., 2012; Watchko et al., 2002; Bowles et al.; 2012;). Viral vectors engineered for use in gene therapy harness the exceptional ability of a virus to deliver exogenous genetic material, and they exploit this skill to augment

the host genomic DNA with a therapeutically designed sequence or plasmid. A popular strategy is to deliver a normal or 'wild-type' version of the gene that augments the host genetic code and produces functional protein while diluting the mutated non-functional protein. This strategy is most appropriate to compensate for recessive loss of function mutations. A different strategy, designed to overcome the effect of a dominant mutation, is to deliver a gene of closely related function whose protein can compensate for the mutation but is not impacted by the defect of the mutated protein. Many other experimental strategies have been proposed, from silencing translation of mutated protein with siRNA sequences (Maeda et al., 2005), to targeted repair of the genome *in vivo* using newly developed gene editing technologies like CRISPR/Cas (Mali et al., 2013; Long et al., 2014; Lu et al., 2015). In order for any of these strategies to be successful, vectors must target a large population of the affected cell type in order to have a therapeutic effect, without being otherwise detrimental to the organism. Achieving high levels of viral vector transduction while simultaneously limiting the expression of the gene products to specific cell types has been a great challenge, and the current tools to tackle this challenge are limited (Thomas et al., 2003; Kotterman and Schaffer 2014). Additionally, the viral vector itself must be proven benign to cellular function. Early clinical trials of gene therapy in humans overlooked the severity of these risks and unfortunately resulted in the death of an 18-year-old Jesse Gelsinger in 1999 after an injection of adenovirus designed to treat a liver enzyme deficiency resulted in viral stimulation of a fatal immune response (Wilson 2009). Additionally, use of a

retroviral vector, which integrates randomly into the genome, to treat severe-combined immune deficiency (SCID) was halted when it was discovered that several patients had developed leukemia as a result of retroviral insertion into a hematopoietic oncogene (Gore 2003, Couzin and Kaiser 2005). Thankfully other vectors with no known human disease association have been developed, such as adeno-associated virus (AAV), and these may minimize triggering of an immune response typical of a vector like adenovirus, which causes the common cold. Even for a non-pathogenic vector like AAV, the immune system is a challenge in a different respect because pre-existing neutralizing antibodies create a formidable barrier to the efficiency of genetic therapy by sequestering viral particles for elimination before they have a chance to reach their target. Additionally, stimulated T-cells are capable of identifying AAV capsid antigens and eliminating tissue transduced with the therapeutic vector (Kotterman and Schaffer 2014). These factors should continue to be addressed as the field of gene therapy matures.

The application of gene therapy as a treatment is dependent on the ability to identify candidate patients and to assess their disease-specific functioning. In the case of inherited deafness, genetic testing and assessment of auditory function is already in use. Newborn hearing screening using Auditory Brainstem Response (ABR) or Distortion Product Otoacoustic Emmision (DPOAE) testing is now mandatory throughout the United States (Alford et al., 2014), and microarray or gene sequencing tests are available for many hearing loss genes whose common mutations have already been identified (Kothiyal et al., 2010; Shearer et

al., 2010; Diaz-Horta et al., 2012). The continued technical development of Whole Exome Sequencing (WES) and Whole Genome Sequencing (WGS) has the potential to identify novel human hearing loss mutations and genes that are not prevalent enough to have already been identified, while reducing the cost to do so. In fact, the potential benefit of newborn screening and genetic diagnosis has become so important that in 2013 the National Institutes of Health (NIH) awarded $25 million dollars in funding for a project called **N**ewborn **S**creening **I**n **G**enomic Medicine and Public **H**eal**T**h (NSIGHT), which will investigate the ability to provide genetic diagnoses from sequencing of newborn DNA and determine if that information is useful to patients and doctors. Genetic hearing loss is identified as one of the few diagnoses that are currently medically actionable in this project (Powell et al., 2014). Interestingly, 90%-95% of newborns confirmed with hearing loss are born to normal hearing parents (Mitchell et al., 2004; Alford et al., 2014), which makes genetic screening all the more important for identifying children not born into large consanguineous families that have a known predisposition to genetic hearing loss. It is estimated that 56% of newborns with inherited deafness suffer from recessive non-syndromic hearing loss, which is the term used to describe a gene that must be inherited from both parents and affects hearing but no other systems in the body (Alford et al., 2014). This population represents the majority of people that are likely to benefit from wild-type gene augmentation therapy. A list of non-syndromic hearing loss genes and loci is maintained online by Dr. Guy Van Camp and Dr. Richard Smith (*hereditaryhearingloss.org*) and regularly updated as new genes are identified.

The convention for naming non-syndromic hearing loss genes has been to label the deafness (DFN) loci as they were discovered: DFNA refers to a dominant mode of inheritance, DFNB refers to a recessive mode of inheritance, DFNX refers to an X-linked mode of inheritance, and DFN alone refers to a mitochondrial mode of inheritance.

The most prevalent form of non-syndromic deafness is DFNB1, which contributes to about 50% of recessive cases in some human populations (Pandya et al., 2003; Alford et al., 2014). The gene associated with DFNB1 is *GJB2* and encodes for the gap junction protein connexin26. Interestingly, connexin 26 is not expressed in the sensory cells of the inner ear, but instead localizes to supporting structures that are linked to an extensive potassium-recycling pathway (Kikuchi et al., 1995, Wangemann 2002). Two studies using gene therapy in mice have attempted to target this extensive supporting cell network to rescue gap junction functioning, but have failed to restore hearing likely due to the challenge of re-establishing connexin26 communication between all individual cells involved in the potassium recycling chain (Crispino et al., 2011; Yu et al., 2014). For reasons discussed in the following chapter, the sensory cells themselves, called hair cells, present a more accessible target. Hair cells convert mechanical stimuli into electrical signals and are essential for normal auditory and balance function. The first study to restore auditory function in deaf mice was able to use gene therapy vectors to target hair cells in mice lacking VGLUT3, a glutamate transport protein that is expressed in auditory inner hair cells and is required for synaptic transmission from inner hair cells to postsynaptic neurons of

the 8th cranial nerve (Akil et al., 2012). The authors of the study used adeno-associated viral (AAV) vectors to deliver the wild-type coding sequence for VGLUT3 into inner hair cells of early post-natal VGLUT3 knock-out mice. While this was an important advance, VGLUT3 mutations are not common in humans and when present, are dominant, suggesting the clinical utility of a VGLUT3 augmentation strategy may be limited. To explore gene therapy for a common form of genetic hearing loss that affects hair cells, we used mice that carry mutations in Transmembrane channel-like gene 1 (*Tmc1*). *TMC1* mutations are a common cause of genetic deafness in humans, accounting for 4%-8% of recessive non-syndromic deafness in some populations (Kitajiri et al., 2007; Sirmaci et al., 2009). To date, 44 mutations have been identified in *TMC1* that cause deafness in humans (Nakanishi et al., 2014; Zhao et al., 2014). Most are recessive and cause prelingual deafness, while at least five are dominant and cause progressive hearing loss with onset during the mid-teen years (Kawashima et al., 2015), suggesting possible windows of opportunity for clinical intervention. The experiments I propose here will take the auditory gene therapy approach a step further by investigating whether two closely related genes from the novel TMC gene family, *Tmc1* and *Tmc2*, are able to act as functional substitutes for one another to treat hearing loss in mouse models for human recessive (DFNB7/11) and dominant (DFNA36) genetic deafness.

Chapter II: Background

The Structure and Function of the Inner Ear

The inner ear is an exquisitely tuned system responsible for the transduction of sound or vibration energy into electrical impulses encoding frequency, amplitude, phase, duration, acceleration, and rotation, among other information. In the case of the auditory system, sound pressure entering the ear canal travels to the eardrum, known as the tympanic membrane, and vibrates the membrane in an oscillatory motion in accordance with the frequency and amplitude of the sound (Fig. 2-1). Directly coupled to the medial side of the tympanic membrane is the chain of middle ear bones. The functional role of the middle ear bones is to transmit and focus sound pressure energy from the large surface of the tympanic membrane onto the small area occupied by the stapes footplate. The size ratio of the surfaces of the tympanic membrane to the stapes footplate is approximately 17:1, which is responsible for a gain in sound pressure of about 20-26 dB SPL (Hughes and Pensak 2007). The stapes is embedded in the oval window, the portal opening into the bone encapsulated structure of the cochlea. The stapes footplate, acting as a piston, presses on the oval window membrane in synchrony with tympanic membrane displacements causing a compression of the fluid inside the membranous labyrinth of the cochlea. Compression of the fluid creates a traveling wave that moves along the length of the cochlear duct, which contains three parallel fluid filled chambers called the scala tympani, scala media, and scala vestibuli. The scala media, bound

superiorly by Reissner's membrane and inferiorly by the basilar membrane, contains the organ of Corti. The organ of Corti rests upon the flexible basilar membrane and contains the sensory hair cells that transduce mechanical movement of their hair bundles into neuronal impulses (Fig. 2-1).

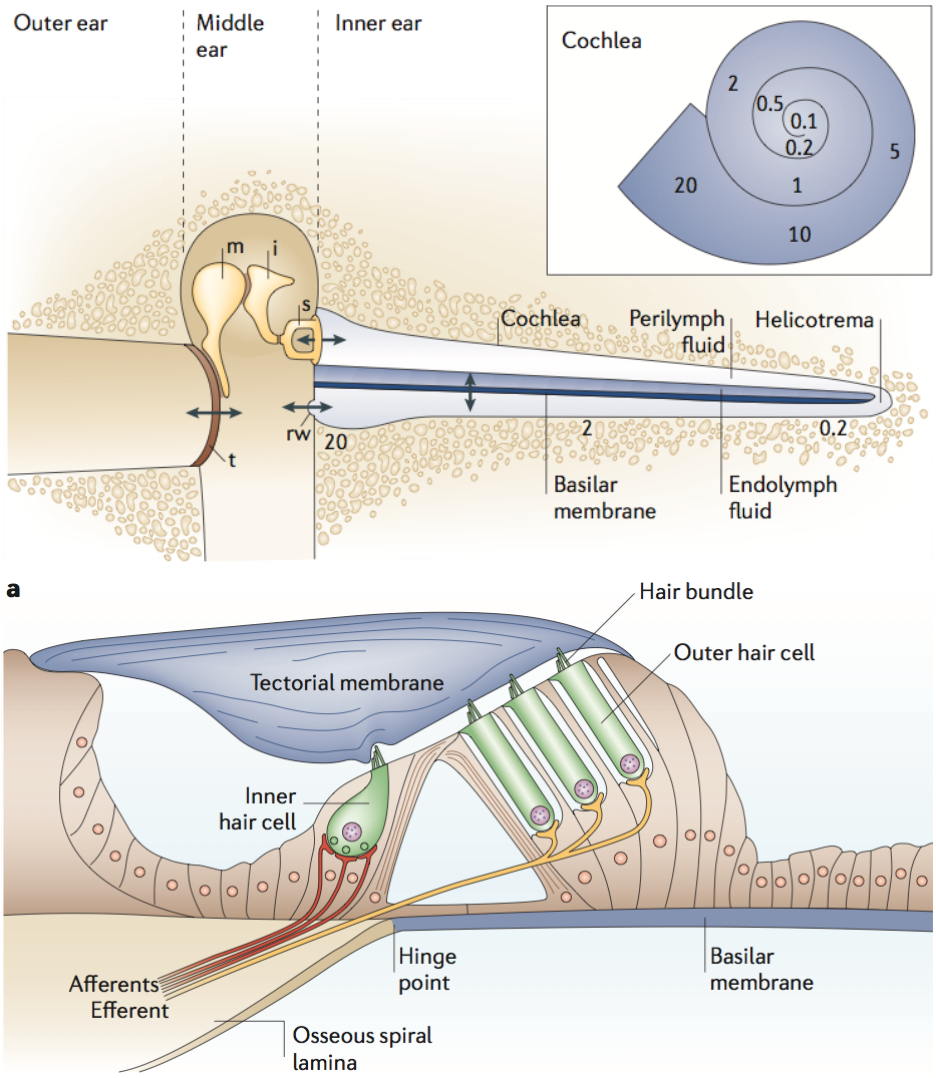

Figure 2-1. A diagramatic representation of an "uncoiled" mammalian cochlea and the sound conduction pathway. Inset is a frequency distribution map in kHz represented along a coiled human cochlea. Below is a cross section of the cochlea displaying the organ of Corti, which includes inner and outer hair cells, afferent and efferent neurons, the tectorial membrane and basilar membrane. Reprinted with permission from Macmillan Publishers Ltd: [Nature Reviews Neuroscience] (Fettiplace and Hackney, 2006), copyright (2006).

The frequency spectrum of the traveling wave is segregated along the length of the basilar membrane so that high frequency waves are shunted through the basilar membrane at the base of the cochlea, whereas low frequency waves travel all the way to the apex before shunting through the basilar membrane. The unique structural properties of the basilar membrane, which is thicker, narrower, and stiffer at the base of the cochlea while thinner, wider, and more compliant at the apex, facilitates the segregation of sound frequency along its length. The human cochlea can respond to sound stimuli in the frequency range of 20Hz to 20kHz and this frequency range is mapped in a logarithmic scale along the basilar membrane (Hudspeth, 2005).

As the traveling wave moves along the cochlear duct, it displaces the basilar membrane up and down. The oscillatory motion of the basilar membrane drives the tips of the sensory hair bundles against the overlying acellular matrix called the tectorial membrane, causing hair bundle deflection through a shearing motion (Fig. 2-1). The hair bundle is organized into three rows of stereocilia, each row increasing in height, where within a column of stereocilia the tip of the shorter stereocilium is connected to the next tallest neighboring stereocilium by a single link called the tip link (Fig. 2-2, C). Shearing motion of the stereocilia bundle against the tectorial membrane increases tension on the tip links, which in turn forces open mechanically gated ion channels. Mechanically gated ion channels, also known as mechanotransduction channels, are the basic molecular component necessary for mechano-electrical transduction (MET) in the hair cell and allow positively charged ions (K^+, Ca^{2+}, and Na^+) to enter and depolarize the

hair cell. Depolarization of the hair cell causes calcium influx through voltage gated calcium channels in the basolateral membrane and glutamate neurotransmitter release at its basal pole. Glutamate released by the hair cell crosses the synaptic cleft and binds glutamate receptors on bipolar spiral ganglion neurons (SGNs). The SGNs then relay the synaptic impulses up the central auditory pathway to the cochlear nucleus and on to the brain.

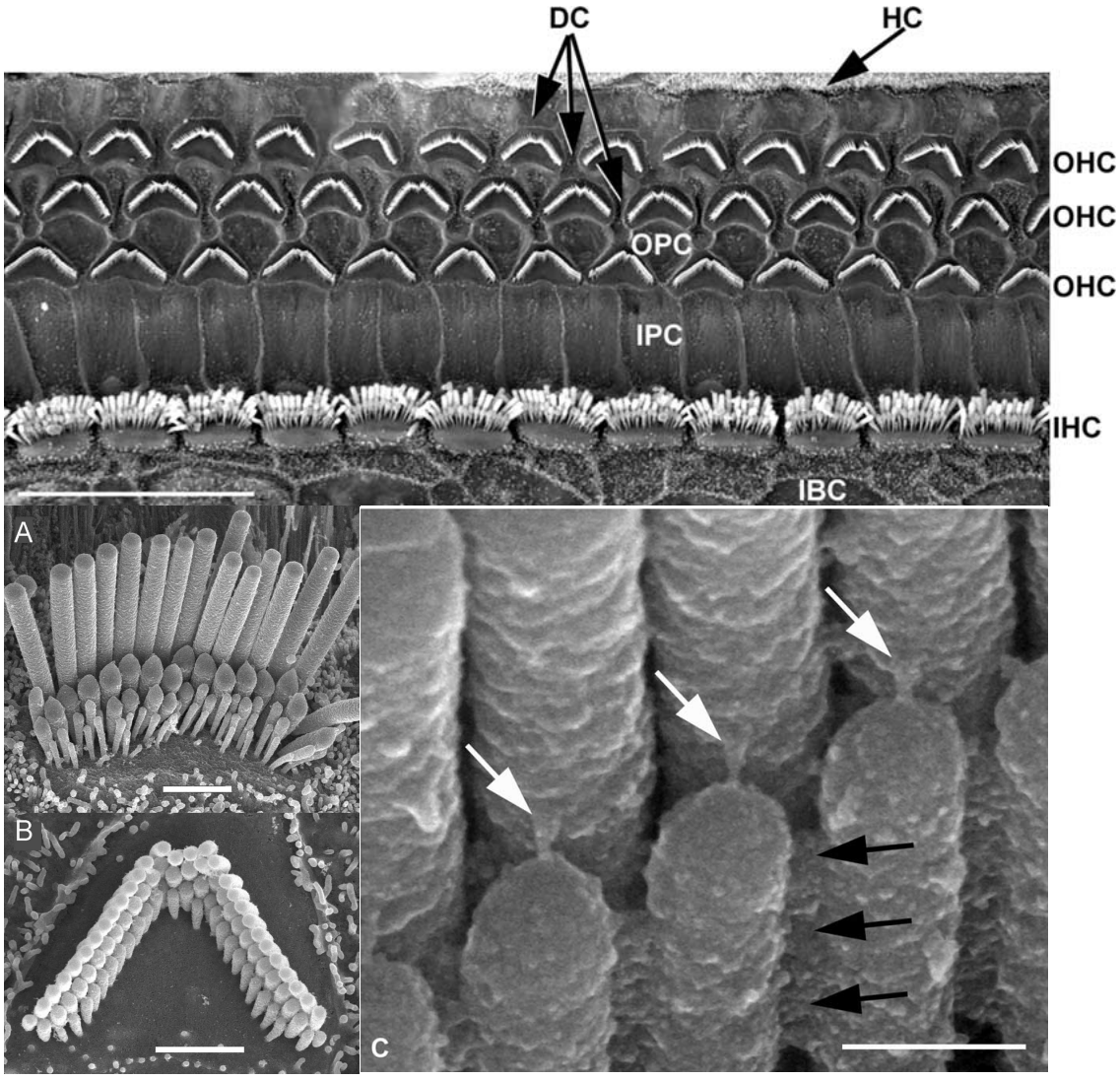

Figure 2-2. Scanning electron micrographs showing the apical view of the mammalian organ of Corti and sensory hair bundles after tectorial membrane removal. The top image displays the organization of one row of inner hair cells (IHCs) and three rows of outer hair cells (OHCs) in the organ of Corti, as well as other non-sensory supporting cell types. DC = Deiter cells, HC = Hensen's cells,

OPC = outer pillar cells, IPC = inner pillar cells, IB = inner border cells (Quint and Steel 2003). The bottom image displays the different morphology of bundles from inner (A) and outer (B) hair cells (A&B from Beurg et al., 2006; Reprinted with permission from the Society for Neuroscience). Tip-links connect the tips of shorter stereocilium to the shaft of taller stereocilium (C, white arrows) while other fibrous side links can also be seen (C, black arrows). Reprinted by permission from Elsevier: [Current Topics in Developmental Biology] (Quint and Steel, 2003), copyright (2003)

In the auditory system there are actually two types of auditory hair cells: inner hair cells (IHCs) and outer hair cells (OHCs) (Figs. 2-1, 2-2). The human inner ear contains roughly ~4,000 IHCs and ~12,000 OHCs, while the mouse inner ear contains about ~700 IHCs and ~2,300 OHCs (Willott 2001). Inner and outer hair cells are distinct from each other based on their location and function. IHCs form a single file row along the length of the cochlea, and serve as the primary sensory inputs to the brain through innervation by 90-95% of the afferent SGNs (Liberman 1980). OHCs are separated from inner hair cells by pillar cells, and form three rows parallel to the strip of IHCs (Fig.2-2). OHCs have sparse afferent innervation by 5% of SGNs, and dense efferent innervation by cholinergic fibers from the olivary nuclei in the brainstem. Consequently, OHCs have been shown to contribute to afferent signaling only during very high amplitude stimuli (Weisz et al., 2009), and are mainly thought to respond to efferent feedback from the brain. Unlike IHCs, the primary function of OHCs is to amplify the energy of the basilar membrane and sharpen the frequency tuning of the cochlea. OHCs have a specialized lateral membrane packed with the protein prestin, a voltage-sensitive protein that through conformational shape changes acts as an area motor in the membrane and endows outer hair with electro-motile properties (See Fig. 2-3). At depolarized membrane potentials, such as when the

hair bundle is deflected and the MET channels open allowing positive current into the cell, the body of the OHC shortens in length. The OHC elongates as the MET channels close, positive current decreases, and the membrane voltage shifts back to the hyperpolarized resting membrane potential. As the basilar membrane oscillates, the hair cell membrane voltage is predicted to activate OHC contraction and expansion on a cycle-by-cycle basis. When considering the mechanics of the organ as a whole, the contraction and expansion of OHCs are able to amplify the movement and sharpen the response of the basilar membrane specifically at low sound pressure amplitudes below 80dB SPL (Holley & Ashmore, 1988; Hudspeth 2008; Huspeth 2014). When OHC function is lost by selectively eliminating OHCs with aminoglycosides (Ryan and Dallos, 1975), or genetically rendering the prestin motor protein insensitive to voltage (Liberman et al., 2002; Dallos et al., 2008), it results in a loss of auditory threshold sensitivity by 40-60 dB SPL and a broadening of the basilar membrane response.

Cochlear Amplification

The process of cochlear amplification remains an active area of research in the auditory field (Ashmore et al., 2010). It is agreed upon that in addition to the passive physical properties of the basilar membrane, there is an active process present in outer hair cells that is capable of tuning basilar membrane responses and amplifying selected frequencies at low sound pressures while allowing the passive properties of the basilar membrane to dominate at higher

sound pressures (Hudspeth 2014). A divide exists in the field between whether this active process is part of the hair bundle mechanotransduction machinery, or whether it is due to the somatic motility of the outer hair cell body. Additionally, the two processes are not mutually exclusive and could exist simultaneously or even work in a coordinated manner.

Active bundle motion is correlated and possibly coupled with the opening or closing of the MET channel, as well as adaptation of the transduction current (Fettiplace 2006). As a stereocilium is deflected, the gating tension on the MET channel grows but the movement of the bundle remains constant. However, once the MET channel opens, increased movement of the bundle occurs in the direction of stimulation. The opposite occurs as the MET channel closes, which results in a movement opposite the direction of stimulation. Like adaptation, where the amplitude of the mechanotransduction current decreases in response to a constant stimulus, the active bundle response relies upon the entry of calcium into the cell. Active bundle movements are abolished by decreasing extracellular calcium, blocking the MET channel, or depolarizing the cell to positive potentials (Ricci et al., 2000; Beurg et al., 2008). In the last two cases calcium is either prevented from entering the cell or reduced by decreasing its diving force for entry into the cell. The suggested mechanism for this effect is that calcium both binds directly to the MET channel making it harder to open, as well as binds the gating spring making it more compliant. Movement of the bundle during active motion is hypothesized to amplify the swinging motion of the hair bundle, which in turn could exert a force against the stationary tectorial

membrane and amplify the motion of the basilar membrane. No studies have yet proven that active hair bundle movement is necessary for amplification in the mammalian auditory system.

On the other hand, evidence has already been generated that somatic motility is necessary for cochlear amplification, as described in the previous section discussing outer hair cell function. The OHC protein prestin is an incomplete anion transporter that is thought to allow movement of intracellular Cl^- or bicarbonate ions partially across the cell membrane in response to depolarization of the membrane potential. The movement of Cl^- ions creates an effect of gating charge movement in and out of the membrane, and this charge movement can be measured in OHCs as non-linear capacitance. The movement of this negative charge corresponds to a conformational change in the shape of prestin, and a change in membrane surface area (Ashmore, 2008). Accordingly, changes in membrane surface area translate into length changes of the OHC, and amplification of basilar membrane movement during sound stimulation.

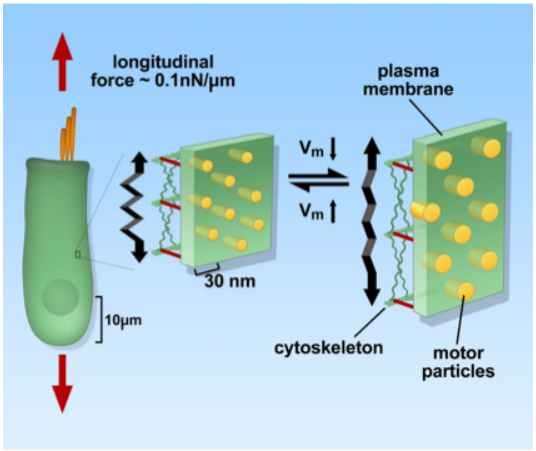

Figure 2-3. Prestin functions as an area motor so that as membrane voltage oscillates, voltage-sensing prestin proteins undergo a conformational shape change to shrink or expand laterally while anchored in the outer hair cell body.

A cooperative theory, which suggests that the active bundle movement and OHC somatic motility mechanisms work together, is that active bundle motion functions to amplify sound energy, while somatic motility serves to set the height of the OHC so that the operating point of the hair bundle is optimal for creating active forces (Kennedy et al., 2005). Until the MET channel and gating spring are molecularly identified, it will be impossible to genetically manipulate active bundle motion in a specific manner that could reveal the fundamental mechanism behind the cochlear amplifier.

The Endocochlear Potential and Ion Homeostasis in the Cochlea

Endolymph is an extracellular solution unique to the scala media of the cochlea. It differs from perilymph and cerebrospinal fluid in that is composed of a high K^+ concentration (150mM) and low concentrations of Na^+ and Ca^{2+} (1mM and 0.05mM respectively) (Smith et al., 1954). Both the high K^+ endolymph concentration accompanied by a +90mV endocochlear potential in the scala media are necessary to provide the proper driving force for K^+ entry into cochlear hair cells through MET channels (Nin et al., 2008; P. Wangemann et al., 2004). A reduction in the endocochlear potential to below +30mV results in a decrease of auditory sensitivity and threshold shift of up to 50 dB SPL (Gow et al., 2004; Kitajiri et al., 2004). The endocochlear potential is generated by the cells of the stria vascularis through the secretion of potassium ions into the scala media, and through electrical compartmentalization mediated by tight junctions between cells

that prevent ionic diffusion out of the scala media. The stria vascularis is composed of basal cells and intermediate cells that secrete K^+ into the intrastrial space via KCNJ10 potassium channels. Potassium ions are then transported by $Na^+/2Cl^-/K^+$ co-transporters and Na^+/K^+ ATPase pumps from the intrastrial space into the marginal cells that make up the apical boarder of the stria vascularis. Marginal cells then secrete the K+ from their apical surface into the endolymph via KCNQ1+KCNE1 channels. Potassium from the endolymph enters hair cells through MET channels and exits the cells via outward potassium currents present in the basolateral portion of the cells. KCNQ4 mediated I_{Kn} allows K^+ to exit hair cells even at rest, and this represents a major route for how K^+ is able to reach the perilymph and surrounding supporting cells (Spicer and Schulte 1996; Wangemann 2002) In addition to the KCNQ4 channels active at rest, the calcium activated BK and SK potassium channels, as well as I_K, become activated at depolarized potentials and help serve as the shunt for K^+ out of the hair cell and into the perilymph or adjacent supporting cells. After leaving the hair cell, K^+ is thought to be recycled through the perilymph and supporting cells back to the stria vascularis via specialized fibrocytes in the lateral wall. Evidence for this part of the recycling pathway is indirect and relies upon immuno-localization of K^+/Cl^- co-transporters Kcc3 and Kcc4 in supporting cells, as well as the gap junction proteins connexin26 and connexin30 (*Gjb2* and *Gjb6*) located in the outer sulcus and lateral wall fibrocytes. The protein products of *Kcnj10, Kcnq1, Kcne1, Kcnq4, Kcnma1, Kcnn2, Kcc3, Kcc4, Gjb2 and Gjb6* are produced in various different cell types involved in the putative K^+ recycling pathway and are each associated

with deafness in mouse models and humans. Additionally, there is at least one ion transporter not involved in the potassium-recycling pathway, but that is necessary for maintaining appropriate calcium levels in hair cells. Plasma Membrane Ca^{2+} ATPase (PMCA) calcium pumps extrude calcium from the hair cell stereocilia, and defects in PMCA transport proteins cause hearing loss in mice (Kozel et al., 1998). Combined with the fact that intracellular calcium buffering proteins are plentiful in hair cells and may protect against cell death due to acoustic overstimulation (Hackney et al. 2005), it is clear that both potassium and calcium must be tightly regulated for normal auditory functioning.

Mechanotransduction and Hair Cell Currents Involved in the Receptor Potential

Sensory hair cells in the cochlea are capable of detecting displacements of the stereocilia on the scale of a few nanometers (Rhode & Geisler, 1967). The hair cell responds to deflections of its stereocilia only on the axis of bundle sensitivity, which is aligned with the push and pull polarity of the tip links (Shotwell et al., 1981). Deflection of the bundle increases tension on the tip links between stereocilia, which gates the opening of the MET channels. The tip link itself is made up of a pair of two parallel protein dimers, where the upper tip link is composed of two Cadherin-23 (CDH23) proteins and the lower tip link is composed of Protocadherin-15 (PCDH15) proteins (Siemens et al., 2004; Söllner et al., 2004; Ahmed et al., 2006; Kazmierczak et al., 2007). The bond between PCDH15 and CDH23 proteins is formed by the presence of calcium (Assad et al., 1991; Lelli et al., 2010), and reducing or eliminating calcium breaks tip links and

results in a loss of mechanotransduction. The tips of stereocilia have been identified as the location where ionic influx of the MET current occurs (Hudspeth & Jacobs, 1979; Jaramillo & Hudspeth, 1991), and influx happens only at the lower end of the tip link as indicated by intracellular Ca^{2+} sensitive dye (Beurg et al., 2009). It is currently unknown how the tip link opens the MET channel, either through a direct coupling or indirect transmission of force. The hair cell MET channel has a reversal potential near 0mV, which is consistent with being a non-selective cation channel that passes calcium, potassium, and sodium (Corey & Hudspeth, 1979a; Lumpkin et al., 1997). While the hair bundle is at rest there remains tension on the tip link between stereocilia, mediated in part by myosin molecular motors (Holt et al., 2002; Kros et al., 2002), that is thought to be responsible for allowing a percentage of channels to open spontaneously. It is estimated that the resting open probability of MET channels is about 3%-10% in IHCs and 30%-40% in OHCs (Corns et al., 2014). The pore of the channel is at least 1.2 nm in diameter (Pan et al., 2012), which is large enough to allow passage of aminoglycoside antibiotics (Ricci et al., 2003) and the styryl dye FM1-43 (Gale et al., 2001; Meyers et al., 2003; Farris et al., 2004). The single channel conductance of the MET channel is estimated to be between 100-200 pS (Crawford et al., 1991; Géléoc et al., 1997; Beurg et al., 2006; Pan et al., 2013), which depending on the number of stereocilia corresponds to about 1-2 channels per stereocilium (Ricci et al., 2003; Stauffer and Holt, 2007). MET currents develop at post-natal day (P) P0-P2 in mouse cochlear hair cells and peak in the first post-natal week (Lelli et al., 2009), while the onset of hearing in mice occurs

around P10-P12. The MET current activates so quickly (within ~10 micro-seconds) that mechanical force most likely gates channel opening directly, making it highly improbable that the process could be carried out by a second messenger system as is done in photoreceptor transduction (Corey & Hudspeth, 1979b). Broad acceptance for the molecular identity of the hair cell MET channel has yet to be established, although the best candidates to date are Transmembrane Channel-like protein family members TMC1 and TMC2. These proteins are necessary for mechanotransduction, bind with PCDH15, and influence pore properties of the MET channel itself (Kawashima et al., 2011; Pan et al., 2013; Maeda et al., 2014). The function of TMC proteins in hair cells will be discussed in greater detail in the following section, but the recent identification of TMIE and TMHS proteins as crucial components for the generation of transduction currents demonstrates that the MET channel transduction complex may be constituted of a diverse set of protein players (Xiong et al., 2012; Zhao et al., 2014; Beurg et al., 2015). TMIE and TMHS are each transmembrane spanning proteins that localize to stereocilia tips, but have just two or four transmembrane-spanning domains, respectively. It is unclear whether they possess or influence core MET channel properties besides aiding in the mechanical gating of transduction currents and possibly connecting the mechanotransduction complex to Pcdh15 proteins.

While the MET channels allow inward current to enter the stereocilia and depolarize the hair cell, there are several types of ion channels located in the basolateral membrane that are responsible for shaping the hair cell receptor

potential, facilitating neurotransmitter release, and repolarizing the cell membrane (Marcotti & Kros, 1999). IHCs have several potassium currents, namely: the calcium activated potassium current from BK channels that mediates I_{Kf}; a delayed rectifier potassium current sensitive to 4-AP that mediates I_{Ks}; and a negative voltage activated delayed rectifier current from KCNQ4 channels that mediates I_{Kn}. IHCs also have a voltage-gated L-type calcium current mediated in part or in full by $Ca_v1.3$ channels. OHCs possess a similar composition of currents, namely I_{Kn} and $I_{Cav1.3}$. However, OHCs have a much more prominent I_{Kn}, and express two additional potassium currents. One is the calcium-activated potassium current through SK channels that mediate I_{SK}, which is activated by calcium influx through nicotinic acetylcholine receptors. The other, called I_K, is a delayed rectifier current similar to I_{Ks} that is also sensitive to 4-AP. I_K in OHCs and I_{Ks} in IHCs have not yet been assigned specific molecular correlates. Lastly, although BK channel expression is low in OHCs, BK channels also contribute to a portion of the OHC outward potassium currents (Nenov et al., 1997).

TMC Proteins Involved in Hair Cell Mechanotransduction and Mouse Models for DFNB7/11 and DNFA36

TMC genes are found in a diverse set of organisms including worms, flies, chickens, mice and humans (Keresztes et al. 2003, Mutai et al. 2005). *TMC1* has been identified as the causative gene for human recessive deafness DFNB7/11 and dominant deafness DFNA36 (Kurima et al., 2002), and 44 different mutations have been discovered to cause human deafness (Nakanishi et al., 2014; Zhao et

al. 2014). While both *Tmc1* and *Tmc2* are found specifically in hair cells of the early post-natal cochlea and vestibular system as identified by *in situ* hybridization, only TMC1 has been associated with hearing dysfunction in humans or mice (Kurima et al., 2002; Vreugde et al., 2002; Marcotti et al., 2006; Kawashima et al., 2011; Pan et al., 2013). However, mice missing both *Tmc1* and *Tmc2* suffer from severe loss of balance in addition to being deaf (Kawashima et al., 2011), indicating dysfunction of both auditory and vestibular hair cells and suggesting a redundant nature of the two genes in hair cells. The TMC gene family is made up of 8 members that encode proteins with 6 predicted transmembrane domains and a putative pore-loop that includes the TMC region, a motif of 120 amino-acids unique to this gene family (Kurima et al., 2003). The presumptive location of this loop between transmembrane domains 4 and 5 deviates from canonical potassium channel structure, but in most other aspects TMC proteins are remarkably reminiscent of an ion-channel, transporter, or receptor (Labay et al. 2010). Although the function of TMC proteins at the molecular level has not been definitively confirmed, they are the strongest candidate gene family to date for the long sought-after hair cell MET channel. A distant homolog for mouse *Tmc2* found in *C. elegans* (*tmc-1*) demonstrates cation non-specific channel activity when expressed in heterologous cell lines and is activated specifically by high sodium concentrations (Chatzigeorgiou et al., 2013). Although no similar function for mammalian TMC2 has yet been demonstrated, this discovery increases the likelihood that TMC proteins function as ion channels. To date, attempts to test this hypothesis have been

unsuccessful due an inability to express mammalian TMC proteins in heterologous cell surface membranes (Labay et al., 2010). Recently, Pan et al., 2013 demonstrated that TMC proteins determine core properties of the MET current itself, including single channel size and calcium permeability. Single channel analysis of inner hair cell MET currents generated by repeated displacement of an individual stereocilium showed average single channel current amplitudes of -22.6pA for *Tmc2* only expressing mice, -12.4pA for *Tmc1* only expressing mice, and -8.4pA for mice expressing only *Tmc1* containing the dominant *Bth* point mutation (*Tmc1*^{Bth}) at position M412K (Fig. 2-4 D).

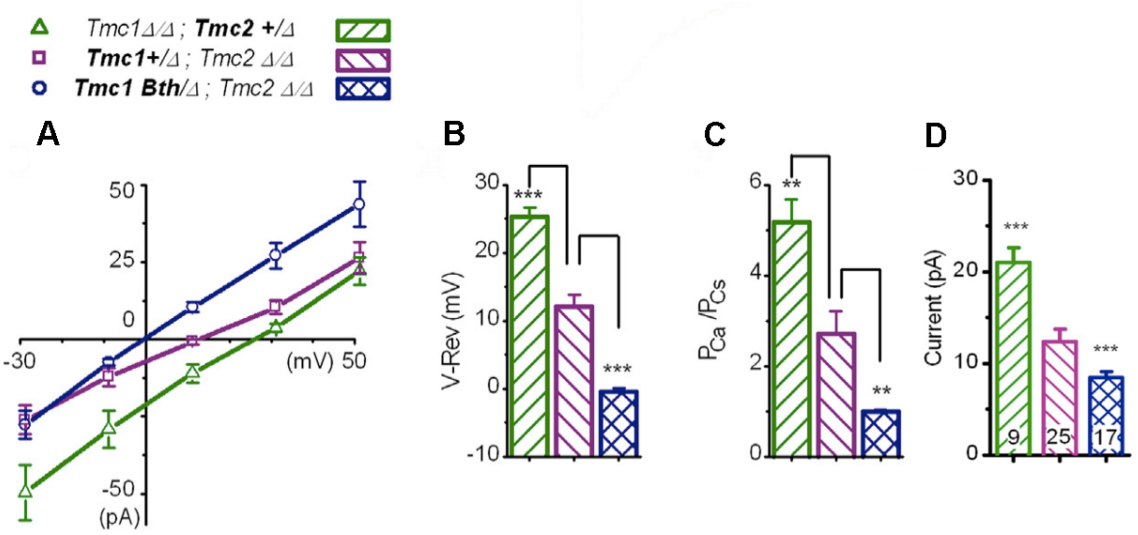

Figure 2-4. *Tmc* genes dictate whole cell MET current reversal potential (A&B) whole cell MET current calcium permeability (C), and single channel MET current amplitudes (D) for the genotypes listed above. Reproduced with permission from Elsevier: [Neuron] (Pan et al., 2013), copyright (2013).

When the calcium reversal potential for MET currents was measured for the same mice during saturating bundle deflection at different voltage steps, inner hair cells each had different mean reversal potentials: 25mV for *Tmc2,* 12mV for *Tmc1*, and 0mV for *Tmc1*^{Bth} MET currents (Fig. 2-4 A&B). Calcium permeability

could then be calculated for this experiment using the Goldman-Hodgkin-Katz equation because external calcium and internal cesium were the only permeant ions present. This evidence crucially demonstrated that the *Tmc1 Bth* point mutation causes nearly a ~3 fold decrease in MET calcium permeability compared to wild-type Tmc1 accompanied by a decrease in single channel amplitude of Tmc1 mediated MET currents, both properties which are traditionally dictated by ion channel proteins or their auxiliary subunits. Furthermore, mice without *Tmc1* & *Tmc2* genes (***Tmc1$^{\Delta/\Delta}$; Tmc2$^{\Delta/\Delta}$***) demonstrate a complete lack of MET currents (Fig. 2-5, Pan et al., 2013; Kawashima et al. 2011).

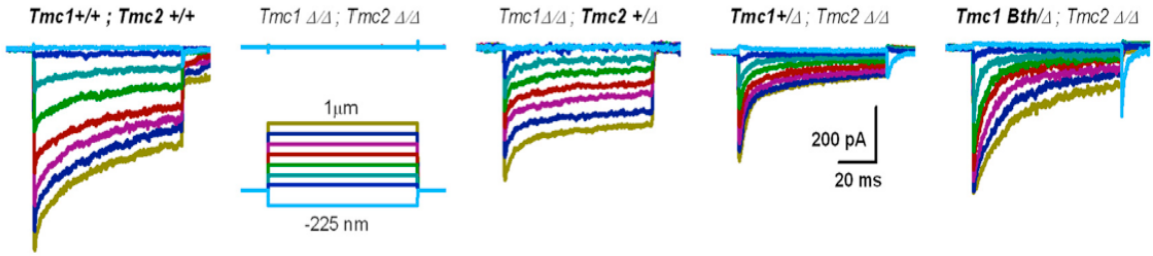

Figure 2-5. Representative mechanotransduction currents from inner hair cells generated from mice expressing different TMC proteins. Single inner hair cells were recorded from using patch clamp electrophysiology while their bundle was displaced according to the step protocol (inset) using a stiff glass probe. Reprinted with permission from Elsevier: [Neuron] (Pan et al., 2013), copyright (2013)

Few mouse models demonstrate a MET current impairment as severe as *Tmc1$^{\Delta/\Delta}$; Tmc2$^{\Delta/\Delta}$* mice, save for genetically dysfunctional models for the tip link proteins Pcdh15 & Cdh23 (Senften et al. 2006, Caberlotto et al. 2011), and the transduction complex associated protein Tmie (Zhao et al., 2014). Additionally, Tmc1 and Tmc2 demonstrate binding interactions with tip-link protein Pcdh15 in yeast two-hybrid screening (Maeda et al., 2014). Tmc1 and Tmc2 proteins fused

with green fluorescent protein localize to stereocilia when their gene products are introduced by gene gun into vestibular and cochlear hair cells (Kawashima et al., 2011). As discussed in the next chapter, antibody staining for the FLAG epitopes contained within the exogenous TMC protein sequence also demonstrates Tmc1 or Tmc2 labeling in stereocilia tips and the hair cell cytoplasm when over-expressed by viral transduction (Fig. 3-8A&B). Lastly, when *Tmc1* or *Tmc2* genes are re-introduced into $Tmc1^{\Delta/\Delta}$; $Tmc2^{\Delta/\Delta}$ hair cells, FM1-43 uptake and MET currents are rescued *in vitro* (Kawashima et al., 2011) demonstrating further support for their principal role in the MET current.

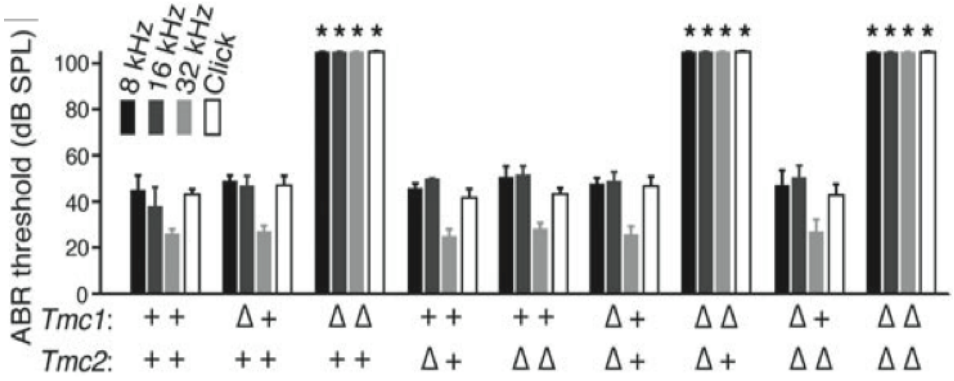

Figure 2-6. (Reproduced from Kawashima et al. 2011) Mice lacking *Tmc1*, but not *Tmc2*, have elevated Auditory-Evoked Brainstem Response (ABR) thresholds at 12 weeks of age. Additionally, raw ABR traces from *Tmc1* KO mice demonstrate no reproducible responses even at the highest stimuli amplitude of 100dB sound pressure level (raw traces not shown). Reprinted with permission from the American Society for Clinical Investigation: [Journal of Clinical Investigation] (Kawashima et al., 2011), copyright (2011).

Mice missing *Tmc1* (***Tmc1***$^{\boldsymbol{\Delta/\Delta}}$;$Tmc2^{\Delta/+}$) lack auditory-evoked brainstem responses (ABR), a measure of summed electrical activity along the auditory circuit from the sensory hair cells to auditory nuclei of the brainstem in response to sound stimuli, while mice missing *Tmc2* ($Tmc1^{\Delta/+}$;***Tmc2***$^{\boldsymbol{\Delta/\Delta}}$) retain normal hearing thresholds (Fig. 2-6). Kawashima et al. 2011 show that in wild-type mice,

Tmc2 participates in the acquisition but not the maintenance of MET currents in the cochlea. The rise in relative expression level of *Tmc2* mirrors the tonotopic development of MET currents during the first post-natal week, but mRNA levels ultimately decline to near zero in the second post-natal week (Fig. 2-7). The decline of *Tmc2* expression corresponds to the loss of MET currents in $Tmc1^{\Delta/\Delta}$; $Tmc2^{+/+}$ mice after P8 (Kim et al., 2013).

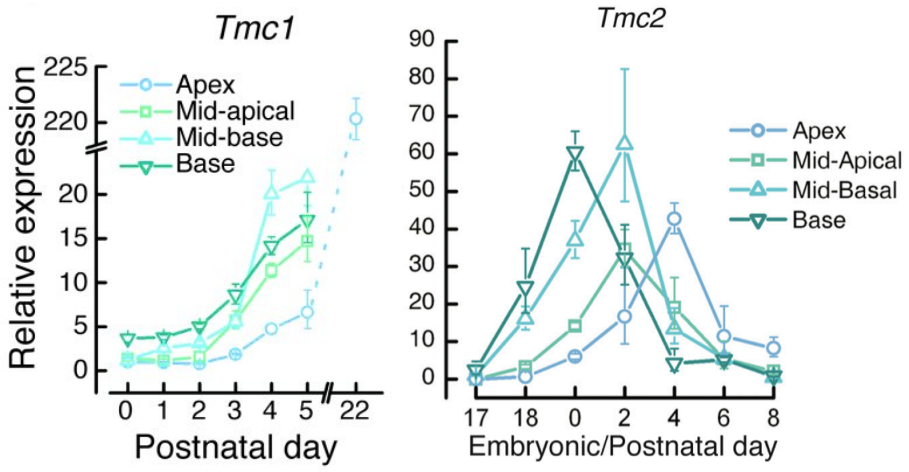

Figure 2-7. TMC2 RNA is expressed from birth in mouse cochlea as detected by quantitative PCR (qPCR), and in situ hybridization (not shown). However, qPCR analysis demonstrates that TMC2 expression peaks from P0-P4 and then declines by the second post-natal week, where as TMC1 RNA expression begins to ramp up only after post-natal day 3 to 4. This suggests that the initial acquisition of transduction is due to expression of TMC2 proteins while TMC1 expression persists at high levels and is responsible for mechanotransduction in the adult animal. Reproduced with permission from the American Society for Clinical Investigation: [Journal of Clinical Investigation] (Kawashima et al., 2011), copyright (2011).

Hair cells begin to develop MET currents in the base of the cochlea beginning at P0, and the development of transduction progresses to the apex by P2 (Lelli et al. 2009). While *Tmc1* expression lags acquisition of transduction by 2-3 days, its expression is maintained throughout adulthood (Fig. 2-7), which corresponds to the persistence of MET currents in $Tmc2^{\Delta/\Delta}$ mice after P8 (Pan et al., 2013). This

developmental switch from *Tmc2* to *Tmc1* is a reasonable explanation as to why *Tmc1*$^{\Delta/\Delta}$ mice lack normal ABR thresholds at P30 while *Tmc2*$^{\Delta/\Delta}$ mice retain normal thresholds. Despite the presence of intact tip links, hair cells from *Tmc1*$^{\Delta/\Delta}$*; Tmc2*$^{\Delta/\Delta}$ mice fail to take up the transduction channel permeable dye FM1-43, they begin to display disorganized stereocilia in the cochlea beginning at P5-P7, and degeneration of hair cells becomes evident after P15 (Kawashima et al., 2011). *Tmc1*$^{\Delta/\Delta}$ mice have normal cochlear stereocilia organization but still suffer hair cell death beginning after P15, while no bundle disorganization or hair cell degeneration has been reported in *Tmc2*$^{\Delta/\Delta}$ mice.

Evidence that both TMC1 and TMC2 proteins are integral to hair cell function was first demonstrated by Kawashima et al., 2011 who showed that in addition to undetectable ABR thresholds, *Tmc1*$^{\Delta/\Delta}$*; Tmc2*$^{\Delta/\Delta}$ mice lack vestibular-ocular reflexes as well. This vestibular defect is a consequence of the fact that *Tmc1*$^{\Delta/\Delta}$*; Tmc2*$^{\Delta/\Delta}$ vestibular hair cells also lack MET currents. In the vestibular system hair cells retain expression of both *Tmc* genes throughout adulthood, and the presence of either *Tmc1* or *Tmc2* alone is sufficient to retain vestibulo-ocular reflexes and balance on rotarod tests. Unlike in the cochlea, *Tmc1*$^{\Delta/\Delta}$*; Tmc2*$^{\Delta/\Delta}$ vestibular hair cells all maintain normal bundle structure and survival despite cellular and behavioral indications that they lack MET currents and balance function. Thus, both Tmc1 and Tmc2 play a role in vestibular function while Tmc1 is responsible for normal function in the mature cochlea.

Based on *Tmc1* mouse models, recessive loss-of-function mutations are predicted to cause human deafness in DFNB7/11 (Nakanishi et al., 2014), while

at least one cause of DFNA36 is a dominant gain-of-function mutation in *Tmc1* (Pan et al., 2013; Zhao et al., 2014). Prior to the generation of $Tmc1^{\Delta/\Delta}$; $Tmc2^{\Delta/\Delta}$ knock-out mice, studies identified the effects of *Tmc1* recessive *dn* and dominant *Bth* mutations in the mouse cochlea (Vreugde et al., 2002; Marcotti et al. 2006). The $Tmc1^{dn}$ mutation is identified to cause a 1.6kb in-frame deletion, and results in RNA encoding the full length of *Tmc1* minus 171 base pairs normally encoded by exon 14 (Kurima et al. 2002). This 57 amino acid deletion occurs in the area of the putative pore region between transmembrane domains 4 and 5, and includes a portion of the TMC motif. Mice homozygous for the deafness mutation ($Tmc1^{dn/dn}$) have no compound action potential responses (summed electrical responses of auditory spiral ganglion neurons to sound stimulus) while $Tmc1^{dn/dn}$; $Tmc2^{-/-}$ cochlear hair cells lack mechanotransduction currents (Marcotti et al., 2006; Kim et al., 2013). Previous work has demonstrated that even at the onset of mouse hearing (P12-P20), cochlear microphonic responses (the summed electrical receptor potentials of outer and inner hair cells) are not present in $Tmc1^{dn/dn}$ mice (Bock and Steel 1983). Cochlear hair cells from $Tmc1^{dn/dn}$ mice begin to degenerate at age P15 through P30. Thus, the function, morphological development, and eventual degeneration of cochlear hair cells are consistent between $Tmc1^{\Delta/\Delta}$ and $Tmc1^{dn/dn}$ mice, making the $Tmc1^{\Delta/\Delta}$ mouse a suitable model for DFNB7/11.

As mentioned previously, the dominant *Bth* mutation is a methionine to lysine substitution at position 412 in Tmc1, and recently the orthologous mutation was identified in human TMC1 at position 418 involving the same amino acids,

making the *Bth* mouse an excellent model for DFNA36 (Vreugde et al., 2002; Zhao et al. 2014). Hair cells null for *Tmc2* and expressing $Tmc1^{Bth/\Delta}$, heterozygous for *Tmc2* expressing $Tmc1^{Bth/\Delta}$, or wild-type for *Tmc2* expressing $Tmc1^{Bth/+}$ all retain large MET currents, indicating that the mutation is not dominant negative or a dominant loss of function (Marcotti et al., 2006; Pan et al., 2013). $Tmc1^{Bth/+}$ mice develop hearing loss in the mid to high frequencies by P30, but low frequency hearing remains and is consistent with hair cell survival in the low frequency region (Marcotti et al., 2006). The intermediate loss of hearing in $Tmc1^{Bth/+}$ mice, as compared to homozygous $Tmc1^{Bth/Bth}$ mutants that are profoundly deaf by P30, indicates a gene dosage effect that acts in a semi-dominant fashion. Indeed, Pan et al. identified the *Bth* mutation as a gain-of-function that decreases Ca^{2+} permeability of the MET channel and eventually leads to hair cell death. Interestingly, virtually all the inner hair cells degenerate in $Tmc1^{Bth/Bth}$ mutant mice by P30, indicating that cell death is the primary cause of their hearing loss. It is unclear how a reduction in Ca^{2+} permeability is related to or brings about hair cell degeneration. One possibility is that hair cells rely on calcium-dependent gene regulation, and a decrease in calcium entry could interrupt transcription of genes necessary for hair cell survival (Holt et al., 2014). So far no calcium dependent gene regulatory mechanisms have been investigated in hair cells. However, recognizing that Tmc2 mediated MET currents have greater Ca^{2+} permeability than Tmc1, it would be interesting to test whether hair cell survival is improved in $Tmc1^{Bth}$ mice by expression of exogenous *Tmc2*. It is currently unknown whether Tmc1 or Tmc2 are capable of

forming heteromeric complexes with each other, as no dominant negative mutations that could aid in probing this type of question have yet been found. Thus, the study of TMC proteins is important not only to characterize their role in mechanotransduction and hair cell survival, but also to investigate how treatments may be devised to rescue dominant (DNFA36) and recessive (DFNB7/11) forms of deafness in humans.

Use of Adeno-Associated Virus (AAV) Vectors in Inner Ear Gene Therapy

The mammalian inner ear is a relatively closed system encased in bone that contains a sensory epithelium separating two fluid filled chambers (Fig. 2-1, 2-8). The fluid can be externally accessed by surgical means with a micropipette through a narrow window covered by a thin elastic membrane called the round window membrane (RWM), or by drilling a hole called a cochleostomy (CO) through the bone of the cochlea (Fig. 2-8). This combination of isolation and accessibility is ideal for administering gene therapy to the sensory cells with limited distribution to other tissues in the body. The mechanosensory bundles of the hair cells exist within a fluid filled compartment called the scala media that remains electrically and ionically isolated from the rest of the body by tight junctions between epithelial cells surrounding the luminal surface of the scala. The fluid filled compartments of the inner ear are also isolated from central circulation by a blood-labyrinthine barrier made up of pericytes and endothelial cells that line cochlear capillaries (Harris et al., 1995). The scala media is filled with endolymph and may be accessed by surgical means, however this involves

puncturing the cochlea lateral wall after a cochleostomy, which can disrupt the natural barriers that maintain the endocochlear potential causing significant auditory threshold shift (Iizuka et al., 2008; Shibata et al., 2009; Wang et al., 2013). The fluid in the scala tympani and scala vestibuli surrounds the scala media and is called perilymph, which is similar in composition to cerebrospinal fluid. The perilymph can be accessed atraumatically through the RWM by micropipette, and is therefore safer because it does not typically lead to hearing loss (Liu et al., 2005; Iizuka et al. 2008; Shibata et al., 2009; Xia et al., 2012; Akil et al., 2012). Furthermore, accessing the inner ear through the RWM is the preferred route of cochlear implantation in humans, which supports the notion that using the RWM approach in the mouse is clinically relevant for human gene therapy administration (Richard et al., 2012).

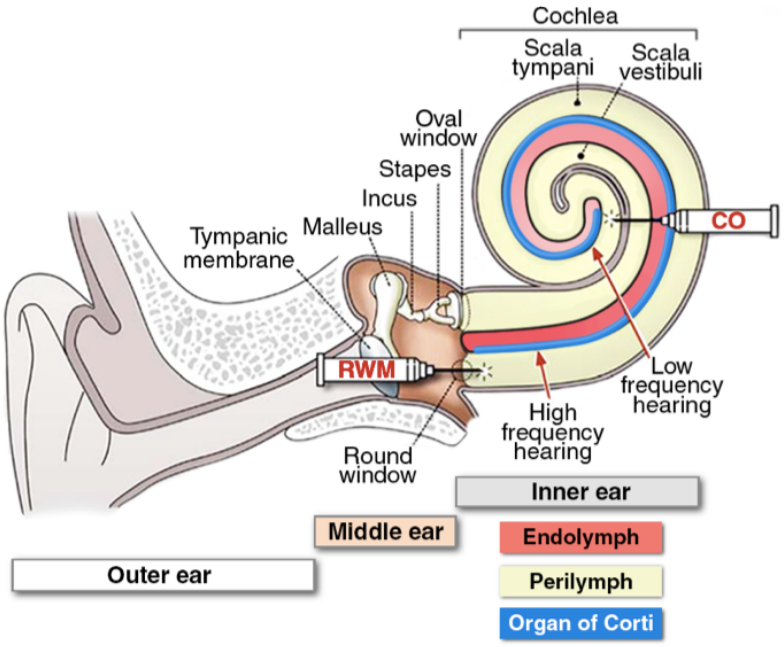

Figure 2-8. A schematic representation of cochlear anatomy demonstrates the different fluid filled compartments of the inner ear and routes for viral vector administration. The scala tympani can be accessed by micropipette through the

round window membrane (RWM), which contains perilymph and bathes the basolateral hair cell surfaces. The scala media can be accessed by cochleostomy (CO) and contains endolymph that bathes the apical hair cell bundles. Image adapted with permission from Macmillan Publishers Ltd: [Molecular Therapy] (Holt and Vandenberghe 2012), copyright (2012).

An important consideration for the translation of mouse studies to humans is the difference between their auditory systems, and key distinctions exist in their maturation. The inner ear of the human completes most of its development in utero, and the peripheral auditory system becomes able to transduce signals to the brain beginning in the middle of the 2nd trimester (Birnholz and Benacerraf 1983; Hepper and Shahidullah 1994). The mouse inner ear completes development after birth, and the peripheral ear does not transduce external auditory information to the brain until the mid second post-natal week. This distinction has important consequences for the treatment of non-syndromic hearing loss, because while successful gene therapy investigations can be done in early post-natal mice before inner ear pathology develops, it is unclear how early inner ear pathology develops in congenitally deaf humans or how early interventions on humans must be performed in order to preserve sensory structures. Of course, severity and onset of human inner ear pathology is dependent on the type of gene involved and whether there are functionally redundant genes present with the potential to prolong sensory cell survival in the absence of the primary gene. It is unknown if the same developmental switch that occurs in mice from primarily *Tmc2* to *Tmc1* expression also occurs in humans, but if so it would be useful to know when redundant *Tmc* expression is lost in order to inform future clinical protocols of the critical period for intervention.

If present, the persistence of *TMC2* expression in humans could potentially support hair cell survival until after birth.

Exploration of viral vectors to infect hair cells of the inner ear began in the 1990s, as the theory of using viruses to deliver therapeutic genes *in vivo* became reality. The first studies focused on use of adenovectors (Raphael et al., 1996; Holt et al., 1999), which were effective for both *in vitro* and *in vivo* infection at relatively low concentrations (~$1x10^7$ vp/mL). Although adenovirus proved highly infectious for hair cells and many cell types in the cochlea, it was demonstrated to have detrimental effects on hearing thresholds (Lubke et al., 2001; Sheffield et al., 2011). The cellular toxicity *in vivo* appears to result when either the first or second generation versions of the virus are used, despite the reported depletion of immunogenic viral replication genes in the second generation adenovirus (Sheffield et al., 2011). Along with sequences of the adenoviral genome, the capsid or protein coat of the adenovirus was discovered to elicit a robust host immune response (Molinier-Frenkel et al., 2002; Raper et al., 2003; Aldhamen et al., 2011) and its associated toxicity to hearing thresholds makes it less attractive for *in vivo* use despite the advantage of its use to deliver large (5-10kb) transgenes *in vitro* (Holt 2002; Kesser et al., 2007). Since it does not produce any known disease in humans, adeno-associated virus was explored as a less toxic alternative to adenovirus. As a dependovirus, AAV is naturally incapable of replicating in the absence of a helper virus, such as adenovirus or herpes virus, and requires their viral replication machinery to complete the viral life cycle (Atchison et al., 1965). This is another attractive feature of AAV for in vivo gene

therapy, since the vector cannot proceed to the lytic phase of its life cycle alone and infection cannot spread from the primary transduced cells. The only AAV wild-type DNA sequence necessary for packaging of a therapeutic transgene cassette is the inverted terminal repeat (ITR) hairpin structures that flank either end of the cassette (Samulski et al., 1983; Samulski et al., 1987). When co-transfected into cultured cells with an adenovirus helper vector and an AAV capsid vector, the therapeutic transgene cassette is packaged into the AAV capsids and the therapeutic vector remains replication incompetent. The ITR sequence of AAV serotype 2 was the first to be isolated, and since its 145-nucleotide structure bears little difference to ITRs of other serotypes, AAV2 has been used to cross package transgene cassettes into the capsid of other serotypes in a process called pseudotyping (Xiao et al., 1999; Burger et al., 2004). Pseudotyped vectors for AAV serotypes 1-9 (e.g. AAV2/1, 2/2, 2/3, 2/4, etc.) have demonstrated that capsid structure plays a contributing role in tissue specific targeting known as tropism, and therefore investigators have attempted to find the most efficient vector for targeting their tissue through trial and error screening of different serotypes (Burger et al., 2004). Although the wild-type form of the AAV2 replication (Rep) sequence is capable of site-specific insertion into a parental virus pre-integration site (AAVSI) in the host genome due to sequence homology, the Rep gene sequences are removed from recombinant AAV and the majority of viral genomes are retained as stable circular episomes in the cell nucleus after viral transduction (Xiao et al., 1996). Since AAV is a single stranded DNA virus, it must complete second strand synthesis inside the host cell before

expression proceeds, where onset of expression typically occurs 5-7 days after infection depending on cell type, AAV serotype, kinetics of viral uncoating, and DNA polymerase activity (Ferrari et al., 1996; McCarty et al., 2001; Kaspar et al., 2002; Zincarelli et al., 2008). The exception is AAV2, which has been shown to take 2 weeks to initiate expression and 4 weeks to reach full expression (Zincarelli et al., 2008). Transgene expression from AAV vectors is very stable and long lived in non-dividing cells, and cells transduced *in vivo* are shown to retain expression for at least a year in mouse cochlear hair cells (Akil et al., 2012), or for over 6 years and counting in non-human primate muscle (Rivère et al., 2006). One major drawback to the use of AAV vectors in gene therapy is their packaging size restriction, which is limited to 4-5kb (Grieger et al., 2005). Fortunately, many genes involved in non-syndromic hearing loss are small enough to fit within this packaging capacity (*hereditaryhearingloss.org)*.

Initially, investigations demonstrated that AAV infection in the cochlea is effectively zero when compared with equivalent titers of adenovirus (~$1x10^8$ PFU/mL, Holt et al., 1999; Luebke et al., 2001). However, with the improvement of AAV production techniques, the virus could be produced at titers near 10^{10}-10^{13} gc/mL (Zolotukhin et al., 2002), and this became the key to the successful AAV infection in the cochlea. The first study to demonstrate convincing infection of cochlear hair cells with high titer AAV (10^{10} genomic copies) utilized an *in vitro* primary culture of dissected P0 cochleas and green fluorescent protein (GFP) as a reporter of vector expression driven by the chicken beta-actin (CBA) promoter in AAV capsid serotypes 1, 2, and 5 (Stone et al., 2005). They observed reporter

expression in IHCs (16-43%) and OHCs (37-66%) after viral transduction with AAV1 or AAV2, but no reporter expression with AAV5. They showed that *in vitro* the majority of infected hair cells are of the outer hair cell type. The first study to take high titer AAV ($5x10^{10}$ genomic copies) transduction *in vivo* used a RWM approach to inject CBA-driven GFP reporter vectors for AAV serotypes 1-5, 7, and 8 into adult mice (Liu et al., 2005). Their study showed that AAV serotypes 1, 3, 5, 7, and 8 all infected IHCs at a high rate but did not infect OHCs. This was the first indication of a discrepancy between *in vitro* and *in vivo* viral infection rates in the cochlea. A handful of later studies repeated investigation of RWM injections with different AAV serotypes into adult rodent cochleas to examine the effects of serotype and promoter, and the consensus data indicate that either CBA or cytomegalovirus (CMV) promoters drive expression in inner hair cells with serotypes 1, 2, or 8 but do not infect outer hair cells even at higher viral titers of 10^{10}-10^{13} (Liu et al., 2007; Iizuka et al., 2008; Konishi et al., 2008). However, when AAV was injected *in utero* into the developing otocyst at embryonic day 12, it was discovered that high rates of both inner (~80%) and outer (~60%) hair cells could be infected using AAV1 (Bedrosian et al., 2006). This data suggested that younger tissue is more receptive to AAV infection, and that AAV1 is capable of infecting both IHCs and OHCs *in vivo*.

The next advance in the field was to use a synergy of the knowledge generated from these earlier studies, and apply it to treatment of a hair cell specific non-syndromic deafness. The authors of Akil et al. 2012 investigated RWM injections into young mice, age P0-P10, using AAV1 and the CBA

promoter to drive expression of a vesicular glutamate transporter (VGLUT3) found specifically in inner hair cells. Vglut3 is necessary to package glutamate into vesicles for synaptic transmission from inner hair cells to spiral ganglion neurons, and without this transporter synaptic transmission fails (Seal et al., 2008). Their study was the first to restore auditory function in deaf mice by using a gene augmentation strategy into Vglut3 knock-out mice, and demonstrated that even though inner hair cells in this mouse model continue to survive through adulthood, they recover greater hearing sensitivity that lasts for a longer duration when they intervened at P0 as opposed to P10. Interestingly, when antibody staining was done to localize expression of the exogenous Vglut3, the authors found that labeling was restricted to inner hair cells despite the use of a ubiquitously expressed promoter. The Akil el al. study was a major success because they took advantage of the ability to infect the majority of inner hair cells at either P0 or P10, and the near 100% viral transduction rate of inner hair cells resulted in rescue of auditory thresholds to wild-type levels because outer hair cell functioning remains intact in VGLUT3 KO mice. However, Akil et al. 2012 left several questions unresolved. What was the mechanism that limited Vglut3 expression to inner hair cells? Were outer hair cells also targeted by AAV1 at P0, and would their approach work for other non-syndromic hearing loss genes expressed in both auditory hair cell types? Others have reported that use of AAV8 targets inner and outer hair cells *in vivo* after inoculation of the scala media in adult mice (Kilpatrick et al. 2011). Is there a difference between AAV1 and AAV8 or is it the route of administration that influences tropism for outer hair

cells? Unfortunately, variability between individual studies in the body of cochlear gene therapy literature (especially in routes of AAV vector administration, vector titer, vector serotype, vector production, and the age of the target tissue) has demonstrated problems to reproducibility which have led many researchers to independently confirm what vectors perform the best for their application in the inner ear (Sacheli et al., 2013).

The experiments outlined in the next chapter seek to independently confirm the tropism of AAV1-*Cba* driven vectors in hair cells in the cochlea, to investigate whether *Tmc1* and *Tmc2* can serve redundant functions to support hearing, and to test gene augmentation and gene substitution strategies as a therapy in DFNB7/11 and DFNA36 mouse models. The outcomes of this study will advance our understanding of the capacity and limitations of gene therapy to restore hearing in patients who suffer from *TMC1* gene mutations.

Chapter III: Transmembrane Channel-like (*Tmc*) Gene Therapy Restores Auditory Function in Deaf Mice[1]

Introduction

Hearing loss is the most common sensory deficit in the world with both genetic and environmental factors causing dysfunction of the primary sensory cells of the inner ear, known as hair cells (Géléoc and Holt, 2014). Hair cells convert mechanical stimuli into electrical signals and are essential for normal auditory and balance function. Unfortunately, hair cells lack the ability to regenerate; thus hair cell damage or death is cumulative, causing progressive hearing loss. The current standards of care for hearing loss are hearing aids or cochlear implants, which provide incomplete restoration of function in a limited patient population. Pharmacologic, stem-cell and gene therapies are being explored as alternative therapies (Géléoc and Holt, 2014). Of these possible strategies, gene therapy may be best suited for restoration of hair cell function in genetic hearing loss (Kesser et al., 2007; Kesser et al., 2008; Kohrman and Raphael, 2013; Géléoc and Holt, 2014). However, few studies have provided proof-of-principle evidence supporting gene therapy as a viable strategy for restoration of auditory function in mouse models of genetic hearing loss. One notable exception is the restoration of auditory function in mice lacking vesicular glutamate transporter 3 (VGLUT3), a glutamate transport protein, expressed in

[1] This chapter is a reproduction of Askew et al., 2015 *Science Translational Medicine*. It has been reformatted with expanded text and figures to match the thesis style. It is reprinted here in accordance with the AAAS Author License to Publish Policy.

auditory inner hair cells, required for synaptic transmission from inner hair cell to postsynaptic neurons of the 8th cranial nerve (Akil et al., 2012). The authors of that study used adeno-associated viral (AAV) vectors to deliver the coding sequence for VGLUT3 into inner hair cells of early post-natal VGLUT3 knockout mice. Although an important advancement, VGLUT3 mutations are not common in humans and when present, are dominant, suggesting the clinical utility of VGLUT3 augmentation may be limited.

To explore gene therapy for a common form of genetic hearing loss that affects hair cells, we used mice that carry mutations in Transmembrane channel-like gene 1 (*Tmc1*). *TMC1* mutations are a common cause of genetic deafness in humans, accounting for up to 4%-8% of genetic deafness in some populations (Kitajiri et al., 2007; Simraci et al., 2009). To date, 44 *TMC1* mutations have been identified that cause deafness in humans (Nakanishi et al., 2014; Kawashima et al., 2015). Most are recessive and cause prelingual deafness, while at least five are dominant and cause progressive hearing loss with onset during the mid-teen years (Nakanishi et al., 2014), suggesting possible windows of opportunity for clinical intervention.

Although the precise molecular function of TMC1 is unclear, there is agreement that TMC1 and its closely related ortholog, TMC2*,* affect permeation properties of sensory transduction channels in auditory hair cells (Kawshima et al., 2011; Pan et al., 2013; Beurg et al., 2015) and are likely channel components (Pan et al., 2013). Mice deficient in *Tmc1* and *Tmc2* lack sensory transduction, are deaf, and suffer severe balance dysfunction, despite the presence of normal

hair cell morphology (Kawashima et al., 2011) and hair cells that survive into mature stages (Marcotti et al., 2006). Mice that carry the *Beethoven (Bth,* Vreugde et al., 2002*)* point mutation (p.M412K) in *Tmc1* retain sensory transduction but have reduced calcium-permeability (Pan et al., 2013). *Beethoven* mice are an excellent model for dominant-progressive hearing loss (DFNA36) in humans who carry an identical substitution in the orthologous position (p.M418K) of the human *TMC1* gene (Zhao et al., 2014). Mice that carry *Tmc1* deletions (Kawashima et al., 2011) are good models for recessive hearing loss (DFNB7/11) in humans with loss-of-function mutations in *TMC1*.

Previously, adenoviral vectors were used *in vitro* to introduce the coding sequence for *Tmc1* or *Tmc2* into hair cells excised from mice deficient in *Tmc1* and *Tmc2* (Kawashima et al., 2011). These experiments demonstrated partial restoration of sensory transduction in cultured hair cells *in vitro*. To extend these studies to an *in vivo* setting and to develop gene therapy strategies to treat genetic deafness in humans, we designed AAV vectors that carried the coding sequence for *Tmc1* or *Tmc2* and injected them in the ears of *Tmc1* mutant mice. Here we demonstrate that *Tmc1* and *Tmc2* are functionally redundant, and that either gene can restore sensory transduction and partial auditory function *in vivo* in mice that carry recessive *Tmc1* mutations. In addition, we used *Tmc2* gene therapy to preserve auditory function and hair cell survival in mice that carried dominant *Bth* mutations in *Tmc1*. Our results support continued development of gene therapy strategies for hearing restoration in humans with genetic deafness. Further work will be required to identify refined strategies capable of gene

delivery to greater numbers of outer hair cells *in vivo* and to maximize hair cell preservation and recovery of auditory function.

Methods

Study design

The aim of this study was to identify AAV serotypes and promoters for delivery and expression of exogenous Tmc1 and Tmc2 in hair cells of the mouse cochlea and to evaluate the ability of these vectors to restore function in mouse models of genetic deafness in humans. AAV vectors were injected in vivo, and the outcomes were evaluated using quantitative RT-PCR, immunolocalization and confocal microscopy, imaging FM1-43 uptake, single-cell recording, histology and imaging of whole cochleas, measurement of ABRs, DPOAEs, and acoustic startle reflexes. Left ears were injected and right ears were used as uninjected controls. Each experiment was replicated as indicated by n values in the figure legends. All experiments with mice and viral vectors were ap- proved by the Institutional Animal Care and Use Committee (protocols #2146 and #2878) at Boston Children's Hospital and the Institutional Biosafety Committee (protocol #IBC-P00000447).

Mice

Wild-type control mice were C57BL/6J (Jackson Laboratories) or Swiss Webster mouse lines (Taconic). Mice that carried mutant alleles of *Tmc1* and *Tmc2* were on a C57BL/6J background as described previously (Kawashima et al., 2011). Three genotypes of *Tmc* mutant mice were used: $Tmc1^{\Delta/\Delta}$,

Tmc1$^{\Delta/\Delta}$;*Tmc2*$^{\Delta/\Delta}$ and *Tmc1*$^{\Delta/\Delta}$;*Tmc2*$^{\Delta/+}$. Mice homozygous for the *Tmc1 Beethoven* (*Bth*) point mutation (p.M412K) were also used (Vreugde et al., 2002). Mice age P0-P2 were used to generate cochlear cultures or for *in vivo* delivery of viral vectors according to protocols approved by the Institutional Animal Care and Use Committee (protocols #2659, #2146) at Boston Children's Hospital.

Tissue preparation

Temporal bones were harvested from mouse pups at P0-P8. Pups were euthanized by rapid decapitation and temporal bones were dissected in MEM (Invitrogen) supplemented with 10 mM HEPES, 0.05 mg/mL Ampicilin, and 0.01 mg/mL Ciprofloxacin at pH 7.40. The membranous labyrinth was isolated under a dissection scope, Reissner's membrane was peeled back, and the tectorial membrane and stria vascularis were mechanically removed. Organ of Corti cultures were pinned flatly beneath a pair of thin glass fibers adhered at one end with Sylgard to an 18 mm round glass coverslip. The tissue was placed in culture and exposed to AAV vectors or used acutely for electrophysiological studies. For mice older than P10, temporal bones were harvested after euthanizing the animal with inhaled CO2, and cochlear whole mounts were generated.

Vector production

Recombinant Adeno-Associated Viral (AAV) vectors were obtained from SignaGen Laboratories at titers of 1×10^{12} – 10^{13} gc/mL which consisted of a *Cmv* promoter driving expression of eGFP packaged into AAV serotypes 2/1, 2/2, 2/6, 2/8, and 2/9. AAV2/1-*Cmv*-eGFP was produced at 4.5×10^{14} gc/mL titer by The

Viral Core at Boston Children's Hospital and was used for *in vivo* injections. AAV2/1-*Cba*-eGFP at a titer of 6×10^{12} gc/mL was obtained from the University of North Carolina Gene Therapy Core. AAV2/1 vectors carrying the coding sequence for mouse *Tmc1* or *Tmc2* driven by a modified Chicken Beta Actin (*Cba*) promoter were generated using a helper virus free system and a double transfection method as previously described (Grimm et al., 2003). A triple flag-tag (FLAG) sequence was fused to the C-terminal end of the *Tmc* coding sequence to enable visualization of the expressed protein. We generated three *Tmc* constructs: 1) AAV2/1- *Cba-Tmc1ex1::FLAG,* 2) AAV2/1-*Cba-Tmc1ex2::FLAG*, 3) AAV2/1-*Cba-Tmc2::FLAG*. AAV2/1-*Cba- Tmc* vectors were purified using an iodixanol step gradient followed by ion exchange chromatography. Titers ranged from 1×10^{12} to 1×10^{13} gc/mL as measured by quantitative PCR using primer sets specific for the human beta-globin intronic element. Virus aliquots were stored at −80°C and thawed just prior to use.

In vitro transduction and quantification

Organotypic cochlear cultures were bathed in 200 µL MEM media with vectors added directly to the culture medium and incubated with the tissue for 24 hours. The tissue was exchanged with 3 mL of MEM supplemented with 1% fetal bovine serum (FBS). Cultures were maintained for an additional 6 days and fixed in 4% paraformaldehyde for 1 hour. The tissue was stained with Alexafluor546-conjugated phalloidin, mounted on glass slides and imaged by confocal microscopy. Stacks of confocal images (20-50 µm thick) were collected along the entire length of the cochlea. Viral transduction rates for each AAV serotype were

determined for the base, mid-base, middle, mid-apex, and apex of the cochlea as the number of eGFP-positive hair cells divided by total number of cells with visibly labeled hair bundles. Cochlear cultures from *Tmc1*$^{\Delta/\Delta}$*;Tmc2*$^{\Delta/\Delta}$ mice were generated in a similar fashion and were exposed to AAV2/1-*Cba-Tmc1ex1::FLAG,* AAV2/1-*Cba-Tmc1ex2::FLAG* or AAV2/1-*Cba-Tmc2::FLAG*. To evaluate *Tmc* expression *in vitro* we used FM1-43 uptake, FLAG-tag localization, and electrophysiology recordings after 5-7 days in culture.

In vivo injection of viral vectors

Mouse pups (P0-P2) were injected via the round window membrane (RWM) using beveled glass microinjection pipettes. Pipettes were pulled from capillary glass on a P-2000 pipette puller (Sutter Instruments) and were beveled (~20 μm tip diameter at a 28° angle) using a micropipette beveler (Sutter Instruments). EMLA cream (lidocaine 2.5% and prilocaine 2.5%) was applied externally for analgesia using sterile swabs to cover the surgical site (left mastoid prominence). Body temperature was maintained on a 37°C warming pad for 30-60 minutes prior to surgery. Pups were anesthetized by rapid induction of hypothermia for 2-3 minutes until loss of consciousness, and this state was maintained on a cooling platform for 10-15 minutes during the surgery. The surgical site was disinfected by scrubbing with Betadine and wiping with 70% ethanol in repetition three times. A post-auricular incision was made to expose the transparent otic bulla, a micropipette was advanced by micromanipulator (MP-30, Sutter Instrument Company) through the bulla and overlying fascia, and the RWM was penetrated by the tip of the micropipette. Approximately 1 μL of

virus was injected unilaterally at 0.1 µL/min into the left ear using a pneumatic microinjector (WPI Nanoliter 2010). The skin incision was closed using a 6-0 monofilament suture (Ethicon). Pups were then returned to the warming pad for recovery.

Quantitative RT-PCR analysis

Two *Tmc1*$^{\Delta/\Delta}$*;Tmc2*$^{\Delta/+}$ mice were injected in the left ear at P1. Cochlea were excised from left and right ears and maintained in culture for 3 days, the equivalent of P10. RNA was extracted and quality was confirmed using an Agilent Bioanalyzer (Agilent Technologies), and it was reverse transcribed into cDNA for quantitative RT-PCR analysis with efficient primer sets specific to either *Tmc1* with SYBR GreenER qPCR reagent (Invitrogen) as previously described (Kawashima et al., 2011). To amplify a fragment of *Tmc1* we used primers:

5'-CATCTGCAGCCAACTTTGGTGTGT-3' and

5'- AGAGGTAGCCGGAAATTCAGCCAT-3'.

Expression levels were normalized to those of *Actb* (encoding β-actin) amplified with primers:

5'-TGAGCGCAAGTACTCTGTGTGGAT-3' and

5'- ACTCATCGTACTCCTGCTTGCTGA-3'.

All primers were designed to span introns, and validated using melt curve analysis and negative controls. Data were analyzed using the ΔΔCT method, relative to *Actb* and the difference between injected and uninjected ears.

Immunofluorescence

Immunostaining was performed on cultured or freshly dissected organs of Corti, immersion fixed for 1hr at room temperature with 4% paraformaldehyde diluted in PBS. For older animals, P25-P30 day old mice, temporal bones were isolated and perfused with 4% paraformaldehyde diluted in PBS and decalcified in 120mM EDTA for 24 hours before microdissecting the organ of Corti. The tissue was then rinsed in PBS, permeabilized in 0.01-0.1% Triton X-100 for 30 minutes, and counterstained for 1 hour with AlexaFluor546-phalloidin (Molecular Probes, 1:200 dilution) to label filamentous actin. For localization of exogenously expressed TMC::FLAG fusion proteins, the tissue was blocked for 1 hour using 2% BSA and 5% Normal Goat Serum, and was an incubated overnight at 4°C with an antibody to the FLAG motif (BD Biosciences, 1:200 dilution). For hair cell counts, tissue was blocked in Normal Goat Serum for 1 hour, stained with a rabbit anti-Myosin VIIa primary antibody (Proteus Biosciences, 1:1000 dilution) at 4°C overnight, and labeled with goat anti-rabbit antibody conjugated to AlexaFluor488 (Life Technologies, 1:200 dilution) for 1 hour. Samples were mounted on glass coverslips with Vectashield mounting medium (Vector Laboratories), and imaged at 10X-63X magnification using a Zeiss LSM700 confocal microscope. Three dimensional projection images were generated from Z-stacks using Image-J (NIH).

FM1-43 labeling

FM1-43 dye loading experiments were performed as described previously (Gale et al., 2011; Meyers et al., 2003; Géléoc and Holt, 2003). Coverslips with

adherent cochlear cultures were placed under an upright microscope (Zeiss Axioscope FS Plus) on a glass-bottomed chamber. Five μM FM1-43FX (Invitrogen) diluted in artificial perilymph was applied for 10 sec and the tissue was washed three times in artificial perilymph to remove dye from the outer leaflet of the cell membrane. After 5 minutes, intracellular FM1-43 was imaged using an FM1-43 filter set and an epifluorescence light source with a 63X water immersion objective. The tissue was fixed and processed for immunofluorescence as described above.

Hair cell electrophysiology

Organotypic cochlear cultures were bathed in standard artificial perilymph containing (in mM): 137 NaCl, 0.7 NaH_2PO_4, 5.8 KCl, 1.3 $CaCl_2$, 0.9 $MgCl_2$, 10 HEPES, 5.6 D-Glucose. Vitamins (1:50) and amino acids (1:100) were added to the solution from concentrates (Invitrogen) and NaOH was used to adjust final pH to 7.40 (310 mOsm/kg). Recording pipettes (3-5MΩ) were pulled from R6 capillary glass (King Precision Glass) and filled with intracellular solution containing (in mM): 135 CsCl, 5 HEPES, 5 EGTA, 2.5 $MgCl_2$, 2.5 Na_2-ATP, 0.1 CaCl2, where CsOH was used to adjust the final pH to 7.40 (285 mOsm/kg). Whole-cell, tight-seal voltage-clamp recordings were done at −84mV at room temperature (22-24°C) using an Axopatch 200B amplifier (Molecular Devices). Sensory transduction currents were filtered at 10kHz with a low-pass Bessel filter and digitized at ≥20kHz with a 16-bit acquisition board (Digidata 1440A) and pClamp 10 software (Molecular Devices). Data were stored for off-line analysis

using OriginPro 8 (OriginLab). Results are presented as means ± SD unless otherwise noted.

Mechanical stimulation

Angled stiff glass probes were fabricated from capillary glass using a fire polisher (WPI) to create a rounded probe tip of ~3-5 μm in diameter as previously described (Stauffer and Holt, 2007). The back end of the glass probe was mounted on a one-dimensional PICMA chip piezo actuator (Physik Instruments) and driven by a 400 mA ENV400 amplifier (Piezosystem Jena). Voltage steps were used to evoke bundle deflections with the stimulus waveform filtered at 10 kHz by a low-pass 8-pole Bessel filter (Krohn-Hite) to eliminate residual probe resonance. Bundle deflections were monitored via video microscopy during the recording to ensure linear probe motion and coupling of the probe to the hair bundle during mechanical steps.

Auditory brainstem responses (ABR)

ABR recordings were conducted as previously described (Maison et al., 2010). Briefly, P25-P30 mice were anesthetized by via IP injection (0.1mL/10g body weight) with 50 mg of ketamine and 5 mg of xylazine diluted into 5 mL of 0.9% saline. ABR experiments were performed at 32°C in a sound-proof chamber. To test hearing function, mice were presented pure tone stimuli of 5.6 kHz, 8 kHz, 11.3k Hz, 16 kHz, 22.6 kHz, or 32 kHz at intensities between 10 decibel sound pressure level (dB SPL) and 115 dB SPL in 5 dB steps until a threshold intensity that evoked a reproducible ABR waveform (peaks I-IV) was

detected. Using an alternating polarity stimulus, 512 to 1024 responses were collected and averaged for each sound level. Waveforms with amplitude larger than 15 μV (peak-to-trough) were discarded by an “artifact reject” function. Prior to the onset of ABR testing, the flap of skin and cartilage that typically obscures the entrance of the external auditory meatus was trimmed away with dissecting scissors, and sound pressure at the entrance of the ear canal was calibrated for each individual test subject at all stimulus frequencies. Acoustic stimuli were delivered directly to the studied ear through a custom probe tube speaker/microphone assembly (EPL PXI Systems) consisting of two electrostatic earphones (CUI Miniature Dynamics) to generate primary tones and a Knowles miniature microphone (Electret Condenser) to record ear-canal sound pressure. Sound stimuli consisted of 5-ms tone bursts (0.5ms rise–fall with a cos2 onset, delivered at 40/s). ABR signals were collected using subcutaneous needle electrodes inserted at the pinna (active electrode), vertex (reference electrode), and rump (ground electrode). ABR potentials were amplified (10,000x), pass-filtered (0.3-10kHz), and digitized using custom data acquisition software (LabVIEW). Sound stimuli and electrode voltage were sampled at 40 μs intervals using a digital I-O board (National Instruments) and stored for offline analysis. Threshold was defined visually as the lowest decibel level at which any wave (I-IV) could be detected and reproduced with increasing sound intensities. ABR thresholds were averaged within each experimental group and used for statistical analysis.

Distortion product otoaccoustic emissions (DPOAE)

DPOAE data were collected under the same conditions, and during the same recording sessions as ABR data. Primary tones were produced at a frequency ratio of 1.2 (f2/f1) for the generation of DPOAEs at 2f1-f2, where the f2 level was 10 dB below f1 level for each f2/f1 pair. The f2 levels were swept in 5 dB steps from 20 to 80 dB SPL. Waveform and spectral averaging were used at each level to increase the signal-to-noise ratio of the recorded ear-canal sound pressure. The amplitude of the DPOAE at 2f1-f2 was extracted from the averaged spectra, along with the noise floor at nearby points in the spectrum. Iso-response curves were interpolated from plots of DPOAE amplitude versus sound level. Threshold was defined as the f2 level required to produce DPOAEs at 0 dB SPL.

Acoustic startle reflexes (ASR)

Mice were tested for startle reflexes in response to broadband auditory stimulation at varying intensities. The animals were tested in a sound shielded startle booth (Kinder Scientific) and the force generated by foot movement was sensed by piezoelectric motion sensor fixed beneath an elevated platform. Mice were placed in a smaller sub-chamber anchored to the topside of the platform, which restricted them from rearing on their limbs but freely permitted penetration of the sound stimulus. Sound stimuli were calibrated using a sound pressure level meter (Allied Electronics) with the microphone mounted in the position normally occupied by the animal holder with the door closed. The generation of sound stimuli and recording of force amplitude signals was performed by startle

monitor software (Kinder Scientific). Broadband white noise was presented at a background level of 60 dB SPL throughout the experiment and auditory test stimuli consisted of 50 msec broadband white noise pulses in 10 dB steps from 60 to 120 dB. Different intensities of the test stimulus were presented in a pseudo random order at randomized inter trial intervals (ITI) that varied between 8-22 seconds, with no ITI repeated more than 3 times. Five repetitions were averaged for each of the intensities for one test subject. ASR testing was conducted prior to ABR testing so that the experimenter had no anticipation of which of the injected mice demonstrated recovery of auditory thresholds. The results are presented as mean and standard error for each group.

Statistical analysis

All mean values and error bars presented in the figures represent mean ±SD. Comparisons for statistical significance between injected ears were performed using a two-tailed paired *t* test. $P < 0.05$ was considered significant.

Results

AAV2/1 targets cochlear hair cells in vitro

To identify AAV serotypes with the highest viral transduction rate in cochlear hair cells, we incubated AAV-Cmv-eGFP reporter vectors containing capsid serotypes 1, 2, 6, 8, or 9, at titers that ranged from $3x10^{10}$ to $4x10^{13}$ genome copies (gc)/mL, with organotypic mouse cochlear cultures. GFP-positive hair cells were evident in all cultures. Confocal images from the mid-basal region of the organ of Corti demonstrate viral transduction of hair cells for each serotype

tested at an effective viral concentration of $3x10^{10}$ to $3x10^{11}$ gc/mL (Fig. 3-1A). We quantified the number of GFP-positive hair cells in each cochlea and defined viral transduction rate as the percentage of total hair cells, counted as cells with Alexa546-phalloidin-labelled hair bundles (Fig. 3-1B). The total number of hair cells per cochlea ranged from 1,575 to 3,046, depending on the quality of the dissection, with an average of 2,348 ± 389 (*n* = 28). Quantification of viral transduction rates for whole cochleas revealed that AAV serotype 2/1 transduced greater numbers of hair cells with equivalent viral titers for each serotype. AAV2/1 transduced an average of 58 ± 6.6% hair cells along the length of the cochlea, compared with 14 ± 8.4% for AAV2/6, the serotype with the next highest viral transduction rate (Fig. 3-1B). We also noted a tonotopic gradient for viral transduction, apparent for AAV2/1 at all concentrations tested (Fig. 3-1C), with more hair cells expressing GFP in the base (up to 95%) of the cochlea than at the apex (up to 54%). The rate of viral transduction of inner hair cells declined sharply from base to apex (from 81% to 5%; *n* = 7), while viral transduction rates in outer hair cell persisted at higher rates along the base to apex axis (from 84% to 57%; n=7). The mechanism of the basal-apical gradient is not clear.

Promoter activity in cochlear cultures

Next we examined the activity of different promoters in cochlear cultures *in vitro* using the AAV2/1 vector for delivery and enhanced GFP (eGFP) expression as a readout of promoter activity. Promoters were chosen from three different sources that are known to have constitutive activity in most cells types:

Cytomegalovirus (*Cmv*), Chicken beta-actin (*Cba*), and mouse Phosphoglycerate Kinase 1 (*Pgk1*). Additionally, we investigated the activity of the Synapsin 1 (*Syn1*) promoter, which is known to be active in cells with synaptic machinery, but has not been investigated in hair cells. We found that both *Cmv* and *Cba* promoters drove robust eGFP expression in hair cells, as well as many types of supporting cells in the cochlea (Fig. 3-1D). Surprisingly, although phosphoglycerate kinase is an enzyme present in most cells, we found that the *Pgk1* promoter drove eGFP expression only in supporting cells of the inner sulcus (Fig. 3-1D). We also observed *Syn1*-driven eGFP expression in spiral ganglion neurons (Fig. 3-1D), consistent with a recent report (Hernandez et al., 2014) and localization of synapsin protein (Safieddine and Wenthold, 1999). There was no detectable eGFP expression in inner or outer hair cells, despite the presence of ribbon synapses in these cells. Because both *Cmv* and *Cba* drove robust exogenous gene expression in hair cells, these promoters were chosen for further characterization of AAV2/1 transduction *in vivo* using eGFP as a reporter.

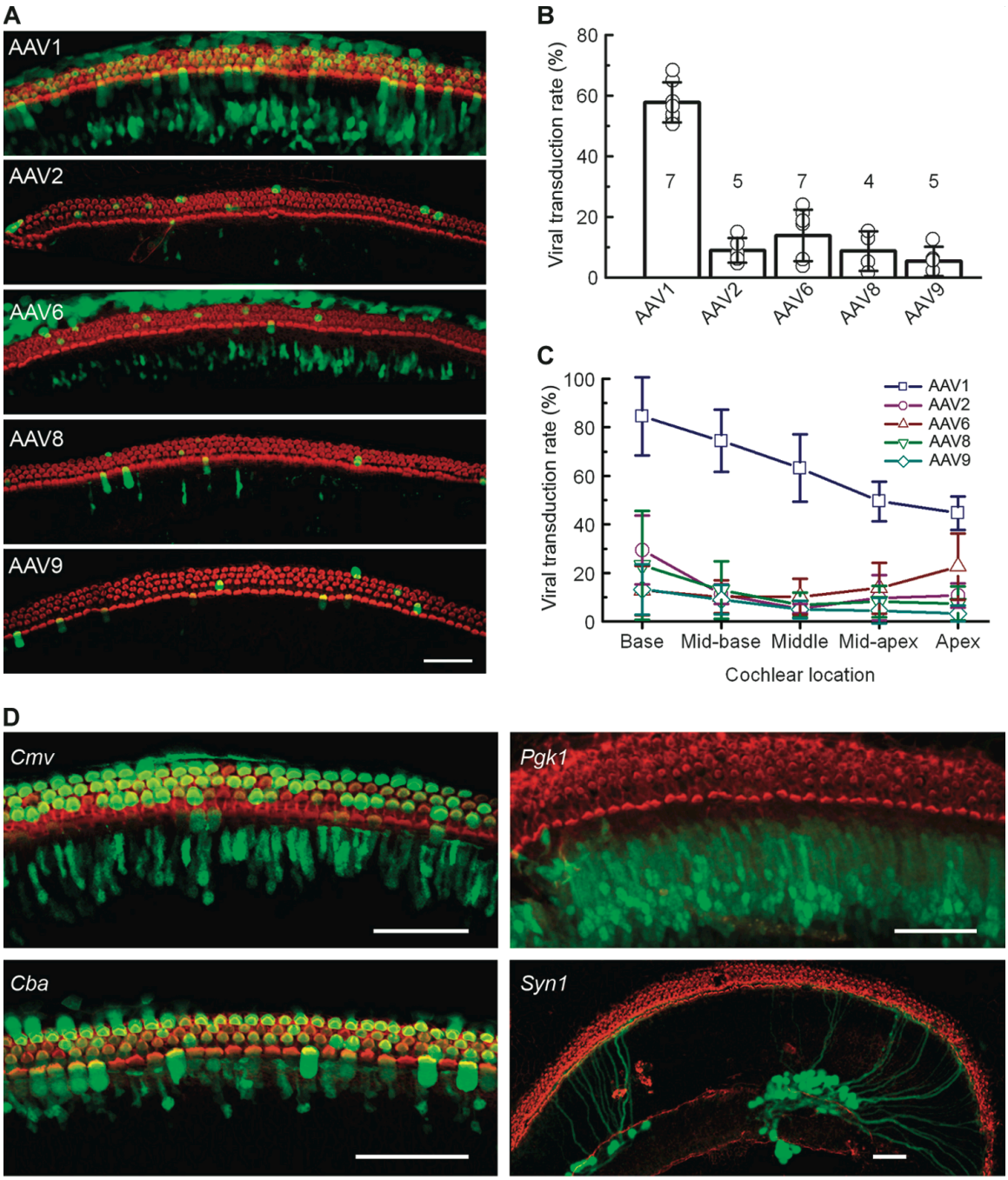

Fig. 3-1. Screen for AAV serotype and promoter in cochlear hair cells.
(**A**) Representative confocal images of the mid-base of cochlear cultures exposed to AAV-*Cmv*-eGFP with capsid serotypes indicated. Wild-type cochleas were dissected at P0 and exposed to viral concentrations of $3.3x10^{10}$ gc/mL (AAV 2/1, 2/2 and 2/6), or $3.3x10^{11}$ gc/mL (AAV 2/8 and 2/9) for 24 hours. The tissue was cultured for 7 days, fixed, stained with Alexa546-phalloidin (red) and imaged for GFP (green) on a Zeiss 700 confocal microscope. Projection images were generated from stacks of 20-40 optical sections collected at 1.2 µm intervals. Scale bar = 50 µm. (**B**) Viral transduction rates were determined from

the number of eGFP-positive hair cells (green) divided by the total hair cells with phalloidin-positive hair bundles. The bar graph represents mean, symbols show transduction rates for each cochlea. Data are mean ± SD (*n* = number of cochleas). Symbols show transduction rates for each cochlea. (**C**) Viral transduction rates subdivided into five equal regions and plotted for the entire length of the tonotopic axis. Data are mean ± SD [*n* as shown in (B)]. (**D**) Representative images of cochleas dissected from P0 WT mice, exposed to AAV2/1-eGFP vectors with promoters indicated (titers: $1x10^{11-12}$ gc/mL). Scale bars = 50 μm. CA and HA performed experiments, collected images, and analyzed data. EC helped analyze data, and BP collected the *Pgk1* promoter activity image.

Round window injection of AAV2/1 targets hair cells

To investigate expression of AAV vectors in the cochlea *in vivo*, we developed a method for viral delivery to the perilymphatic spaces via round window membrane (RWM) injection into early postnatal mice (P0-P2). Our RWM injection protocol is similar to other methods (Akil et al., 2012), except that we left the bulla intact and drove a beveled glass injection pipette directly through the overlying fascia until it penetrated both the bulla and RWM into the scala tympani (Fig 3-2). In initial experiments, successful targeting of the perilymphatic spaces was confirmed using 1 μL of fast green dye which filled the membranous labyrinth. Dye-filled turns of the cochlea were visually discernible, demonstrating distribution of the injection fluid (Fig.3-2).

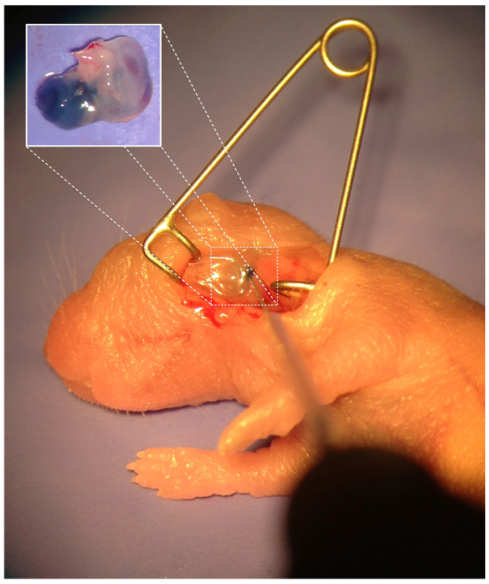

Figure 3-2. *In vivo* injection technique. A P2 mouse was injected with 1μL of fast green dye to visualize the injected spaces. A post-auricular incision exposed the otic bulla and retractors held the overlying tissue out of the target field. A beveled micropipette was then inserted through the bulla and penetrated the round window. The inset shows the excised dye filled cochlea post injection. (C. Askew, unpublished data).

In the next series of experiments we injected 1 µL of either AAV2/1-*Cba*-eGFP or AAV2/1-*Cmv*-eGFP unilaterally into the left ear through the RWM of P0-P2 wild-type mice. When injected ears were harvested at P8-P10, eGFP fluorescence revealed that both the AAV2/1-*Cba*-eGFP (Fig. 3-3) and AAV2/1-*Cmv*-eGFP (Fig. 3-5) vectors targeted hair cells and supporting cells, and drove transgene expression throughout the cochlea. However, unlike the *in vitro* results, eGFP was mainly expressed in inner hair cells *in vivo.* GFP-positive outer hair cells were seen sporadically in the basal half of the cochlea, near the injection site, but very few GFP-positive outer hair cells were found in the apical half of the cochlea. In cochleas injected with AAV2/1-*Cba*-eGFP, 59 ± 2% (*n* = 2) of inner hair cells were eGFP-positive and 70 ± 9% were eGFP-positive in AAV2/1-*Cmv*-eGFP (*n* = 4) injected cochleas. Additional cochleas were injected with *Cmv*-eGFP reporter vectors to confirm poor *in vivo* viral transduction rates for AAV8, -6, and -2 (Fig. 3-6), and representative images demonstrated similar results to the *in vitro* screen. Utricles of AAV2/1 injected mice also displayed eGFP expression in vestibular hair cells and supporting cells (Fig. 3-4), which confirmed that the injections distributed viral particles throughout the membranous labyrinth. We did not see evidence of GFP expression upon gross inspection of the auditory brainstem or other bodily tissues.

Both *Cmv* and *Cba* drove robust expression of eGFP in hair cells, but we opted to focus on the *Cba* promoter, which has recently been shown effective for driving exogenous *Vglut3* expression in inner hair cells *in vivo* (Akil et al., 2012). To assay for possible deleterious consequences on hair cell function we

measured sensory transduction currents from AAV2/1-*Cba*-eGFP-transduced wild-type hair cells following RWM injections at P0- P2, harvested at P6-P7, and cultured for 2 days. Whole-cell, tight-seal recording revealed sensory transduction currents from eGFP-positive inner hair cells that were similar to those of GFP-negative control hair cells from the same tissue (Fig. 3-3 C-F) and similar to currents of uninjected control cells (Pan et al., 2013). The sensitivity of the cells, as indicated by the steepness of the stimulus-response relationship, was unaltered in the eGFP-positive cochlear hair cells relative to control cells (Fig. 3-3 D&F). Current amplitudes (Fig. 3-3E) and adaptation properties (Fig. 3-3C) were also unaffected, suggesting that viral transduction and eGFP expression does not appear to alter sensory transduction. Since sensory transduction has not been previously recorded following *in vivo* injection of viral vectors, these data offer assurance that hair cell function is not compromised by AAV2/1 injection or eGFP expression.

To assay for possible consequences of intra-cochlear injection of AAV2/1-*Cba*-eGFP on auditory function, we recorded auditory brainstem responses (ABR) from ears of injected and uninjected wild-type mice at P25 (Fig. 3-3G). The ABR assay uses scalp electrodes to monitor the summed electrical activity of the auditory brainstem, with the first peak representing activity in the 8th cranial nerve. Consistent with prior studies that showed no detrimental effect on ABRs following *in utero* injection (Bedrosian et al., 2006) or adult injection (Kilpatrick et al., 2011), we found that auditory thresholds measured during ABR tests showed no significant difference between uninjected wild-type control mice,

wild-type mice that received a sham RWM injection with PBS (P = 0.27) or wild-type mice that received RWM injection that contained AAV2/1-*Cmv*-eGFP (P = 0.95; Fig. 3-3H). In summary, neither the injection technique, AAV transduction, nor eGFP expression affected hair cell or auditory function in any of our assays, suggesting AAV2/1 vectors are safe for delivery of exogenous genes into the inner ears of neonatal mice.

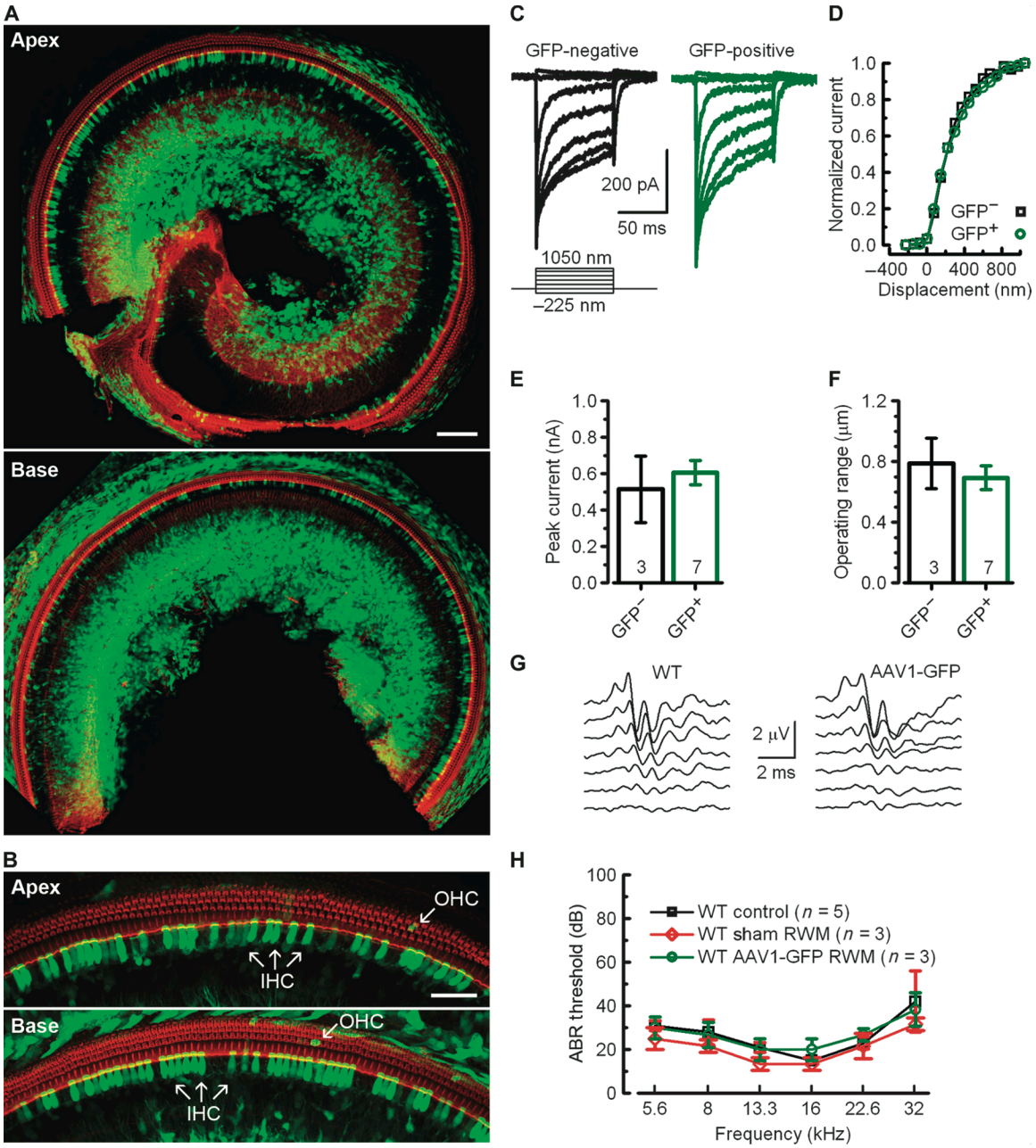

Fig. 3-3. *In vivo* injection of AAV2/1-*Cba*-eGFP through the RWM. (**A**) Representative confocal images from the apex and base of a wild-type cochlea injected through the RWM with 1µL of AAV2/1-*Cba*-eGFP ($6x10^{12}$ gc/mL) at P2, harvested at P9 and stained with Alexa546-phalloidin (red) and imaged for GFP (green). Scale bar = 100 µm. (**B**) Apex and base from the same cochlea in (A) at higher magnification. Scale bar = 50 µm. (**C**) Families of sensory transduction currents evoked by mechanical displacement of inner hair cell bundles from control (GFP-negative) cells and GFP-positive cells. Scale bars and displacement protocols are provided. (**D**) Stimulus-response curves for GFP-negative and GFP-positive cells revealed no difference in sensitivity. (**E** and **F**) Peak sensory transduction currents (E) and 10-90% operating range (F) from control and GFP-positive cells. Data are means ± SD for control and GFP-

positive cells (*n* = number of cells). (**G**) Families of ABR waveforms recorded at P25 from uninjected WT (left) and AAV2/1-*Cba*-eGFP- injected ears (right). The stimulus was an 8 kHz tone burst between 25 and 70 dB SPL in 5-dB increments. (**H**) Auditory thresholds plotted as a function of stimulus frequency for uninjected wild-type mice, sham-injected wild-type mice, and AAV2/1-*Cba*-eGFP-injected mice. Data are means ± SD (*n* = number of mice). CA performed experiments, collected images, and analyzed data. BP performed inner hair cell transduction recordings.

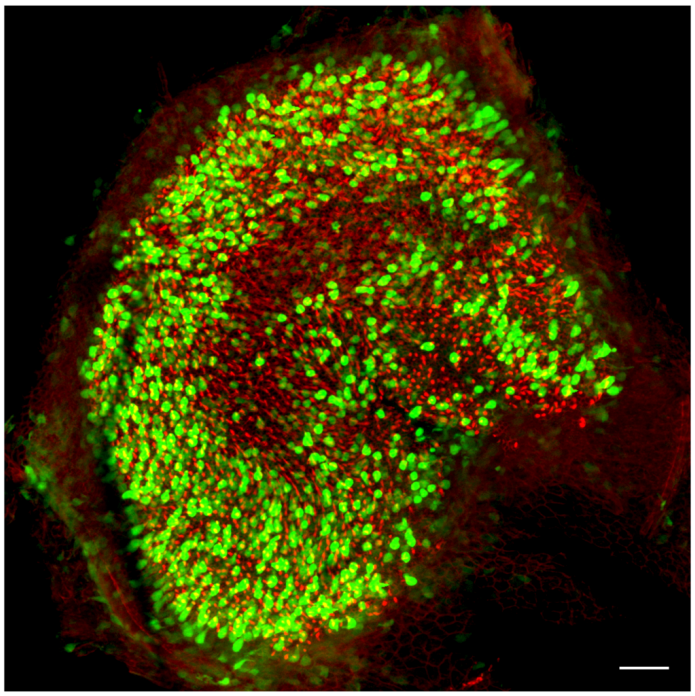

Figure 3-4. *In vivo* injection also targets vestibular hair cells. The utricle epithelium from a mouse injected with AAV2/1-*Cmv*-eGFP (the mouse and conditions are the same as Fig. 3-5, see figure legend for description). GFP-positive vestibular hair cells are evident throughout the tissue, suggesting exogenous gene constructs can target vestibular organs via RWM injection of AAV vectors. Scale bar = 50 μm. CA performed all experiments and collected images.

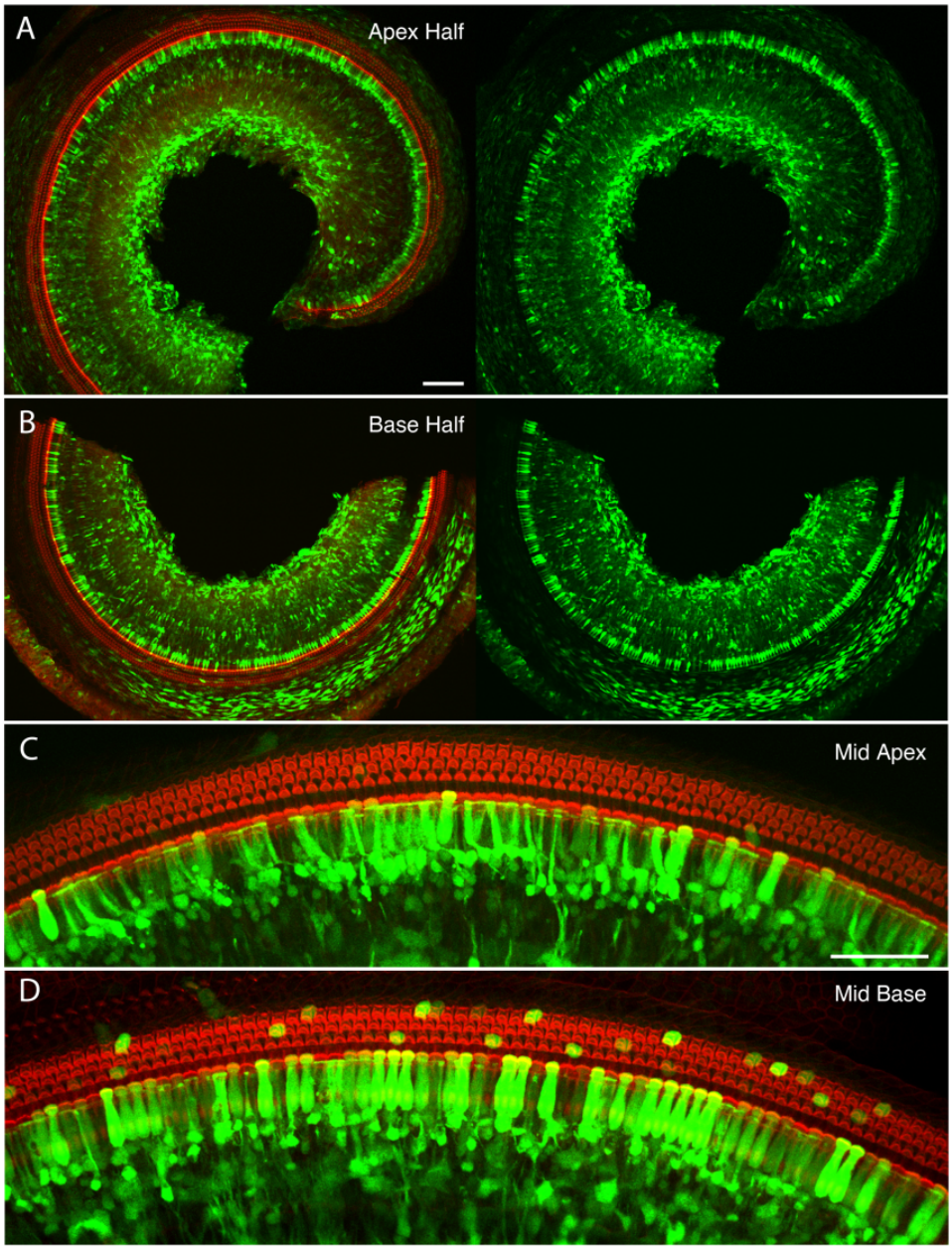

Figure 3-5. *In vivo* injection of AAV2/1-*Cmv*-eGFP through the RWM. Confocal images of cochleas injected through the round window membrane (RWM) with 1µl of AAV2/1-*Cmv*-eGFP at $4.4x10^{12}$ gc/mL. Injections were at P2 on wild-type mice and then the cochleas were harvested 7 days post injection, mounted, fixed and stained for confocal microscopy with Alexa546-phalloidin (red) and imaged for GFP (green). Representative confocal images of an *in vivo* injected cochlea tissue from the apex (**A**) and base (**B**) collected at 10x magnification. Scale bar = 100 µm. The apex (**C**) and base (**D**) from the same tissue (A&B) is shown at higher magnification (25x). Scale bar = 50 µm. The images revealed expression of eGFP in inner hair cells along the entire length of

the cochlea. Outer hair cell transduction and eGFP expression was sparse. CA performed all experiments and collected images for Fig. 3-5 and Fig. 3-6.

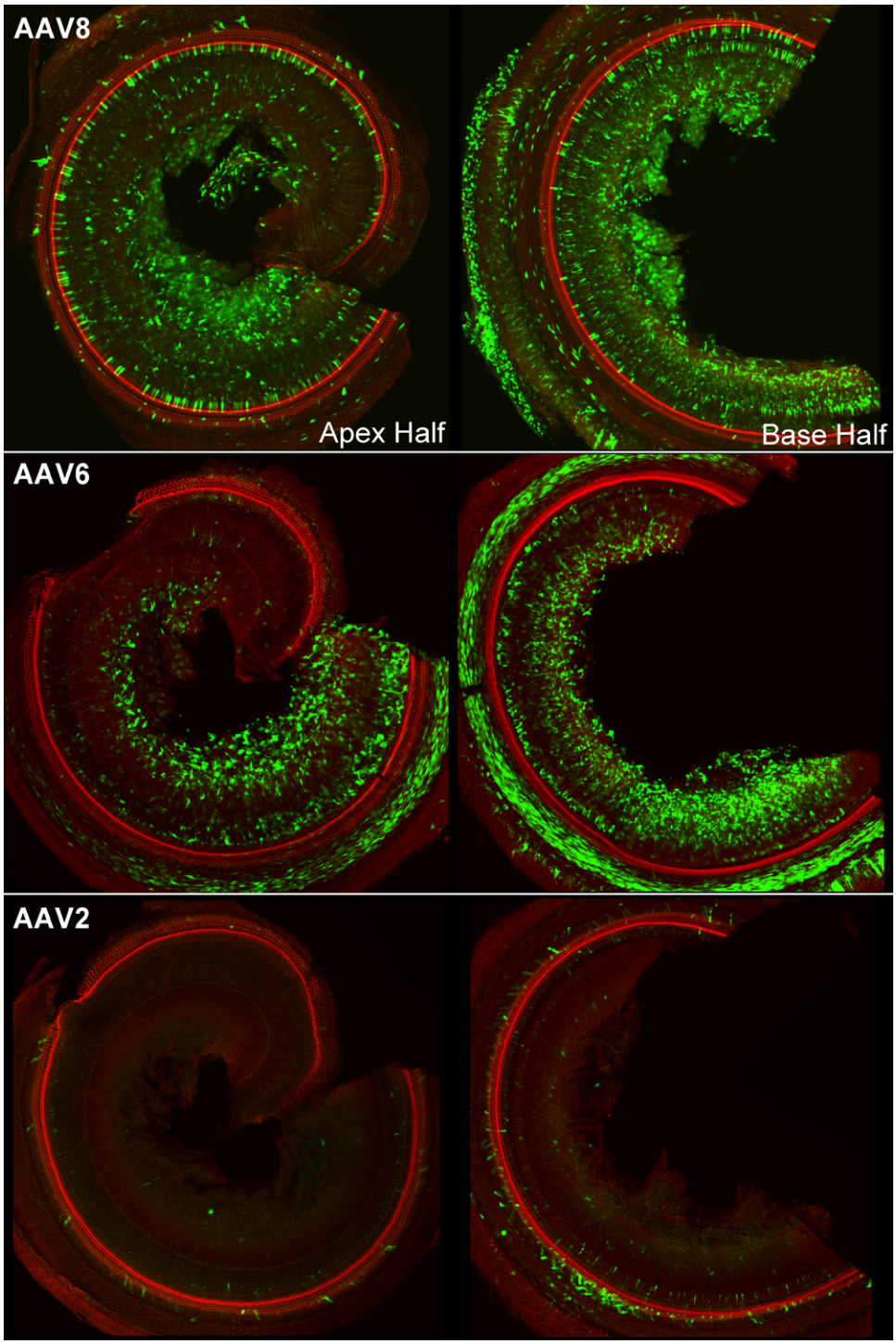

Figure 3-6. *In vivo* injection of alternate serotypes of AAV-*Cmv*-eGFP through the RWM. Confocal images of the apex (left column) and base (right column) halves of cochleas injected with 1µl of either AAV2/8-*Cmv*-eGFP

($1.16x10^{13}$ gc/mL), AAV2/6.2-*Cmv*-eGFP ($7.83x10^{12}$ gc/mL), or AAV2/2-*Cmv*-eGFP ($2.12x10^{12}$ gc/mL) as indicated. Injections were performed at P1 on wild-type mice and then cochleas were harvested 7 days post injection, mounted, fixed and stained for confocal microscopy with Alexa546-phalloidin (red) and imaged for GFP expression (green). Images were collected at 10x magnification. The images revealed a moderate level of inner hair cell transduction from AAV8-*Cmv*-eGFP expression while outer hair cell eGFP expression was sparse. Very few hair cells expressed eGFP after transduction by serotypes AAV6 or AAV2.

AAV2/1-Cba-Tmc vectors rescue hair cell function in vitro

To assess the potential for gene therapy restoration of hair cell and auditory function, we generated AAV2/1-*Cba* vectors that carried the coding sequence for wild-type *Tmc1* or *Tmc2* fused to 3xFLAG tags at their C-termini. To evaluate the functionality of these vectors, we used organotypic cochlear cultures excised at P0 from $Tmc1^{\Delta/\Delta};Tmc2^{\Delta/\Delta}$ mice, which lack TMC1 and TMC2 protein expression, are deaf and lack sensory transduction in both outer hair cells (Kawashima et al., 2011) and inner hair cells (Pan et al., 2013). AAV2/1-*Cba-Tmc1* or AAV2/1-*Cba-Tmc2* vectors were added directly to the culture media for 24 hours, and the cultures were maintained *in vitro* for 5-7 days. We found that hair cells of $Tmc1^{\Delta/\Delta};Tmc2^{\Delta/\Delta}$ mice exposed to AAV2/1-*Cba-Tmc1* or AAV2/1-*Cba-Tmc2* recovered FM1-43 uptake (Fig. 3-A), a styryl dye that permeates transduction channels open at rest (Gale et al., 2001; Meyers et al., 2003; Géléoc and Holt, 2003). Since uninfected hair cells from $Tmc1^{\Delta/\Delta};Tmc2^{\Delta/\Delta}$ do not take up FM1-43 (Kawashima et al., 2011), dye uptake in cells exposed to AAV2/1-*Cba-Tmc* vectors indicates recovery of sensory transduction.

Sensory transduction currents were recorded from both inner and outer hair cells. Representative currents were recorded from $Tmc1^{\Delta/\Delta}; Tmc2^{\Delta/\Delta}$ hair

cells and hair cells in the same tissue 5-7 days after exposure to AAV2/1-*Cba-Tmc1* or AAV2/1-*Cba-Tmc2* (Fig. 3-7B). Peak sensory transduction currents from outer hair cells ranged in amplitude from 66 to 420 pA and inner hair cells from 50 to 800 pA (Fig. 3-7B). The average peak transduction current for inner hair cells rescued by AAV2/1-*Cba-Tmc1* was 306 ± 211 pA (*n* = 4), for outer hair cells the mean was 289 ± 98 pA (*n* = 10). For inner hair cells rescued by AAV2/1-*Cba-Tmc2,* the mean peak transduction current was 766 ± 142 pA (*n* = 2). Together, these results demonstrate that either *Tmc1* or *Tmc2* can restore sensory transduction at the cellular level when delivered into non-functional hair cells *in vitro*. The data raise the potential for therapeutic use of AAV1-*Cba-Tmc* vectors to rescue hair cell function *in vivo*.

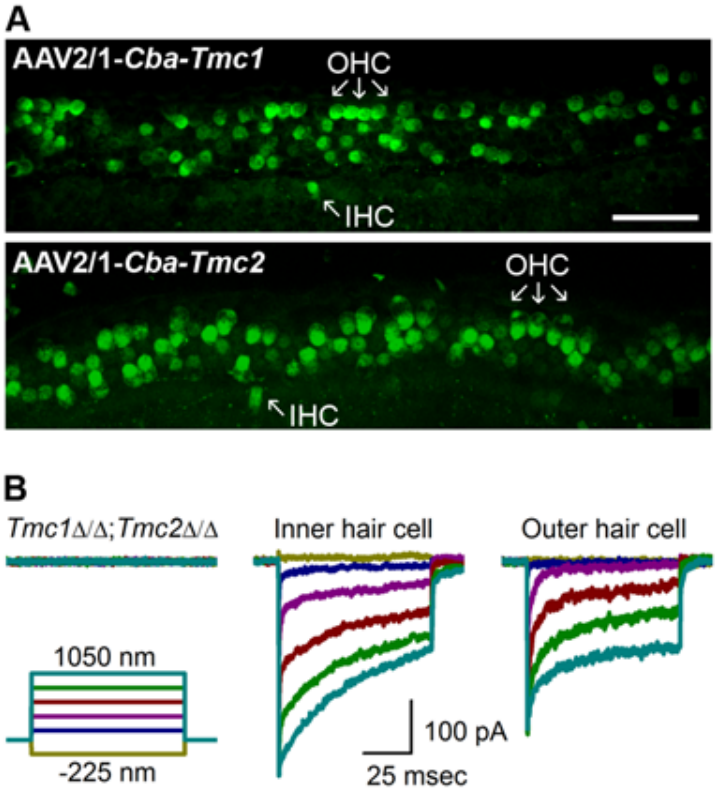

Fig. 3-7. Exogenous *Tmc* expression restores sensory transduction in *Tmc*-deficient hair cells *in vitro*. (**A**) Cochlear cultures generated from P0 $Tmc1^{\Delta/\Delta};Tmc2^{\Delta/\Delta}$ mice were exposed to either AAV2/1-*Cba-Tmc1* or AAV2/1-*Cba-Tmc2* vectors and cultured for 5-7 days. Cultures were perfused with 5 μM FM1-43FX for 10 seconds followed by 3 full bath exchanges to washout excess dye. The tissue was then fixed and mounted for imaging of FM1-43 uptake (green) in IHCs and OHCs. (**B**) Representative families of sensory transduction currents recorded in voltage-clamp mode at −84 mV from a $Tmc1^{\Delta/\Delta};Tmc2^{\Delta/\Delta}$ inner hair cell (left), an

IHC exposed to AAV2/1-*Cba-Tmc1* (middle) and an OHC exposed to AAV2/1-*Cba-Tmc1* (right). Scale bar and stimulus protocol applies to all current families. CA performed experiments, collected images, and analyzed data. BP performed inner hair cell transduction recordings.

AAV2/1-Cba-Tmc vectors restore sensory transduction in vivo

To evaluate the ability of AAV2/1-*Cba-Tmc1* vectors to drive exogenous expression of *Tmc1 in vivo*, we used quantitative RT-PCR with primers specific for *Tmc1* mRNA (Kawashima et al., 2011). *Tmc1*$^{\Delta/\Delta}$ mice were injected at P1 with 1 µL AAV2/1-*Cba-Tmc1* at a titer of 2x10^{13} gc/mL into the left ear. Cochlear tissue from the injected side (left) and uninjected side (right) was excised 7 days post-injection and incubated for an additional 3 days in culture. We extracted total RNA and measured *Tmc1* mRNA expression in cochlear tissue from injected ears relative to tissue from uninjected ears. Injected cochleas had *Tmc1* mRNA expression levels that were 13-fold higher than uninjected cochlea (n = 4 biological samples, 6 technical replicates), suggesting robust expression of exogenous *Tmc1* (Fig. 3-8A).

To test the ability of the AAV2/1-*Cba-Tmc* vectors to restore hair cell function *in vivo* we used RWM injection in *Tmc1*$^{\Delta/\Delta}$*;Tmc2*$^{\Delta/\Delta}$ mice at P0-P2. We injected 1 - 1.2 µL AAV2/1-*Cba-Tmc1* or AAV2/1-*Cba-Tmc2* at titers of 2x10^{13} gc/mL into the left ear and excised live cochlear tissue 6-7 days after injection. To evaluate the ability of the vectors to drive the exogenous *Tmc1*-3xFLAG expression, the tissue was fixed and stained with an anti-FLAG antibody conjugated to Alexa488 and counterstained with Alexa546-phalloidin. We observed prominent FLAG staining in the cell bodies of most (65%, 82/127 cells)

inner hair cells (Fig. 3-8 B&C) and, importantly, at the tips of inner hair cell stereocilia (Fig. 3-8D), the site of hair cell sensory transduction, which confirmed that TMC1 and TMC2 were expressed and properly targeted. Consistent with our prior *in vivo* observation (Figs. 3-3, 3-5), we saw little expression of the exogenous protein in outer hair cells (4%, 16/395 cells, Fig. 3-8B).

To assay for rescue of FM1-43 uptake and hair cell sensory transduction, live cochlea were excised at P6-P7 and maintained in organotypic cultures for an additional 2-3 days until the equivalent of P8-P9. Five μM FM1-43FX was pipetted over the tissue for 10 seconds followed by 4 washes of fresh dissection media and immediate fixation. Figure 3-8 E shows a representative image of a cochlear culture harvested from a $Tmc1^{\Delta/\Delta};Tmc2^{\Delta/\Delta}$ mouse exposed to FM1-43FX, which reveals no dye uptake in inner or outer hair cells. In contrast, $Tmc1^{\Delta/\Delta};Tmc2^{\Delta/\Delta}$ mice injected with AAV2/1-*Cba-Tmc1* vectors had robust FM1-43 uptake in most (71%, 57/80 cells) inner hair cells along the entire length of the cochlea in the injected ear (Fig. 3-8F). However, very few outer hair cells took up the dye, consistent with a lack of viral transduction in outer hair cells *in vivo*.

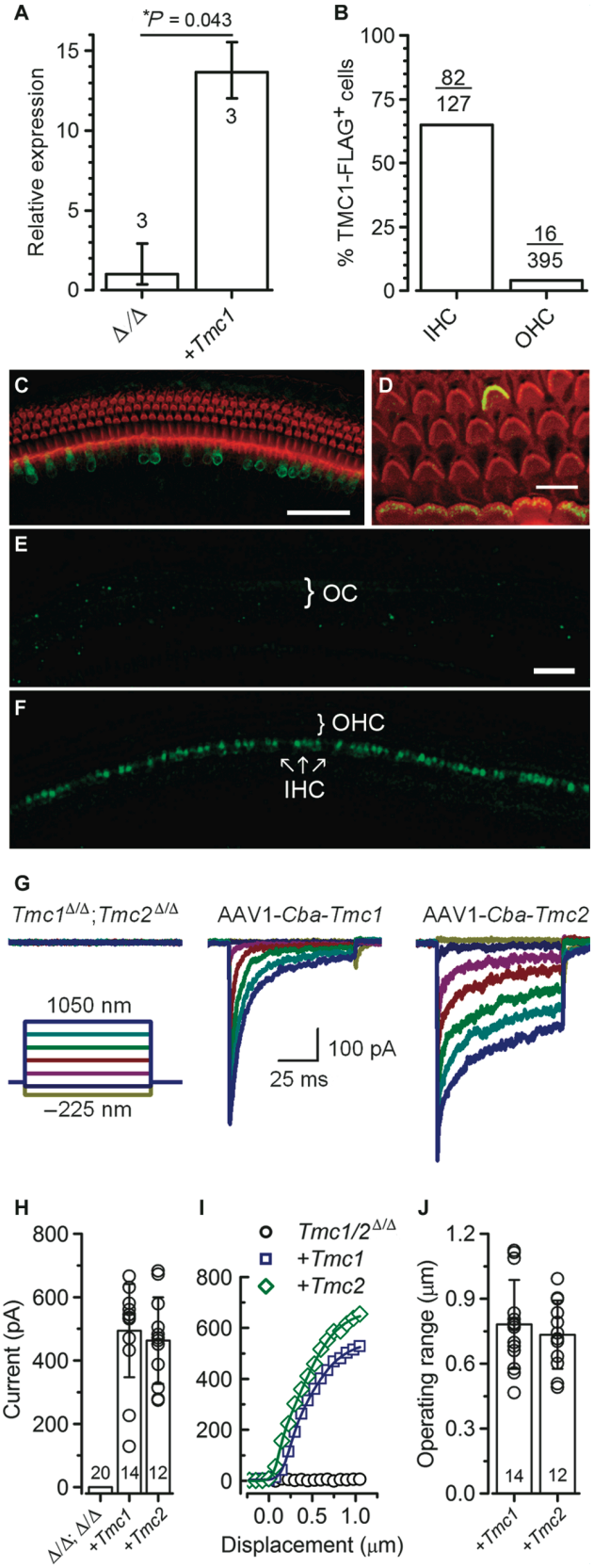

Fig. 3-8. Exogenous, AAV-delivered *Tmc1/2* restores sensory transduction in *Tmc*-deficient hair cells *in vivo*. P0-P2 $Tmc1^{\Delta/\Delta};Tmc2^{\Delta/\Delta}$ mice were injected via the RWM with AAV2/1-*Cba-Tmc1* ($2.4x10^{13}$ gc/mL) or AAV2/1-*Cba-Tmc2* ($1.8x10^{13}$ gc/mL). Cochleas were harvested 6-7 days after injection. (**A**) Quantitative PCR expression analysis of *Tmc1* mRNA from total RNA harvested from two uninjected $Tmc1^{\Delta/\Delta}$ cochleas and two $Tmc1^{\Delta/\Delta}$ cochleas injected with AAV2/1-Cba-Tmc1 (*n* = 3 technical replicates). (**B**) Percent of TMC1-FLAG positive hair cells in AAV2/1-*Cba-Tmc1* injected cochleas (*n*, number of FLAG-positive cells over total number of cells). (**C**) Confocal image of a cochlea injected with AAV2/1-*Cba-Tmc1*, stained with Alexa488 anti-FLAG antibody (green) and Alexa546-phalloidin (red). Scale bar = 50 μm. (**D**) Projection from Z-stack images of a WT cochlea injected with AAV6/1-*Cba-Tmc2* showing FLAG staining at the tips of hair cell stereocilia. Scale bar = 5 μm. (**E** and **F**) FM1-43 uptake in $Tmc1^{\Delta/\Delta};Tmc2^{\Delta/\Delta}$ tissue not injected AAV2/1-*Cba-Tmc* vectors (control, E) or injected (F) with AAV2/1-*Cba-Tmc1*. OC = Organ of Corti, scale bar = 50 μm. $Tmc1^{\Delta/\Delta};Tmc2^{\Delta/\Delta}$ mice injected with AAV2/1-*Cba-Tmc1* showed uptake of FM1- 43 in inner hair cells (IHC), but few outer hair cells (OHC). (**G**) Representative families of sensory transduction currents recorded from inner hair cells of a $Tmc1^{\Delta/\Delta};Tmc2^{\Delta/\Delta}$ mouse injected with AAV2/1-*Cba-Tmc1* that were FM1-43–negative (left) or FM1-43-

positive (middle). FM1-43–positive inner hair cell currents from a *Tmc1*$^{\Delta/\Delta}$*;Tmc2*$^{\Delta/\Delta}$ mouse injected with AAV2/1-*Cba-Tmc2* (right). (**H**) Peak sensory transduction current amplitudes from FM1-43–negative and FM1-43-positive IHCs of *Tmc1*$^{\Delta/\Delta}$*;Tmc2*$^{\Delta/\Delta}$ mice injected with AAV2/1-*Cba-Tmc1* or AAV2/1-*Cba-Tmc2* as indicated. Bars are means ± SD, circles are individual measurements (*n* = number of cells). (**I**) Stimulus-response curves from currents shown in panel G. (**J**) Mean (±S.D.) 10-90% operating range measured from stimulus-response curves shown in (I). Bars are means ± SD, circles are individual measurements (*n* = number of cells). CA performed experiments, collected images, and analyzed data. YA performed qPCR and qPCR analysis. BP injected cochleas for qPCR and performed inner hair cell transduction recordings.

Since FLAG and FM1-43 labeling indicated high viral transduction rates in inner hair cells in AAV2/1-*Cba-Tmc1* injected cochleas, we assayed for rescue of sensory transduction current in cochlear inner hair cells at P7-P9. Sensory transduction currents were recorded from AAV-*Cba-Tmc*-positive inner hair cells that expressed exogenous *Tmc1* or *Tmc2* (Fig. 3-8G), identified by the presence of FM1-43 uptake (20 nM bath application). Peak transduction current amplitudes from FM1-43-positive cells (Fig. 3-8H) were similar to currents from wild-type and GFP-positive controls (Fig. 3-3 C&E). FM1-43-negative cells from the same ear lacked sensory transduction currents entirely (Fig. 3-8 H&I). Although the FM1-43 uptake data showed variable viral transduction throughout the cochlea, cells that were FM1-43-positive had normal sensory transduction current amplitudes (Fig. 3-8H) relative to wild-type controls (Pan et al., 2013) and normal sensitivity (Fig. 3-8 I&J). Interestingly, the difference in adaptation rate and extent between hair cells exposed to AAV2/1-*Cba-Tmc1* versus AAV2/1-*Cba-Tmc2* were similar to those of hair cells expressing endogenous *Tmc1* or *Tmc2* (Pan et al., 2013). The single hair cell physiology data suggest that AAV2/1-*Cba-Tmc* vectors are

capable of complete restoration of sensory transduction *in vivo* with all the properties of native sensory transduction.

AAV2/1-*Cba-Tmc1 rescues auditory brainstem responses in Tmc1-deficient mice*

To model AAV gene therapy for rescue of genetic deafness in patients who carry recessive mutations in *Tmc1*, we injected *Tmc1*-deficient animals (P0-P2) *in vivo* with 1 - 1.2 µL AAV2/1-*Cba-Tmc1* and measured auditory function using the ABR assay at 25-30 days. Figure 3-9A shows families of ABR waveforms recorded in response to 8 kHz tone bursts with sound intensities rising along the vertical axis. The data were recorded from a $Tmc1^{\Delta/\Delta}$ mouse (left), and a $Tmc1^{\Delta/\Delta}$ mouse injected with AAV2/1-*Cba-Tmc1* (right). Uninjected $Tmc1^{\Delta/\Delta}$ mice lacked responses at all stimulus intensities and frequencies tested, which ranged between 5 and 32 kHz and 0-115 dB, indicating profound deafness, consistent with prior reports (Kawashima et al., 2011). However, prominent ABR waveforms, which represented substantial recovery of auditory transmission from the cochlea to the brainstem via the 8th cranial nerve, were present in 50% (8 of 16) of the AAV2/1-*Cba-Tmc1*-injected mice. In the eight mice with no recovery of ABR responses we found little evidence of viral transduction in hair cells, suggesting the injections may have been unsuccessful, perhaps due to clogged or improperly targeted injection needles.

For the eight mice with ABRs we quantified peak I amplitude as a function of stimulus intensity at 8 kHz in AAV2/1-*Cba-Tmc1*-injected mice and in uninjected $Tmc1^{\Delta/\Delta}$ control mice (Fig. 3-9B). Peak I amplitudes increased

monotonically in 8 of 16 *Tmc1*$^{\Delta/\Delta}$ mice injected with AAV-*Cba*- *Tmc1*, indicating stimulus-dependent increase in the auditory response. Minimum ABR thresholds are plotted in Fig. 3-9C and show recovery of auditory function, particularly at frequencies between 5 and 16 kHz for eight *Tmc1*$^{\Delta/\Delta}$ mice injected with AAV2/1-*Cba*-*Tmc1.* The ABR thresholds at 85 to 100 dB SPL (Fig. 3-9C) represent a substantial improvement relative to uninjected *Tmc1*$^{\Delta/\Delta}$ control mice, which are profoundly deaf and have no detectable responses to sound stimuli even at the highest intensities tested, 115 dB SPL. The data demonstrate partial recovery of auditory function at the systems level in the otherwise deaf mice.

In wild-type control mice, auditory thresholds for frequencies between 5 and 16 kHz were substantially lower, occurring between sound pressure levels of 20-40 dB (Fig. 3-3H). Thus, although there was recovery of ABR responses in the AAV2/1-*Cba*-*Tmc1*-injected mice, the responses did not reach wild-type levels. To investigate the reason for the incomplete recovery, including possible toxicity associated with over-expression of *Tmc1*, we injected wild-type C57BL/6 mice with AAV2/1-*Cba*-*Tmc1*. ABR thresholds in the AAV2/1-*Cba*-*Tmc1*-injected wild-type mice were unaltered relative to uninjected controls (Fig. 3-12A). This suggests there is little toxicity associated with the injection procedure, exposure to AAV2/1-*Cba*-*Tmc1* vectors or overexpression of *Tmc1* in hair cells, spiral ganglion neurons or any other cell type necessary for normal auditory function. Furthermore, we did not observe FM1-43 uptake in non-hair cells (Fig. 3-8F), suggesting that mis-expression of *Tmc1* does not lead to the formation of functional channels in other cell types.

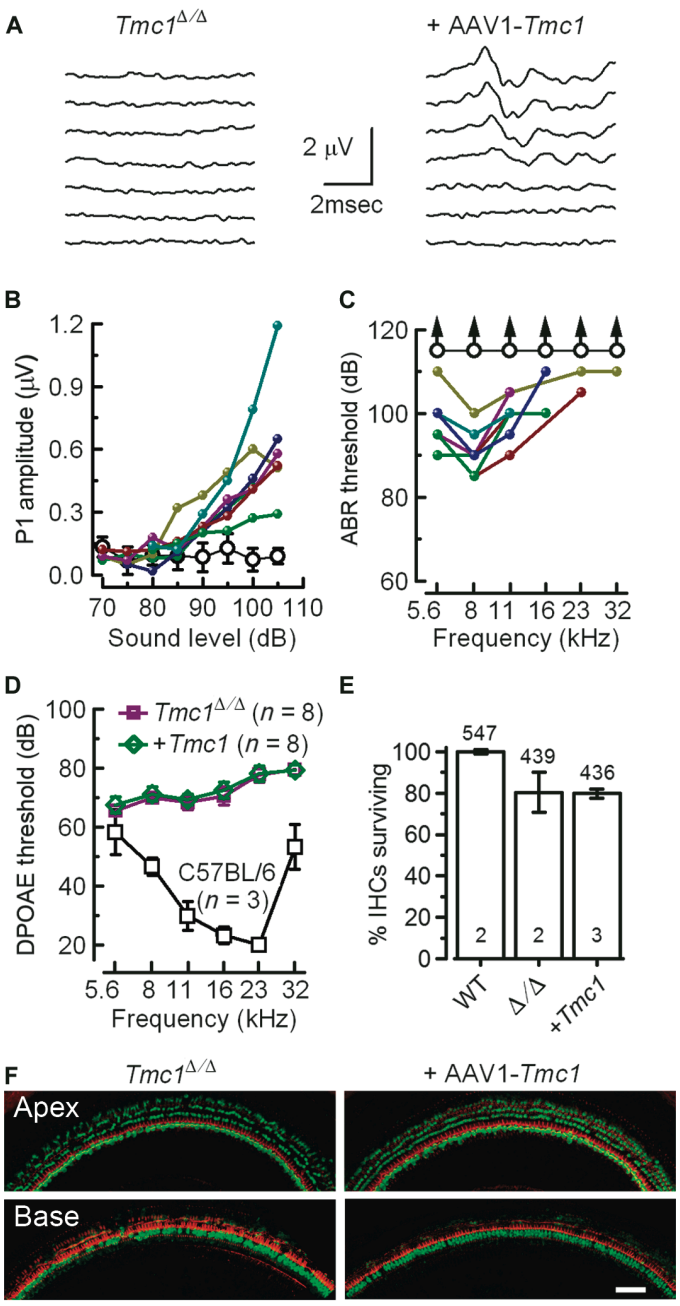

Fig. 3-9. Exogenous *Tmc1* rescues auditory function in *Tmc1*$^{\Delta/\Delta}$ mice. (A) Families of ABR waveforms recorded from an uninjected *Tmc1*$^{\Delta/\Delta}$ mouse (left) and from a *Tmc1*$^{\Delta/\Delta}$ mouse injected with AAV2/1-*Cba-Tmc1* (right). ABRs were recorded at P25-P30 using 8 kHz tone bursts at sound pressure levels between 75 and 105 dB in 5-dB increments. Scale bar applies to both families. (**B**) Peak 1 amplitudes measured from 8 kHz ABR waveforms as shown in (A) for eight *Tmc1*$^{\Delta/\Delta}$ mice injected with AAV2/1-*Cba-Tmc1* vectors. Open circles are mean responses (± SD) from uninjected *Tmc1*$^{\Delta/\Delta}$ mice (*n* = 8). (**C**) ABR thresholds plotted as function of sound frequency for eight *Tmc1*$^{\Delta/\Delta}$ mice injected with AAV2/1-*Cba-Tmc1* vectors. Open circles are means of uninjected *Tmc1*$^{\Delta/\Delta}$ mice (*n* = 8) which had no detectable thresholds at highest sound intensity tested (115-dB, arrows). (**D**) DPOAE thresholds plotted as a function of stimulus frequency for wild-type, uninjected *Tmc1*$^{\Delta/\Delta}$ mice, and *Tmc1*$^{\Delta/\Delta}$ mice injected with AAV2/1-*Cba-Tmc1.* Data are means ± SD (*n* = number of animals). (**E**) Mean percentage (± SD) of surviving IHCs (relative to WT) in 5-mm mid-cochlea sections from *Tmc1*$^{\Delta/\Delta}$ mice and AAV2/1-*Cba-Tmc1*-injected *Tmc1*$^{\Delta/\Delta}$ mice (upper *n*, number of IHCs; lower *n*, number of cochlea). (**F**) Confocal images of cochlear whole- mounts harvested at P30 from an uninjected *Tmc1*$^{\Delta/\Delta}$ mouse and a *Tmc1*$^{\Delta/\Delta}$ mouse injected with AAV2/1-*Cba-Tmc1.* The tissue was stained for MYO7A (green) and phalloidin (red). Scale bar = 50 μm. Fig. 3-13 shows low magnification images of the same cochleas. CA performed all experiments, collected images, and analyzed data.

To investigate other possible causes of the incomplete recovery, we measured distortion product otoacoustic emissions (DPOAEs) in uninjected *Tmc1*$^{\Delta/\Delta}$ mice and *Tmc1*$^{\Delta/\Delta}$ mice injected with AAV2/1-*Cba*-*Tmc1.* The DPOAE assay is a test of outer hair cell function, specifically. Outer hair cells are required for cochlear amplification, enhanced sensitivity and normal auditory function (Hudspeth 2014; Liberman et al., 2002). Interestingly, DPOAE measurements revealed elevated thresholds relative to wild-type and no difference between uninjected *Tmc1*$^{\Delta/\Delta}$ mice and those injected with AAV2/1- *Cba*-*Tmc1* vectors (Fig. 3-9D), which suggests little recovery of outer hair cell function. Uninjected wild-type mice and wild-type mice injected with either AAV2/1-*Cba*-eGFP or AAV2/1-*Cba*-*Tmc1* had normal DPOAE thresholds (Fig. 3-12B), consistent with the suggestion that the injection itself, exposure to AAV2/1 vectors and *Tmc1* overexpression caused little toxicity in outer hair cells or elsewhere in the cochlea.

Following ABR and DPOAE measurements, the mice were euthanized and their inner ear tissue was excised for histological examination. There was no overt evidence of inflammation, tissue damage or decay in the injected ears. Cochlear whole-mounts were prepared and stained with an anti-MYO7A antibody to label hair cells and Alexa546-phalloidin to label hair bundles (Figs. 3-9F, 3-13). Counts of surviving inner hair cells revealed no significant difference (P = 0.6) between uninjected *Tmc1*$^{\Delta/\Delta}$ cochleas and those injected with AAV2/1-*Cba*-*Tmc1* (Fig. 3-9E, 3-15), suggesting that AAV2/1-*Cba*-*Tmc1* injection was neither detrimental nor beneficial for inner hair cell survival at P30. Hair bundle

morphology was also inspected, but since morphology and tip-links remain normal in surviving *Tmc1*$^{\Delta/\Delta}$ hair cells (Kawashima et al., 2011), we did not detect any improvement following AAV2/1-*Cba-Tmc1* injection.

AAV2/1-Cba-Tmc2 restores ABRs in Tmc1 mutant mice

Tmc2, a closely related ortholog of *Tmc1,* is expressed in cochlear hair cells during the first postnatal week, but mRNA levels decline thereafter (Kawashima et al., 2011). *Tmc2* is expressed in *Tmc1*$^{\Delta/\Delta}$ mice, and both inner and outer hair cells of these mice retain sensory transduction through the end of the first postnatal week (Kawashima et al., 2011; Pan et al., 2013). However, because *Tmc2* expression declines thereafter, *Tmc1*$^{\Delta/\Delta}$ mice are deaf. Since AAV2/1-*Cba-Tmc2* restored sensory transduction in *Tmc1*$^{\Delta/\Delta}$*;Tmc2*$^{\Delta/\Delta}$ hair cells *in vitro* and *in vivo* (Figs. 3-7B, 3-8G), we investigated whether injection of AAV2/1-*Cba-Tmc2* into the ears of *Tmc1*$^{\Delta/\Delta}$ mice would also restore auditory function. To test this possibility we used the same injection protocols and measured ABR responses at P25-P30. We measured prominent ABR responses in 9 of 16 *Tmc1*$^{\Delta/\Delta}$ mice injected with AAV2/1-*Cba-Tmc2* (Fig. 3-10A). Peak I amplitudes (Fig. 3-10B) and minimal ABR thresholds (Fig. 3-10C) were similar to those of mice injected with AAV2/1-*Cba-Tmc1* (Fig. 3-9B&C), suggesting that expression of exogenous *Tmc2* is capable of restoring auditory function *in vivo*. Also similar to AAV2/1-*Cba-Tmc1* injection (Fig. 3-9D), AAV2/1-*Cba-Tmc2* injection did not restore DPOAE thresholds (Fig. 3-12B) nor did it impact hair cell survival or death rates relative to uninjected *Tmc1*$^{\Delta/\Delta}$ control mice (Fig. 3-10D, 3-13). There

was no significant (P = 0.44) difference in inner hair cell counts between uninjected *Tmc1*$^{\Delta/\Delta}$ mice and those injected with AAV2/1-*Cba-Tmc2* (Fig. 3-10E, 3-15).

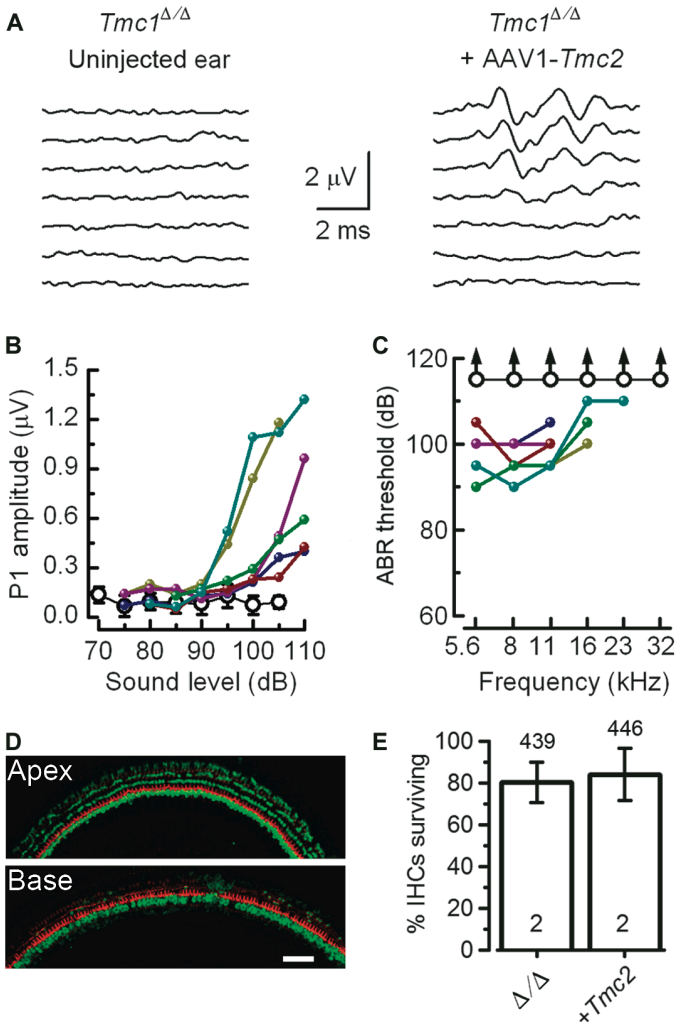

Fig. 3-10. Exogenous *Tmc2* rescues auditory function in *Tmc1*$^{\Delta/\Delta}$ mice. (A) Families of ABR waveforms recorded from the uninjected contralateral ear (left, control) of a *Tmc1*$^{\Delta/\Delta}$ mouse injected with AAV2/1-*Cba-Tmc2* (right, treated ear). ABRs were recorded at P25-P30 using 8 kHz tone bursts at sound pressure levels between 75 and 105 dB in 5-dB increments. Scale bar applies to both families. (**B**) Peak 1 amplitudes measured from 8-kHz ABR waveforms, as shown in panel (A), for six *Tmc1*$^{\Delta/\Delta}$ mice injected with AAV2/1-*Cba-Tmc2* vectors. Open circles are mean (±SD) responses from eight uninjected *Tmc1*$^{\Delta/\Delta}$ mice shown to facilitate comparison (n = 8). (**C**) ABR thresholds plotted as a function of sound frequency for six *Tmc1*$^{\Delta/\Delta}$ mice injected with AAV2/1-*Cba-Tmc2* vectors. Open circles are means of uninjected *Tmc1*$^{\Delta/\Delta}$ mice that had no detectable thresholds at the highest intensity tested (115 dB, arrows). (**D**) Confocal images of cochlear whole mounts harvested at P30 from a *Tmc1*$^{\Delta/\Delta}$ mouse injected with AAV2/1-*Cba-Tmc2.* The tissue was stained for MYO7A (green) and phalloidin (red). Scale bar = 50 μm. Fig. 3-13 shows low magnification images of the same cochleas. (**E**) Mean percentage (± SD) of surviving IHCs (relative to WT) in 5-mm mid-cochlea sections from *Tmc1*$^{\Delta/\Delta}$ mice and AAV2/1-*Cba-Tmc2* injected *Tmc1*$^{\Delta/\Delta}$ mice (upper n, number of IHCs; lower n, number of cochleas). CA performed all experiments, collected images, and analyzed data.

Based on the ability of exogenous *Tmc2* to restore ABR responses in mouse models of genetic deafness due to recessive *TMC1* mutations, we next wondered whether exogenous *Tmc2* expression might be sufficient to overcome dominant *TMC1* mutations and restore auditory function. Previously, Pan et al. 2013 showed that the dominant p.M412K mutation in TMC1, known as *Beethoven* (*Bth*), causes a reduction in calcium permeability, a reduction in single-channel currents, and an increase in the number of sensory transduction channels in inner hair cells. The identical mutation has also recently been described in a human family in the orthologous residue of human TMC1, p.M418K (Zhao et al., 2014), suggesting the *Bth* mouse is an ideal model for genetic hearing loss in humans. To investigate the ability of *Tmc2* to compensate for the *Tmc1-Bth* mutation we injected AAV2/1-*Cba-Tmc2* vectors into the ears of homozygous *Bth* mice and measured their ABRs at P25-P30. Consistent with prior reports, *Bth* mice were completely deaf by P15 (Vreugde at al., 2002; Marcotti et al., 2006). However, 7 of 15 *Bth* mice injected with AAV2/1-*Cba-Tmc2* had prominent ABRs evoked by loud sound intensities (Fig. 3-11A). Peak 1 amplitudes were smaller and the thresholds were elevated (Fig. 3-11 B&C) relative to ABRs evoked in $Tmc1^{\Delta/\Delta}$ mice injected with either AAV2/1- *Cba-Tmc2* (Fig. 3-10 B&C) or AAV2/1-*Cba-Tmc1* (Fig. 3-9 B&C), suggesting the extent of the recovery was more limited. Interestingly, there was a substantial increase in the survival rate of inner hair cells ($P = 0.006$) in the ears of *Bth* mice injected with AAV2/1-*Cba-Tmc2*, relative to the uninjected ear (Fig. 3-11D, 3-14),

suggesting that exogenous expression of *Tmc2* promotes inner hair cell survival (Fig. 3-11E, 3-15).

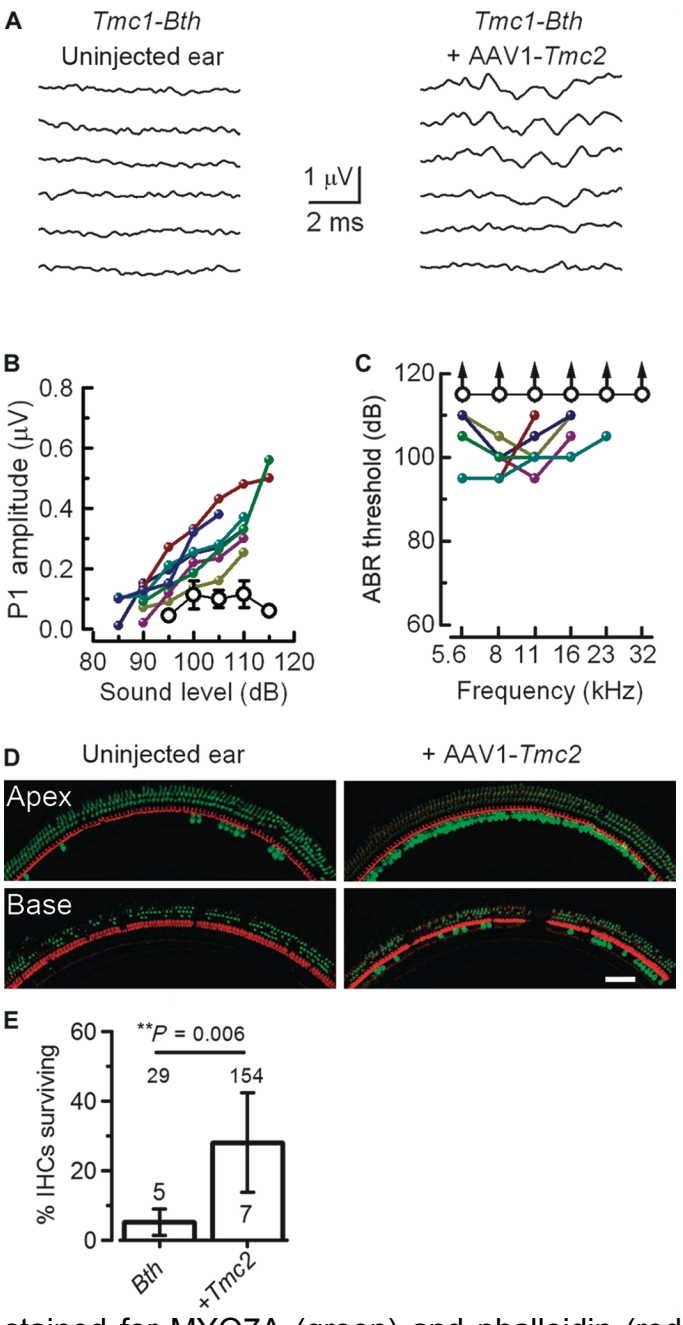

Fig. 3-11. Exogenous *Tmc2* rescues auditory function in *Tmc1-Bth* mice. (A) Families of ABR waveforms recorded from the contralateral ear (left, control) of a *Tmc1-Bth* mouse injected with AAV2/1-*Cba-Tmc2* (right, treated ear). ABRs were recorded at P25-P30 using 8 kHz tone bursts at sound pressure levels between 80 and 110 dB in 5 dB increments. Scale bar applies to both families. (**B**) Peak 1 amplitudes measured from 8 kHz ABR waveforms as shown in panel (A) for seven *Tmc1-Bth* mice injected with AAV2/1-*Cba-Tmc2* vectors. Open circles are mean (±SD) responses from uninjected *Tmc1-Bth* mice (*n* = 5). (**C**) ABR thresholds plotted as function of sound frequency for seven *Tmc1-Bth* mice injected with AAV2/1-*Cba-Tmc2* vectors. Open cirecles are means of uninjected *Tmc1-Bth* mice that had no detectable thresholds at highest sound intensity tested 115 dB (arrows, *n* = 5). (**D**) Confocal images of cochlear whole mounts harvested at P30 from an uninjected *Tmc1-Bth* mouse and one injected with AAV2/1-*Cba-Tmc2.* The tissue was stained for MYO7A (green) and phalloidin (red). Scale bar = 100 μm. Note the increased survival of inner hair cells in the apex and base of the AAV2/1-*Cba-Tmc2* injected cochlea. Fig. 3-14 shows low mag. images of the same cochleas. (**E**) Mean percentage (± SD) of surviving IHCs (relative to WT) in in 5-mm mid-cochlea sections from *Tmc1-Bth* mice and AAV2/1-*Cba-Tmc2* injected *Tmc1-Bth* mice (upper *n*, number of IHCs; lower *n*, number of cochleas). CA performed all

experiments, collected images, and analyzed data.

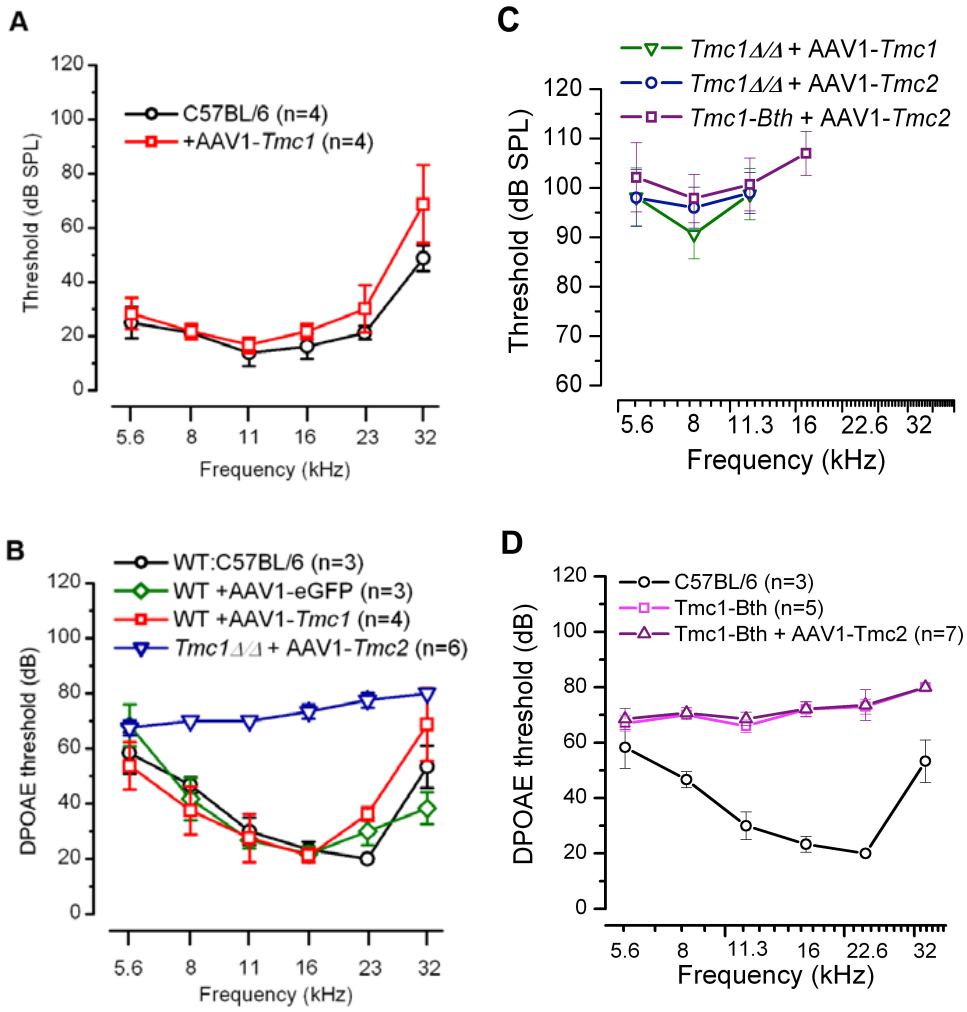

Figure 3-12. Summary of average auditory responses from groups of wild-type and deaf mice injected with AAV vectors. (**A**) Mean ABR threshold responses (± SD) recorded from wild-type C57BL/6 mice at P30 and in wild-type mice injected with AAV2/1-*Cba-Tmc1* at P0-P2. There was no significant difference in thresholds at any frequency tested indicating no evidence of inner ear toxicity. (**B**) Mean DPOAE responses (± SD) recorded at P25-P30 from wild-type C57BL/6 mice, wild-types injected with AAV2/1-*Cba*-eGFP or AAV2/1-*Cba-Tmc1.* There was no significant difference in injected wild-type mice relative to non-injected controls. As with *Tmc1*$^{\Delta/\Delta}$ control mice, *Tmc1*$^{\Delta/\Delta}$ mice injected with either *Tmc1* (see Fig.3-9D) or *Tmc2* (B) demonstrate no OHC response recovery due to lack of viral transduction of these cells. (**C**) Mean ABR threshold responses (± SD) recorded from *Tmc1*$^{\Delta/\Delta}$ mice or *Tmc1-Bth* mice injected with either AAV2/1-*Cba-Tmc1* or AAV2/1-*Cba-Tmc2* as indicated (averaged from mice shown in Fig. 3-9C, 3-10C, 3-11C). (**D**) Mean DPOAE responses (± SD) recorded at P25-P30 from wild-type C57BL/6 mice, *Tmc1-Bth* control mice, or

Tmc1-Bth mice injected with AAV2/1-*Cba-Tmc2* (averaged DPOAE measurements from mice shown in Fig. 3-11C). As with *Tmc* injected *Tmc1*$^{\Delta/\Delta}$ mice, the *Tmc1-Bth* mice lack DPOAE responses at P25-P30. Number of mice (*n*) for each condition is indicated. CA performed experiments and analyzed data. YA collected ABR and DPOAE thresholds from WT+AAV1-*Tmc1* mice.

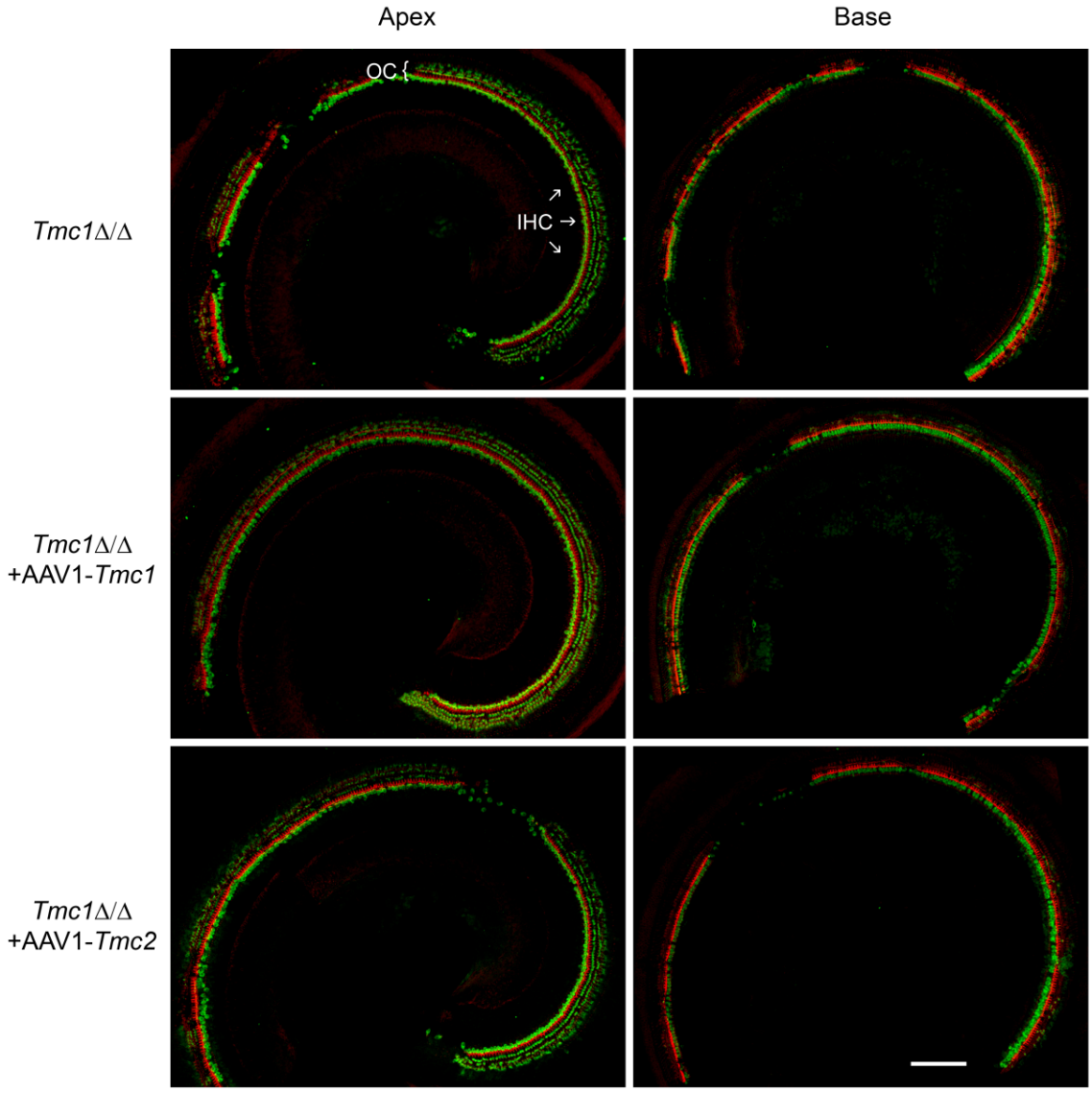

Figure 3-13. Confocal images of *Tmc1*$^{\Delta/\Delta}$ cochleas injected with AAV2/1-*Cba-Tmc* vectors. Representative images of cochlear whole mounts harvested at P30 from a *Tmc1*$^{\Delta/\Delta}$ mouse and *Tmc1*$^{\Delta/\Delta}$ mice injected with AAV2/1-*Cba-Tmc1* or AAV2/1-*Cba-Tmc2* as indicated to the left. The tissue was stained for MYO7A (green) and phalloidin (red). Several breaks in the tissue reveal areas where both outer and inner hair cells, as well as pillar cells have degenerated. Scale bar = 100 µm. Higher magnification images of the same cochleas are shown in Figs. 3-9E and 3-10D. CA performed all experiments, collected images, and analyzed data in Fig. 3-13 and Fig. 3-14.

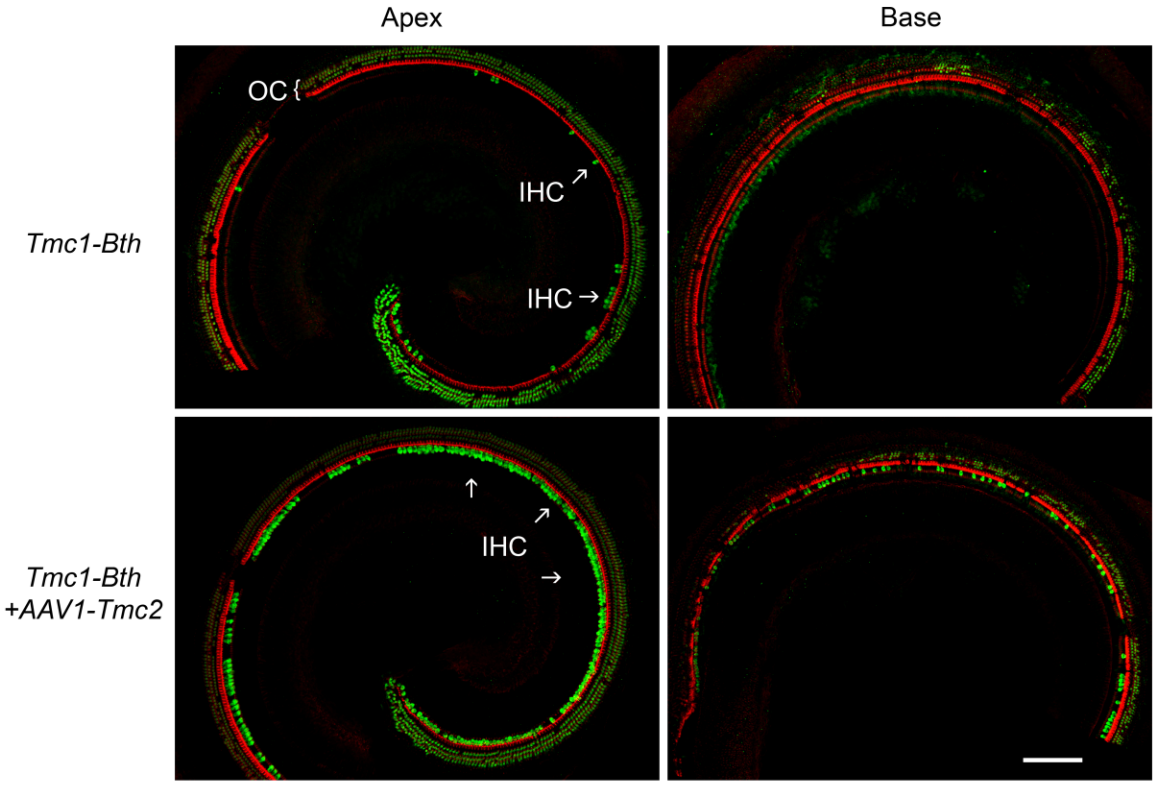

Figure 3-14. Confocal images of *Tmc1-Bth* cochleas injected with AV2/1-*Cba-Tmc2*. Representative images of cochlear whole mounts harvested at P30 from a *Tmc1-Bth* mouse and *Tmc1-Bth* mouse injected with AV2/1-*Cba-Tmc2* as indicated to the left. The tissue was stained for MYO7A (green) and phalloidin (red). Scale bar = 100 µm. The organ of Corti (OC) is indicated by the bracket and the inner hair cells (IHC) are indicated by arrows. Higher magnification images of the same cochleas are shown in Fig. 3-12D.

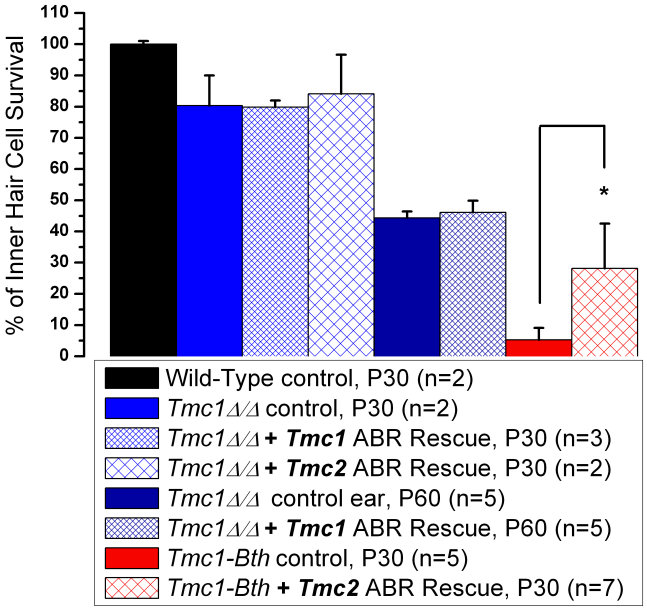

Figure 3-15. Inner hair cell survival in mice with rescued ABR thresholds after injection of *Tmc1* or *Tmc2*. Inner hair cells were counted along the length of dissected whole cochleas (average 5.45mm ± 0.41mm, n=31 cochleas) and the counts for each cochlea were normalized to a length of 5.00mm (*n* = number of mice). The percent survival is reported as # of IHCs relative to # of wild-type control IHCs. Only *Tmc1-Bth* mice injected with the *Tmc2* vector had a significant increase in

hair cell survival (5-fold) compared to non-injected *Tmc1-Bth* control mice (154 ± 74 IHCs vs. 29 ± 24 IHCs respectively, $P = 0.006$). P30 Tmc1$^{\Delta/\Delta}$ mice injected with either *Tmc1* or *Tmc2* vectors showed little difference in IHC survival compared to non-injected controls. Both the injected left ear and uninjected right ear (control ear) of the same mouse were investigated at P60 for Tmc1$^{\Delta/\Delta}$ mice injected with *Tmc1* vectors, but no difference was found in hair cell survival ($P = 0.403$). CA performed experiments and analyzed data. YA helped to collect images from P60 cochleas.

Lastly, because up to 70% of inner hair cells were transduced by reporter vectors *in vivo* and greater than 70% of inner hair cells survive in *Tmc1*$^{\Delta/\Delta}$ control mice at P30 (Fig. 3-15), we reasoned that not enough degeneration had yet occurred at P30 to distinguish the effects of *Tmc1* vectors on hair cell survival. Instead, we waited a longer interval for more hair cell degeneration to progress and quantified cell survival at P60 in *Tmc1*$^{\Delta/\Delta}$ mice injected with AAV2/1-*Cba-Tmc1*. We found that although just over 50% of inner hair cells had degenerated in the uninjected control ear (contralateral), the ear injected with AAV2/1-*Cba-Tmc1* showed no significant increase in cell survival despite rescue of ABR thresholds (Fig. 3-15).

AAV2/1-Cba-Tmc vectors restore behavioral responses to auditory stimuli

To test whether the partial ABR recovery in deaf mice injected with AAV2/1-*Cba-Tmc* vectors resulted in behaviorally relevant sound perception, we tested acoustic startle reflexes at P30 from wild-type control mice, uninjected deaf mice, and deaf mice injected with AAV2/1-*Cba- Tmc* vectors. Wild-type mice had startle responses that were detectable beginning around 80 dB SPL (Fig. 3-16A, open circles). When we measured acoustic startle reflexes in five *Tmc1*$^{\Delta/\Delta}$ mice injected with AAV2/1-*Cba-Tmc1* that lacked ABR responses, we found they

also lacked startle responses (Fig. 7A, open squares). However, we found that 100% (n = 7) of *Tmc1*$^{\Delta/\Delta}$ mice injected with AAV2/1-*Cba-Tmc1* that had ABR responses also had robust startle reflexes (Fig. 3-16A). All seven mice had recovery of startle response thresholds at 90-100 dB SPL with startle amplitudes that increased with increasing sound intensity. Furthermore, we found that the startle reflexes persisted through P60, the latest time point tested: five of five *Tmc1*$^{\Delta/\Delta}$ mice injected with AAV2/1-*Cba-Tmc1* that had positive ABRs also had substantial startle responses (Fig. 3-16B).

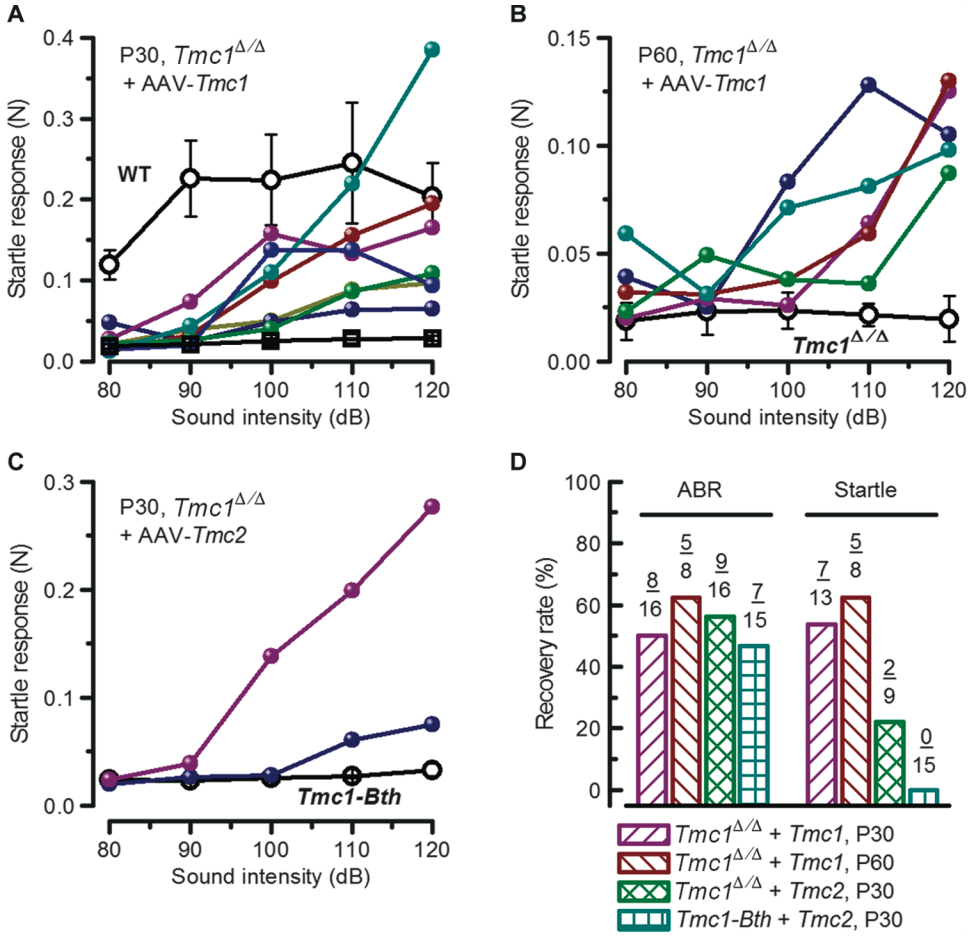

Figure 3-16. Exogenous *Tmc* expression rescues acoustic startle reflexes in *Tmc1* mutant mice. (**A**) Startle response amplitudes (in newtons) measured at P30 and plotted as function of sound intensity for the mean (±SD) of four control C57BL/6 mice (open circles), for seven individual *Tmc1*$^{\Delta/\Delta}$ mice injected

with AAV2/1-*Cba-Tmc1*, and for five AAV2/1-*Cba*-Tmc1-injected mice with no ABR recovery (open squares). (**B**) Startle reflexes measured at P60 and plotted for the mean of four *Tmc1*$^{\Delta/\Delta}$ mice (open circles) and five individual *Tmc1*$^{\Delta/\Delta}$ mice injected with AAV2/1-*Cba-Tmc1*. (**C**) Startle reflexes measured at P30, plotted for two individual *Tmc1*$^{\Delta/\Delta}$ mice injected with AAV2/1-*Cba-Tmc2* and the mean (±SD) of seven *Tmc1-Bth* mice (open circles) injected with AAV2/1-*Cba-Tmc2*. (**D**) Summary bar graph showing percentage of *Tmc1* mutant mice with recovery as assayed by ABRs and startle reflexes for mice injected with either AAV2/1-*Cba-Tmc1* or AAV2/1-*Cba-Tmc2.* Numerator indicates *n* mice with recovery of function; denominator indicates *n* injected mice tested. Not all mice were tested with both assays. CA performed all experiments and analyzed data for Fig. 3-16 and Fig. 3-17.

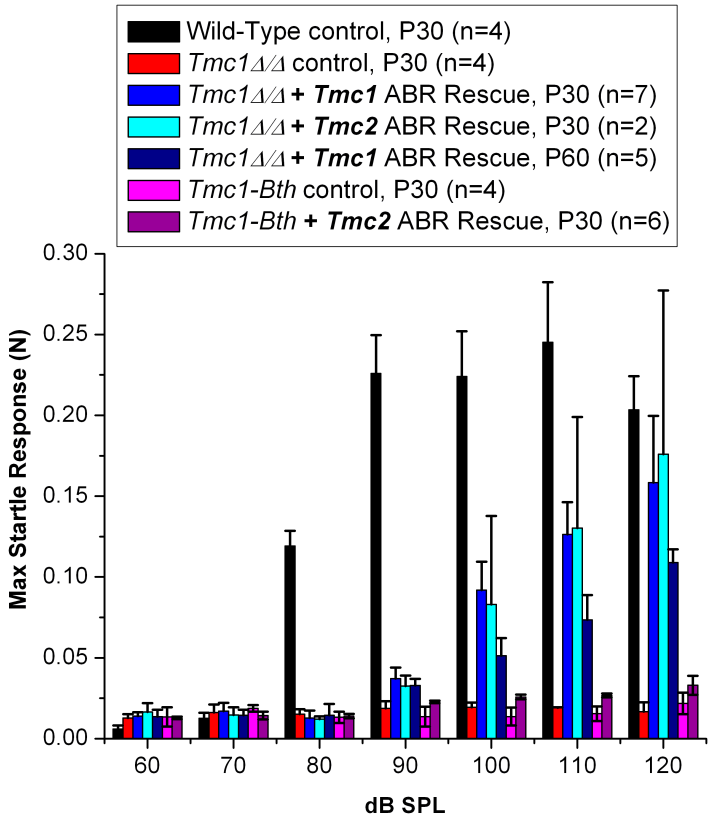

Figure 3-17. Summary of average Acoustic Startle Reflexes (ASR) from groups of control mice and injected mice with ABR recue. Displayed are the mean acoustic startle response amplitudes (±SD) measured in units of force (newtons) from each group listed above (*n* = number of mice). Deaf control mice (*Tmc1*$^{\Delta/\Delta}$ and *Tmc1-Bth*) presented without startle reflex to auditory stimuli. Wild-type mice begin to display a startle reflex at 80 dB SPL, while *Tmc1*$^{\Delta/\Delta}$ mice with hearing rescued by *Tmc1* or *Tmc2* begin to startle at 90 dB SPL.

Next, we examined startle responses in *Tmc1* mutant mice injected with AAV2/1-*Cba- Tmc2.* Although five *Tmc1*$^{\Delta/\Delta}$ mice injected with AAV2/1-*Cba-Tmc2* recovered ABRs and were tested for startle responses, only two of the five had startle responses (Fig. 3-16C). One mouse had substantial responses, similar to those of wild-type mice for the loudest sound intensities (Fig. 3-16C). Seven of

15 *Tmc1-Bth* mice injected with AAV2/1-*Cba-Tmc2* recovered ABR responses, but none had startle responses (Fig. 3-16 C&D), suggesting that exogenous *Tmc2* expression may not be sufficient to overcome the dominant *Bth* mutation in a behaviorally relevant assay. Averaged startle responses for each group of mice are presented in Fig. 3-17, where animals tested is indicated in parenthesis (n). Figure 3-16D summarizes the ABR and startle response data for all 55 *Tmc1* mutant mice injected with AAV2/1-*Cba-Tmc* vectors. Gene augmentation with wild-type *Tmc1* successfully restored both ABR and acoustic startle responses in greater than 50% of the injected mice. Injection of the AAV2/1 vector encoding wild-type *Tmc2* revealed similar success rates for ABR recovery, but was less effective for recovery of startle responses in both $Tmc1^{\Delta/\Delta}$ and *Tmc1-Bth mice.*

Discussion

In this study we characterized several adeno-associated viral serotypes in combination with various promoter sequences for their ability to drive exogenous gene expression in sensory hair cells of the inner ear. AAV2/1 was the most efficient combination for viral expression of transgenes in neonatal mouse cochlear hair cells *in vitro*. Although both inner and outer hair cells were transduced, we noted a tonotopic gradient with ~80% of hair cells expressing eGFP at the basal high frequency end of the cochlea and ~50% at the apical low frequency end. The gradient was not due to viral access, as the experiment was performed in organotypic cultures in which the entire cochlea was bathed in a uniform concentration of viral particles. Thus, we suspect there may be inherent

viral tropism that favors the basal high frequency end of the cochlea. If similar patterns exist *in vivo*, this may be advantageous for gene therapy applications, as many forms of progressive deafness begin as high frequency hearing loss affecting the basal end of the cochlea. In a prior study, Stone et al. (2004) also found AAV1 to be an efficient vector for transducing cochlear hair cells with a similar tonotopic preference for the basal end of the cochlea.

We developed a modified round window injection technique for *in vivo* delivery of AAV vectors into the fluid-filled spaces of the scala tympani. The scala tympani is continuous with the scala vestibuli, both of which contain perilymph, an extracellular solution that bathes the basolateral membranes of hair cells and is similar in composition to cerebrospinal fluid. RWM injection of either AAV2/1-*Cmv*-eGFP or AAV2/1-*Cba*-eGFP drove robust expression of eGFP in cochlear and vestibular hair cells, suggesting the approach may be viable for delivery of therapeutic reagents to target hair cells throughout the human inner ear. Furthermore, we found normal mechanosensory responses and normal ABRs, suggesting the injection technique, AAV2/1 vectors and eGFP expression were safe for *in vivo* use, supporting further development of AAV gene therapy as a strategy for hearing restoration.

To model for DFNB7/11 we used mice deficient in *Tmc1* and engineered AAV2/1 vectors that carried the *Cba* promoter followed by the coding sequence for either *Tmc1* or *Tmc2*. The vectors restored cellular function *in vitro* in cultures harvested from *Tmc1*/*Tmc2* doubly deficient mice. Viral transduction with either construct revealed localization of exogenous TMC1 and TMC2 at the tips of hair

cell stereocilia, uptake of the transduction channel permeable dye FM1-43 and robust mechanosensory transduction currents, in otherwise non-functional hair cells. The data provide compelling evidence that our AAV2/1-*Cba-Tmc1* and AAV2/1-*Cba-Tmc2* vectors can restore function at the cellular level in both inner and outer hair cells *in vitro*.

ABRs were recovered in >50% of *Tmc1*$^{\Delta/\Delta}$ deaf mice injected with AAV2/1-Cba-Tmc1, indicating successful transmission of auditory information from the cochlea to the auditory brainstem. The ABR thresholds were elevated relative to those of wild-type mice indicating partial recovery of auditory function. The lack of recovery in DPOAE responses suggested that ABR thresholds were elevated due to lack of recovery of outer hair cell function, in turn due to low viral transduction rates in outer hair cells (only 4-5% in selected samples). Functional outer hair cells are required for cochlear amplification, a process that provides mechanical feedback to the cochlea by increasing gain to soft sounds, turning down gain for loud sounds and tuning the auditory response in the frequency domain (Hudspeth 2014). Outer hair cell dysfunction is known to yield elevated ABR thresholds, shifted up to 60 dB higher than wild-type thresholds. Thus, in *Tmc1*$^{\Delta/\Delta}$ mice, in which all cochlear hair cells lack sensory transduction, rescue of IHC function but not OHC function yielded ABR thresholds shifted ~60 dB higher than wild-type responses. This magnitude of threshold shift is consistent with thresholds in a different mouse model with outer hair cell dysfunction due to deletion of the outer hair cell specific protein, prestin (Liberman et al., 2002). In the *Vglut3* study (Akil et al., 2012), outer hair cells remained functionally intact,

but the *Vglut3* knockout mice are deaf because of IHC dysfunction. After *Vglut3* gene augmentation, ABR thresholds recovered to near wild-type levels because restoration of function was only required in IHCs, which make up ~25% of the cochlear hair cell population. Our *in vivo* experiments revealed viral transduction rates of IHCs (60-80%) and the transduced cells had mechanosensory currents equivalent to those of wild type, but OHC dysfunction remained. Although the recovery was incomplete, the result was considered a success because normal mechano- sensory function in IHCs is a prerequisite for auditory function. Had the outcome been the converse—restoration of OHC but not IHC function—the animals would still be deaf.

Interestingly, and consistent with prior observations (Akil et al., 2012), when AAV2/1 vectors were injected via the RWM into the inner ears of deaf mice, restoration of cellular function was limited to inner hair cells. We saw little evidence of exogenous gene expression in outer hair cells following injection of four different vectors: AAV2/1-*Cmv*-eGFP, AAV2/1-*Cba*-eGFP, AAV2/1-*Cba*-*Tmc1*, and AAV2/1-*Cba*-*Tmc2*. Because all four vectors were capable of driving exogenous gene expression in outer hair cells *in vitro* when introduced into culture media that bathed both apical and basolateral surfaces of hair cells in organotypic cultures, we suspect that the lack of viral transduction in outer hair cells *in vivo* could be the result of limited viral access to the apical hair cell surface via RWM injection into perilymphatic spaces. Consistent with this notion, Kilpatrick et al. (2011) reported that introduction of AAV vectors into the scala media, which contains fluid that bathes hair cell apical membranes, yielded GFP

expression in both inner and outer hair cells. The challenge of scala media injection is that it requires a more invasive surgical approach and can disrupt the endolymphatic compartment, which contains a unique extracellular fluid with a high K^+ concentration (~140 mM). Mixing of high K^+ endolymph with perilymph can cause hair cell depolarization and cell death. Therefore, to target outer hair cells will require vectors that can enter those cells via the basolateral membrane or delivery methods that target endolymphatic spaces without disrupting endolymph/perilymph barriers.

We also found that AAV2/1-*Cba-Tmc2* vectors were capable of restoring sensory transduction and partial ABR responses in *Tmc1*$^{\Delta/\Delta}$ mice, which supports the hypothesis that *Tmc1* and *Tmc2* perform somewhat redundant functions and can substitute for each other, at least in inner hair cells. The AAV2/1-*Cba-Tmc2* transduction pattern was similar to AAV2/1-*Cba-Tmc1* and was restricted primarily to inner hair cells, resulting in similar recovery at elevated ABR thresholds. That hair cell survival rates were not altered in *Tmc1*$^{\Delta/\Delta}$ mice injected with either AAV2/1-*Cba-Tmc1* or AAV2/1-*Cba-Tmc2* was important for two reasons: 1) neither vector caused loss or decay of hair cells and 2) hair cells remained in uninjected *Tmc1*$^{\Delta/\Delta}$ mice up to P60, suggesting there may be a window of opportunity for therapeutic intervention in mature mice. Whether a similar window exists in humans with recessive *TMC1* mutations is unknown. If patients with TMC1 mutations retain viable hair cells, they may present an opportunity for clinical intervention.

Restoration of auditory function was limited in mice that carried the dominant *Bth* mutation injected with AAV2/1-*Cba-Tmc2*. Interestingly, there was significant preservation of inner hair cells in AAV2/1-*Cba-Tmc2* injected *Bth* mice. The mechanism that promoted inner hair cell survival is unknown. However, based on measurements of sensory transduction and calcium permeability in mice that expressed wild-type *Tmc2*, *Tmc1* or *Tmc1-Bth*, Pan et al. (2013) found a significant reduction in calcium entry in *Tmc1-Bth* inner hair cells, while *Tmc2* cells had high calcium entry. We hypothesize that appropriate levels of calcium entry are required for maintenance and survival of inner hair cells and by introducing exogenous *Tmc2,* calcium homeostasis was restored, which enhanced hair cell survival in the *Bth* mice injected with AAV2/1-*Cba-Tmc2.*

As a final test of auditory function we measured acoustic startle responses in *Tmc1* mutant mice. The otherwise unresponsive $Tmc1^{\Delta/\Delta}$ mice recovered startle responses following injection of AAV2/1-*Cba-Tmc1* and the responses persisted for up to 60 days, the latest time point tested. Fewer AAV2/1-*Cba-Tmc2* injected mice recovered startle responses but one recovered to near wild-type levels. It was unclear why *Tmc1-Bth* mice injected with AAV2/1-*Cba-Tmc2* recovered partial ABR function but did not recover startle responses. The extent of the ABR recovery in the *Tmc1-Bth* mice injected with AAV2/1-*Cba-Tmc2* was less than the ABR recovery in $Tmc1^{\Delta/\Delta}$ mice injected with AAV2/1-*Cba-Tmc2* which suggests there may be a minimal recovery threshold required to drive behavioral responses to loud sounds. The level of ABR recovery in *Tmc2* injected *Tmc1-Bth* mice correlates with their lower average number of surviving

hair cells, which even after recovery was still one 1/3rd the survival rate of injected *Tmc1*$^{\Delta/\Delta}$ mice at P30 (Fig. 3-15). Strategies aimed at restoration of auditory function for dominant DFNA36 deafness may require development of alternate strategies, perhaps by suppressing expression of the dominant allele.

In conclusion, the data provide compelling proof-of-principle evidence demonstrating that gene augmentation strategies in a mouse model of DFNB7/11 are effective at restoring cellular function *in vitro* in both inner and outer hair cells, restoring inner hair cell function *in vivo*, partial recovery of systems level function *in vivo*, and recovery of acoustic startle reflexes at the behavioral level. Thirty-nine mutations have been identified in *TMC1* that cause recessive prelingual deafness in humans, which underscores the significance of TMC1 for normal auditory function and the need for therapeutic reagents to remedy the disorder. Although our gene therapy strategy is not yet ready for clinical application, the challenges that remain are not insurmountable. Continued development of *Tmc* gene therapy will need to provide characterization of the long term expression pattern of the exogenous gene constructs, including their ability to maintain recovery; improved design of vectors, promoters and delivery techniques that drive exogenous gene expression in outer hair cells to expand the extent of the recovery; and evaluation of the therapeutic window of opportunity in human patients with recessive *TMC1* mutations. Finally, we suggest that AAV-mediated gene augmentation in the inner ear may be a model that could be expanded to address some of the over 70 forms of genetic deafness.

Acknowledgments:

We thank M. Charles Liberman for assistance with ABR recordings; Yilai Shu and Zheng-Yi Chen for technical assistance with RWM injections; Vivianne Padrun, Fabienne Pidoux and Aline Aebi at EPFL Brain Mind Institute for technical assistance with AAV production; Behavior and Viral Cores at Boston Children's Hospital (supported by BCH IDDRC, P30 HD18655). **Funding:** This work was supported by the Bertarelli Foundation, Program in Translational Neuroscience and Neuroengineering. **Author contributions:** *Charles Askew:* performed experiments, analyzed data, helped write the manuscript; *Cylia Rochat:* designed and generated vectors; *Bifeng Pan:* performed experiments; *Yukako Asai:* performed experiments and analysis, designed and generated vectors; *Hena Ahmed:* performed experiments, analyzed data; *Erin Child:* analyzed data; *Bernard L. Schneider:* designed and generated vectors, helped design experiments; *Patrick Aebischer:* helped design vectors and experiments; *Jeffrey R. Holt:* conceived the study, designed experiments, analyzed data, helped write manuscript. **Competing interests**: The authors declare no competing interests. **Data and material availability:** Plasmids for AAV vector production are available via a material transfer agreement.

Chapter IV: Conclusions and Future Directions

In summary, we presented evidence that a mouse model for non-syndromic human deafness DFNB7/11 can recover sensory transduction, auditory thresholds, and sound perception with the administration of AAV1 vectors containing wild-type forms of *Tmc1* or *Tmc2*. Additionally, we demonstrated that hearing thresholds and inner hair cell survival improved in a mouse model for DFNA36 with the administration of an AAV1-*Tmc2* vector. Although auditory thresholds in rescued mice did not recover to wild-type levels, we reasonably expect that such recovery is impossible without also targeting the majority of outer hair cells for therapeutic gene delivery. We demonstrated that AAV2/1 targets predominantly inner hair cells along the length of the cochlea at a rate of 60%-80%, while outer hair cells are targeted at < 5%, and these rates were consistent between both GFP reporter vectors and therapeutic *Tmc* vectors *in vivo*. The rescue of ABR responses with elevated thresholds and the absence of DPOAE responses in our deaf mice are consistent with responses in other mouse models where outer hair cells are chemically ablated or genetically immobilized (Ryan & Dallos, 1975; Liberman et al., 2002). In each case, auditory thresholds are increased by ~60 dB SPL. To further assess the capability of *Tmc1* and *Tmc2* genes to rescue *Tmc1* deafness mutations will require the development of vectors that target outer hair cells *in vivo*, in addition to inner hair cells. Despite this limitation, it is encouraging that even a moderate rescue of thresholds with *Tmc* vectors is capable of restoring function at the behavioral

level, and the same level of rescue in humans may still provide some benefit to those with profound DFNB7/11 hearing loss.

Roughly 50% of injected deaf mice recovered hearing in each group (Fig. 3-16D), and we believe this rate was not higher because of the variability inherent to a difficult microinjection of a small target (<1mm^2) where visualization of the RWM is partially obscured by the overlying tissue. We could not confirm proper targeting of the micropipette for every injection because the anatomy of some mice visually obscured the RWM, and at times the pipette could become clogged or expel some vector during the procedure before the tip penetrated the RWM. Greater reliability in targeting of the scala tympani could be achieved by surgically opening the bulla for direct visualization of the RWM, but this approach requires great care not to perforate the stapedial artery or disrupt the tympanic membrane and middle ear bones. Such an approach is more practical on an older mouse where the middle ear structures are more developed and the cartilaginous bulla is thick enough to be drilled. These factors are specific to this surgical approach on the neonatal mouse and may be more easily resolved on a larger and more developed animal.

We also found that the viral transduction rate for the AAV2/1 reporter vector performed differently *in vivo* than *in vitro*. While inconsistency between *in vitro* and *in vivo* infection rate in the inner ear has been reported between studies done by different groups (Sacheli et al., 2013), this study is the first to investigate the two preparations using the same stock of virus (AAV2/1-*Cmv-eGFP*). AAV2/1 targeted outer hair cells *in vitro* at a higher rate than inner hair cells, while *in vivo*

the opposite was true. We hypothesize that there are a number of possible explanations for this result. First, the route of vector access to the hair cell epithelium is likely to be different *in vitro* (vector access to apical surfaces, with possible permeation to basal surfaces) versus scala tympani injection *in vivo* (where vector access is restricted to hair cell basolateral surfaces by scala media luminal tight junctions). Assuming that the route of administration is responsible for the discrepancy in tropism, this could be tested by comparing outer hair cell infection rate for scala tympani injections and scala media injections using the same virus. In fact, a study recently published performed this exact experiment with an AAV8-*Cmv-GFP* reporter vector, comparing administration of the same vector to the scala tympani or scala media in adult mice (Chien et al., 2015). Their results showed that when using high titer AAV8 (10^{13} gc/mL), both injection approaches infected predominantly inner hair cells, while outer hair cell infection was sparse and limited. This result is contrary to Kilpatrick et al. 2011 who demonstrated that scala media inoculation with AAV8 is capable of high rates of inner and outer hair cell infection in the apex of the adult cochlea, although specific infection rates along the whole cochlea were not quantified. Inconsistent with previous reports, Kilpatrick et al. did not report high infection of IHCs or OHCs with AAV1 by scala media injection, and they did not test scala tympani administration with either AAV1 or AAV8. In this study, we found that AAV8 had a very low rate of hair cell infection when tested *in vitro* (<10%, Fig. 3-1). However, when administered to the scala tymapani *in vivo,* AAV8 was able to transduce inner hair cells at moderate levels while outer hair cell transduction was sparse

(Fig. 3-6). The inconsistency between these findings suggests there may be alternative factors impacting the rate of infection (such as subject age). Second, we did not take into account the possibility of vector interactions with the immune system *in vivo*, and factors such as pre-existing neutralizing antibodies against AAV capsid proteins have been shown to significantly impact the level of viral transduction (Rogers et al., 2011; Mingozzi et al., 2013). If neutralizing antibodies against AAV2/1 are present in the inner ear fluid at the time of injection, the vector concentration could be effectively reduced *in vivo* as the antibodies act as a buffer to sequester viral particles and antagonize receptor mediated endocytosis by hair cells. Future experiments could test this hypothesis by incubating the vector in perilymph harvested by micropipette from the scala tympani, and then applying the incubated vector media to an *in vitro* cochlea culture to detect whether viral transduction is reduced when compared to cultures without perilymph incubation. Although speculative, perhaps the observation that predominantly inner hair cells are infected by several different AAV serotypes (1, 2, 3, 5, 7, 8) that are known to enter cells via distinct glycan receptors, is a result of the high endocytic activity of inner hair cells and AAV entry is independent of receptor mediated endocytosis for these cells (Bartlett et al., 2000; Griesinger et al., 2002 & 2005; Mietzsch et al., 2014). This hypothesis could be tested by inhibiting endocytosis using a mouse mutant lacking dynamin and investigating if viral transduction of inner hair cells persists using different AAV serotypes. Third, the expression pattern of cell entry receptors for the different AAV serotypes has not been well established in the inner ear (Ballana et al., 2008), and so a

correlation of serotype targeting with the expression of cell surface receptors remains to be tested. A final consideration is that the purity of the AAV vector has also been demonstrated to influence viral transduction rate independent of cell type or AAV serotype, and different production protocols for AAV could introduce variability between studies (Ayuso et al., 2010).

We observed that AAV2/1 reporter vectors infect not only hair cells but also supporting cells and spiral ganglion neurons in the cochlea. We investigated the localization of TMC proteins produced by our therapeutic vector in the cochlea using FLAG staining, and we occasionally observed supporting cells with FLAG positive signal in their cytoplasm (data not shown). However, when we examined uptake of the transduction channel permeable dye FM1-43 after *in vivo* injections, the FM1-43 signal was limited specifically to the inner hair cells of AAV1-*Tmc* injected *Tmc1*$^{\Delta/\Delta}$*;Tmc2*$^{\Delta/\Delta}$ mice (see Fig. 3-8D). Furthermore, when we introduced *Tmc1* vectors into wild-type mice, we did not observe any negative impact on ABR or DPOAE thresholds (Fig. 3-12), suggesting that if there is ectopic expression of *Tmc* vectors in non-hair cells, it does not negatively impact inner ear function. Currently there is no evidence that TMC proteins have pores that can be mechanically gated or constitutively opened when expressed in non-hair cells, but use of cell specific promoters in future gene therapy experiments could be an important consideration to limit the toxicity or disruptive effects from specific genes that can be detrimental to cell function when expressed in non-native cells.

We made the novel discovery that ectopic expression of *Tmc2* in inner hair cells has the ability to compensate for the function of *Tmc1* in $Tmc1^{\Delta/\Delta}$ mice, and we were able to partially rescue auditory responses to sound stimuli using *Tmc2*. While either *Tmc1* or *Tmc2* is able to restore mechanotransduction of inner or outer hair cells in $Tmc1^{\Delta/\Delta};Tmc2^{\Delta/\Delta}$ mice, it remains to be demonstrated whether *Tmc2* alone can be used to fully restore hearing. Such an experiment will be dependent on targeting of both inner and outer hair cells for *Tmc2* expression in the absence of *Tmc1*. An interesting corollary to this discussion is that while the conductance of whole cell MET currents is known to remain constant for inner hair cells along the length of the cochlea, the conductance of outer hair cell MET currents decreases from base to apex (Beurg et al., 2006). It has been proposed that because *Tmc1* and *Tmc2* generate different single MET channel conductance, titration of *Tmc1* or *Tmc2* expression in outer hair cells could be a mechanism to set up a longitudinal conductance gradient from the base to the apex of the cochlea (Pan et al., 2013; Kim et al., 2013). Little is known about whether *Tmc2* is expressed in normal adult outer hair cells at the base of the cochlea, but regardless of whether the molecular mechanism involves *Tmc2*, we speculate that re-establishment the outer hair cell conductance gradient could be important to the function and tuning of the rescued cochlea.

Although only one copy of the orthologous *Bth* mutation is typical in the development of DFNA36 in humans, we chose to use the homozygous $Tmc1^{Bth/Bth}$ mouse with two affected copies of *Tmc1* because their hearing loss

quickly progresses to total deafness and they suffer from near complete degeneration of IHCs by P30. The lack of residual hearing thresholds or surviving inner hair cells made interpretation of the effects of a therapeutic gene delivery straightforward. Use of the *Tmc1*$^{Bth/Bth}$ mutant is also beneficial in isolating the possible therapeutic interaction of Tmc2 proteins with Tmc1^{Bth} proteins in a hair cell environment devoid of wild-type Tmc1. Therefore, our results demonstrate therapeutic potential for the *Tmc2* gene despite utilizing a genetic model that is more severe than the human manifestation. Had we used the heterozygous *Tmc1*$^{Bth/+}$ mutant for the same experiments, we hypothesize there would be better improvement of auditory thresholds and hair cell survival, due to a decrease in *Bth* gene dosage. Future studies should not ignore this fact, and should continue investigating the therapeutic outcomes of both *Tmc2* and *Tmc1* administration in *Tmc1*$^{Bth/+}$ mice over a longer period of observation (from 2 months up to 1 year). It is unclear whether over expression of *Tmc1* would be able to dilute *Tmc1*^{Bth} expression enough to prolong hair cell survival, but it is apparent that mouse Tmc1^{Bth} proteins do not exert a dominant null effect on Tmc2 in mechano-sensation because transduction current amplitude is undiminished in either *Tmc1*$^{Bth/\Delta}$ + *Tmc2*$^{\Delta/\Delta}$, or *Tmc1*$^{Bth/\Delta}$ + *Tmc2*$^{+/\Delta}$ mice (Pan et al., 2013). Our hypothesis for the use of *Tmc2* to treat *Tmc1*^{Bth} inner hair cells hinged upon the potential of Tmc2 proteins, which have higher calcium permeability than Tmc1, to improve calcium entry. While we did not test this result directly, it would be straightforward to investigate transduction currents from *Tmc1*$^{Bth/\Delta}$ + *Tmc2*$^{+/+}$ mice to determine if they display an intermediate

calcium reversal potential to those of *Tmc1*$^{Bth/\Delta}$ and *Tmc2*$^{+/+}$ mice. Such a result would suggest the indirect ability of *Tmc2* to increase MET current calcium permeability in the presence of the *Bth* mutation. While we do not understand the molecular mechanism for why a decrease in calcium permeability could be detrimental to hair cells, it has been suggested that calcium may act as a survival signal through regulation of gene transcription. Regardless of the mechanism, *Tmc2* gene augmentation resulted in greater survival of inner hair cells in *Tmc1*$^{Bth/Bth}$ + *Tmc2*$^{+/+}$ mice at P30 as compared to uninjected controls of the same background genotype. Future experiments could interrogate the calcium load that auditory hair cells must carry, whether too little or too much, in order to maintain survival.

One line of questioning that could not be fully addressed due to time constraints of this study was whether recovery of MET currents or calcium permeability translates into long-term survival of hair cells. We tried to address this question by investigating hair cell survival in *Tmc1*$^{\Delta/\Delta}$ mice at P60, an age when approximately 50% of inner hair cells have degenerated (Fig. 3-15). We found no difference in hair cell survival after injection of *Tmc1* vectors and ABR recovery in these mice despite an estimated viral transduction rate of ~70% with the therapeutic vector. We could not determine what portion of the surviving adult hair cells in the injected *Tmc1*$^{\Delta/\Delta}$ mice were positive for Tmc1::3xFLAG proteins at P30 or P60, as antibody staining at this age was uninterpretable due to consistently high background signal. Future studies could quantify survival of transduced cells by incorporating a small cytosolic reporter gene, such as a

miniSOG (Shu et al., 2011), capable of fitting into the remaining packaging space in the therapeutic *Tmc* vectors, but driven by an independent promoter so that the fluorescent signal would not be limited by the abundance (or scarcity) of Tmc proteins expressed in the cell. Interestingly, $Tmc1^{\Delta/\Delta}$ mice do not display nearly as much hair cell degeneration as $Tmc1^{Bth}$ mice (Vreugde et al. 2002, Kawashima et al. 2011, Fig. 3-15). Because $Tmc1^{Bth/Bth}$ mice lose the majority of their inner hair cells at P30 (~5% remaining) it was possible to quantify that *Tmc2* gene augmentation was effective at increasing average inner hair cell survival by 5-fold. Still, this surviving population represented only ~28% of the cells found in a normal wild-type mouse at the same age, suggesting that some degeneration of inner hair cells continues even after rescue with *Tmc2*. Ultimately, the question of whether therapeutic *Tmc* vectors can preserve long term hair cell survival will depend on the development of a vector that can virally transduce and rescue function of all the auditory hair cells. Then, quantification of degenerating hair cells will not be complicated by the inability to distinguish which ones are expressing the therapeutic Tmc proteins after injection.

This study has further demonstrated the capacity of gene therapy to successfully restore auditory function caused by inherited hearing loss. I hope to dedicate my career to developing this promising approach into a potential therapy for children with congenital hearing loss and for this research to have broader translational applications. This will certainly be a journey with its own set of challenges, but I am hopeful that these challenges can be overcome.

References:

Ahmed, Z. M., Goodyear, R., Riazuddin, S., Lagziel, A., Legan, P. K., Behra, M., et al. (2006). The tip-link antigen, a protein associated with the transduction complex of sensory hair cells, is protocadherin-15. *Journal of Neuroscience*, 26(26), 7022–7034.

Akil, O., Seal, R. P., Burke, K., Wang, C., Alemi, A., During, M., et al. (2012). Restoration of hearing in the VGLUT3 knockout mouse using virally mediated gene therapy. *Neuron*, 75(2), 283–293.

Aldhamen, Y. A., Seregin, S. S., & Amalfitano, A. (2011). Immune recognition of gene transfer vectors: focus on adenovirus as a paradigm. *Frontiers in Immunology*, 2, 40.

Alford, R. L., Arnos, K. S., Fox, M., Lin, J. W., Palmer, C. G., Pandya, A., et al. (2014). American College of Medical Genetics and Genomics guideline for the clinical evaluation and etiologic diagnosis of hearing loss. *Genetics in Medicine*, 16(4), 347–355.

Ashmore, J. (2008). Cochlear outer hair cell motility. *Physiological Reviews*, 88(1), 173–210.

Ashmore, J., Avan, P., Brownell, W. E., Dallos, P., Dierkes, K., Fettiplace, R., et al. (2010). The remarkable cochlear amplifier. *Hearing Research*, 266(1-2), 1–17.

Askew, C., Rochat, C., Pan, B., Asai, Y., Ahmed, H., Child, E., et al. (2015). Tmc gene therapy restores auditory function in deaf mice. *Science Translational Medicine*, 7(295), 295ra108.

Assad, J. A., Shepherd, G. M., & Corey, D. P. (1991). Tip-link integrity and mechanical transduction in vertebrate hair cells. *Neuron*, 7(6), 985–994.

Atchison, R. W., Casto, B. C., & Hammon, W. (1965). Adenovirus-associated defective virus particles. *Science*, 149(3685), 754–756.

Ayuso, E., Mingozzi, F., Montane, J., Leon, X., Anguela, X. M., Haurigot, V., et al. (2010). High AAV vector purity results in serotype- and tissue-independent enhancement of transduction efficiency. *Gene Therapy*, 17(4), 503–510.

Ballana, E., Wang, J., Venail, F., Estivill, X., Puel, J.-L., Arbonès, M. L., & Bosch, A. (2008). Efficient and specific transduction of cochlear supporting cells by adeno-associated virus serotype 5. *Neuroscience Letters*, 442(2), 134–139.

Bartlett, J. S., Wilcher, R., & Samulski, R. J. (2000). Infectious entry pathway of adeno-associated virus and adeno-associated virus vectors. *Journal of Virology*, 74(6), 2777–2785.

Bedrosian, J. C., Gratton, M. A., Brigande, J. V., Tang, W., Landau, J., & Bennett, J. (2006). In vivo delivery of recombinant viruses to the fetal murine cochlea: transduction characteristics and long-term effects on auditory function. *Molecular Therapy*, 14(3), 328–335.

Beurg, M., Evans, M. G., Hackney, C. M., & Fettiplace, R. (2006). A large-conductance calcium-selective mechanotransducer channel in mammalian cochlear hair cells. *Journal of Neuroscience*, 26(43), 10992–11000.

Beurg, M., Nam, J.-H., Crawford, A., & Fettiplace, R. (2008). The actions of calcium on hair bundle mechanics in mammalian cochlear hair cells. *Biophysical Journal*, 94(7), 2639–2653.

Beurg, M., Fettiplace, R., Nam, J., & Ricci, A. J. (2009). Localization of inner hair cell mechanotransducer channels using high-speed calcium imaging. *Nature Neuroscience, 12*(5), 553-558.

Beurg, M., Xiong, W., Zhao, B., Müller, U., & Fettiplace, R. (2015). Subunit determination of the conductance of hair-cell mechanotransducer channels. *PNAS*, 112(5), 1589–1594.

Birnholz, J. C., & Benacerraf, B. R. (1983). The development of human fetal hearing. *Science*, 222 (4623), 516–518.

Bock, GR and Steel, KP (1983). Inner ear pathology in the *deafness* mutant mouse. *Acta Otolaryngology.* (96), 39-47.

Bowles, D. E., McPhee, S. W. J., Li, C., Gray, S. J., Samulski, J. J., Camp, A. S., et al. (2012). Phase 1 gene therapy for Duchenne muscular dystrophy using a translational optimized AAV vector. *Molecular Therapy*, 20(2), 443–455.

Boye, S. E., Boye, S. L., Lewin, A. S., & Hauswirth, W. W. (2013). A comprehensive review of retinal gene therapy. *Molecular Therapy*, 21(3), 509–519.

Burger, C., Gorbatyuk, O. S., Velardo, M. J., Peden, C. S., Williams, P., Zolotukhin, S., et al. (2004). Recombinant AAV viral vectors pseudotyped with viral capsids from serotypes 1, 2, and 5 display differential efficiency and cell tropism after delivery to different regions of the central nervous system. *Molecular Therapy*, 10(2), 302–317.

Caberlotto, E., Michel, V., Foucher, I., Bahloul, A., Goodyear, R. J., Pepermans, E., et al. (2011). Usher type 1G protein sans is a critical component of the tip-link complex, a structure controlling actin polymerization in stereocilia. *PNAS*, 108 (14), 5825–5830.

Chatzigeorgiou, M., Bang, S., Hwang, S. W., & Schafer, W. R. (2013). Tmc-1 encodes a sodium-sensitive channel required for salt chemosensation in C. elegans. *Nature*, 1–6.

Chien, W. W., McDougald, D. S., Roy, S., Fitzgerald, T. S., & Cunningham, L. L. (2015). Cochlear gene transfer mediated by adeno-associated virus: Comparison of two surgical approaches. *Laryngoscope*. doi:10.1002/lary.25317

Cideciyan, A. V., Jacobson, S. G., Beltran, W. A., Sumaroka, A., Swider, M., Iwabe, S., et al. (2013). Human retinal gene therapy for Leber congenital amaurosis shows advancing retinal degeneration despite enduring visual improvement. *PNAS*, 110(6), E517–E525.

Corey, D. P., & Hudspeth, A. J. (1979a). Ionic basis of the receptor potential in a vertebrate hair cell. *Nature, 281*(5733), 675-677.

Corey, D. P., & Hudspeth, A. J. (1979b). Response latency of vertebrate hair cells. *Biophysical Journal, 26*(3), 499-506.

Corns, L. F., Johnson, S. L., Kros, C. J., & Marcotti, W. (2014). Calcium entry into stereocilia drives adaptation of the mechanoelectrical transducer current of mammalian cochlear hair cells. *PNAS*, 111(41), 14918–14923.

Couzin, J., & Kaiser, J. (2005). Gene Therapy. As Gelsinger case ends, gene therapy suffers another blow. *Science*, 307 (5712) p. 1028.

Crawford, A. C., Evans, M. G., & Fettiplace, R. (1991). The actions of calcium on the mechano-electrical transducer current of turtle hair cells. *The Journal of Physiology, 434*, 369-398

Crispino, G., Di Pasquale, G., Pietro Scimemi, Rodriguez, L., Ramirez, F. G., De Siati, R. D., et al. (2011). BAAV Mediated GJB2 Gene Transfer Restores Gap Junction Coupling in Cochlear Organotypic Cultures from Deaf Cx26Sox10Cre Mice. *PloS One*, 6(8), e23279.

Dallos, P., Wu, X., Cheatham, M. A., Gao, J., Zheng, J., Anderson, C. T., et al. (2008). Prestin-based outer hair cell motility is necessary for mammalian cochlear amplification. *Neuron*, 58(3), 333–339.

Diaz-Horta, O., Duman, D., Foster, J., Sırmacı, A., Gonzalez, M., Mahdieh, N., et al. (2012). Whole-exome sequencing efficiently detects rare mutations in autosomal recessive nonsyndromic hearing loss. *PloS One*, 7(11), e50628.

Dillon, C. F., Gu, Q., Hoffman, H. J., & Ko, C.-W. (2010). Vision, hearing, balance, and sensory impairment in Americans aged 70 years and over: United States, 1999-2006. *NCHS Data Brief*, (31), 1–8.

Farris, H. E., LeBlanc, C. L., Goswami, J., & Ricci, A. J. (2004). Probing the pore of the auditory hair cell mechanotransducer channel in turtle. *The Journal of Physiology*, 558(Pt 3), 769–792.

Ferrari, F. K., Samulski, T., Shenk, T., & Samulski, R. J. (1996). Second-strand synthesis is a rate-limiting step for efficient transduction by recombinant adeno-associated virus vectors. *Journal of Virology*, 70(5), 3227–3234.

Fettiplace, R. (2006). Active hair bundle movements in auditory hair cells. The *Journal of Physiology*, 576(Pt 1), 29–36.

Fettiplace, R., & Hackney, C. M. (2006). The sensory and motor roles of auditory hair cells. *Nature Reviews Neuroscience*, 7(1), 19–29.

Gale, J. E., Marcotti, W., Kennedy, H. J., Kros, C. J., & Richardson, G. P. (2001). FM1-43 dye behaves as a permeant blocker of the hair-cell mechanotransducer channel. *Journal of Neuroscience*, 21(18), 7013–7025.

Géléoc, G. S., Lennan, G. W., Richardson, G. P., & Kros, C. J. (1997). A quantitative comparison of mechanoelectrical transduction in vestibular and auditory hair cells of neonatal mice. *Proceedings of the Royal Society B: Biological Sciences, 264*(1381), 611-621.

Géléoc, G. S. G., & Holt, J. R. (2003). Developmental acquisition of sensory transduction in hair cells of the mouse inner ear. *Nature Neuroscience*, 6(10), 1019–1020.

Géléoc, G. S. G., & Holt, J. R. (2014). Sound strategies for hearing restoration. *Science*, 344(6184), 1241062.

Gore, M. E. (2003). Adverse effects of gene therapy: gene therapy can cause leukaemia: no shock, mild horror but a probe. *Gene Therapy*, 10(1), 4–4.

Gow, A., Davies, C., Southwood, C. M., Frolenkov, G., Chrustowski, M., Ng, L., et al. (2004). Deafness in Claudin 11-null mice reveals the critical contribution of basal cell tight junctions to stria vascularis function. *The Journal of Neuroscience*, 24(32), 7051–7062.

Grieger, J. C., & Samulski, R. J. (2005). Packaging capacity of adeno-associated virus serotypes: impact of larger genomes on infectivity and post-entry steps. *Journal of Virology*, 79(15), 9933–9944.

Griesinger, C. B., Richards, C. D., & Ashmore, J. F. (2002). Fm1-43 reveals membrane recycling in adult inner hair cells of the mammalian cochlea. *Journal of Neuroscience*, 22(10), 3939–3952.

Griesinger, C. B., Richards, C. D., & Ashmore, J. F. (2005). Fast vesicle replenishment allows indefatigable signalling at the first auditory synapse. *Nature*, 435(7039), 212–215.

Grimm, D., Kay, M. A., & Kleinschmidt, J. A. (2003). Helper virus-free, optically controllable, and two-plasmid-based production of adeno-associated virus vectors of serotypes 1 to 6. *Molecular Therapy*, 7(6), 839–850.

Hackney, C. M., Mahendrasingam, S., Penn, A., & Fettiplace, R. (2005). The concentrations of calcium buffering proteins in mammalian cochlear hair cells. *Journal of Neuroscience*, 25(34), 7867–7875.

Harris, J. P., & Ryan, A. F. (1995). Fundamental immune mechanisms of the brain and inner ear. *Otolaryngology - Head and Neck Surgery*, 112(6), 639–653.

Hepper, P. G., & Shahidullah, B. S. (1994). Development of fetal hearing. *Archives of Disease in Childhood*, 71(2), F81–7.

Hernandez, V. H., Gehrt, A., Reuter, K., Jing, Z., Jeschke, M., Schulz, A. M., et al. (2014). Optogenetic stimulation of the auditory pathway. *Journal of Clinical Investigation*, 124(124(3)), 1114–1129.

Holley, M. C., & Ashmore, J. F. (1988). On the mechanism of a high-frequency force generator in outer hair cells isolated from the guinea pig cochlea. *Proceedings of the Royal Society of London.* 232(1269), 413-429.

Holt, J. R., Johns, D. C., Wang, S., Chen, Z. Y., Dunn, R. J., Marban, E., & Corey, D. P. (1999). Functional expression of exogenous proteins in mammalian sensory hair cells infected with adenoviral vectors. *Journal of Neurophysiology*, 81(4), 1881–1888.

Holt, J. R., Gillespie, S. K. H., Provance, D. W., Shah, K., Shokat, K. M., Corey, D. P., et al. (2002). A chemical-genetic strategy implicates myosin-1c in adaptation by hair cells. *Cell*, 108(3), 371–381.

Holt, J. R., Pan, B., Koussa, M. A., & Asai, Y. (2014). TMC function in hair cell transduction. Hearing Research, 311, 17–24.

Hudspeth, A. J. (2005). How the ear's works work: mechanoelectrical transduction and amplification by hair cells. *Comptes Rendus Biologies*, 328(2), 155–162.

Hudspeth, A. J. (2008). Making an effort to listen: mechanical amplification in the ear. *Neuron*, 59(4), 530–545.

Hudspeth, A. J. (2014). Integrating the active process of hair cells with cochlear function. *Nature Reviews Neuroscience*, 15(9), 600–614.

Hudspeth, A. J., & Jacobs, R. (1979). Stereocilia mediate transduction in vertebrate hair cells (auditory system/cilium/vestibular system). *PNAS, 76*(3), 1506-1509.

Hughes, Gordon B. and Pensak, Myles L. “Clinical Otology”, Thieme Publishers, copyright 2007.

Iizuka, T., Kanzaki, S., Mochizuki, H., Inoshita, A., Narui, Y., Furukawa, M., et al. (2008). Noninvasive in vivo delivery of transgene via adeno-associated virus into supporting cells of the neonatal mouse cochlea. *Human Gene Therapy*, 19(4), 384–390.

Jaramillo, F., & Hudspeth, A. J. (1991). Localization of the hair cell’s transduction channels at the hair bundle’s top by iontophoretic application of a channel blocker. *Neuron*, 7(3), 409–420.

Kalos, M., Levine, B. L., Porter, D. L., Katz, S., Grupp, S. A., Bagg, A., & June, C. H. (2011). T cells with chimeric antigen receptors have potent antitumor effects and can establish memory in patients with advanced leukemia. *Science Translational Medicine*, 3(95), 95ra73.

Kaspar, B. K., Vissel, B., Bengoechea, T., Crone, S., Randolph-Moore, L., Muller, R., et al. (2002). Adeno-associated virus effectively mediates conditional gene modification in the brain. *PNAS*, 99(4), 2320–2325.

Kawashima, Y., Géléoc, G. S. G., Kurima, K., Labay, V., Lelli, A., Asai, Y., et al. (2011). Mechanotransduction in mouse inner ear hair cells requires transmembrane channel-like genes. *Journal of Clinical Investigation*, 121(12), 4796–4809.

Kawashima, Y., Kurima, K., Pan, B., Griffith, A. J., & Holt, J. R. (2015). Transmembrane channel-like (TMC) genes are required for auditory and vestibular mechanosensation. *Pflügers Archiv - European Journal of Physiology*, 467(1), 85–94.

Kazmierczak, P., Sakaguchi, H., Tokita, J., Wilson-Kubalek, E. M., Milligan, R. A., Müller, U., & Kachar, B. (2007). Cadherin 23 and protocadherin 15 interact to form tip-link filaments in sensory hair cells. *Nature*, 449(7158), 87–91.

Kennedy, H. J., Crawford, A. C., & Fettiplace, R. (2005). Force generation by mammalian hair bundles supports a role in cochlear amplification. *Nature*, 433(7028), 880–883.

Keresztes, G., Mutai, H., & Heller, S. (2003). TMC and EVER genes belong to a larger novel family, the TMC gene family encoding transmembrane proteins. *BMC Genomics*, 4(1), 24.

Kesser, B. W., Hashisaki, G. T., Fletcher, K., Eppard, H., & Holt, J. R. (2007). An in vitro model system to study gene therapy in the human inner ear. *Gene Therapy*, 14(15), 1121–1131.

Kesser, B. W., Hashisaki, G. T., & Holt, J. R. (2008). Gene transfer in human vestibular epithelia and the prospects for inner ear gene therapy. *Laryngoscope*, 118(5), 821–831.

Kikuchi, T., Kimura, R. S., Paul, D. L., & Adams, J. C. (1995). Gap junctions in the rat cochlea: immunohistochemical and ultrastructural analysis. *Anatomy and Embryology*, 191(2), 101–118.

Kilpatrick, L. A., Li, Q., Yang, J., Goddard, J. C., Fekete, D. M., & Lang, H. (2011). Adeno-associated virus-mediated gene delivery into the scala media of the normal and deafened adult mouse ear. *Gene Therapy*, 18(6), 569–578.

Kim, K. X., & Fettiplace, R. (2013). Developmental changes in the cochlear hair cell mechanotransducer channel and their regulation by transmembrane channel-like proteins. *The Journal of General Physiology*, 141(1), 141–148.

Kitajiri, S.-I., Miyamoto, T., Mineharu, A., Sonoda, N., Furuse, K., Hata, M., et al. (2004). Compartmentalization established by claudin-11-based tight junctions in stria vascularis is required for hearing through generation of endocochlear potential. *Journal of Cell Science*, 117(Pt 21), 5087–5096.

Kitajiri, S.-I., McNamara, R., Makishima, T., Husnain, T., Zafar, A. U., Kittles, R. A., et al. (2007). Identities, frequencies and origins of TMC1 mutations causing DFNB7/B11 deafness in Pakistan. *Clinical Genetics*, 72(6), 546–550.

Kohrman, D. C., & Raphael, Y. (2013). Gene therapy for deafness. *Gene Therapy*, 20(12), 1119–1123.

Konishi, M., Kawamoto, K., Izumikawa, M., Kuriyama, H., & Yamashita, T. (2008). Gene transfer into guinea pig cochlea using adeno-associated virus vectors. *The Journal of Gene Medicine*, 10(6), 610–618.

Kothiyal, P., Cox, S., Ebert, J., Husami, A., Kenna, M. A., Greinwald, J. H., et al. (2010). High-throughput detection of mutations responsible for childhood hearing loss using resequencing microarrays. *BMC Biotechnology*, 10, 10.

Kotterman, M. A., & Schaffer, D. V. (2014). Engineering adeno-associated viruses for clinical gene therapy. *Nature Reviews Genetics*, 15(7), 445–451.

Kozel, P. J., Friedman, R. A., Erway, L. C., Yamoah, E. N., Liu, L. H., Riddle, T., et al. (1998). Balance and hearing deficits in mice with a null mutation in the gene encoding plasma membrane Ca2+-ATPase isoform 2. *The Journal of Biological Chemistry*, 273(30), 18693–18696.

Kros, C. J., Marcotti, W., van Netten, S. M., Self, T. J., Libby, R. T., Brown, S. D. M., et al. (2002). Reduced climbing and increased slipping adaptation in cochlear hair cells of mice with Myo7a mutations. *Nature Neuroscience*, 5(1), 41–47.

Kurima, K., Peters, L. M., Yang, Y., Riazuddin, S., Ahmed, Z. M., Naz, S., et al. (2002). Dominant and recessive deafness caused by mutations of a novel gene, TMC1, required for cochlear hair-cell function. *Nature Genetics*, 30(3), 277–284.

Kurima, K., Yang, Y., Sorber, K., & Griffith, A. J. (2003). Characterization of the transmembrane channel-like (TMC) gene family: functional clues from hearing loss and epidermodysplasia verruciformis. *Genomics*, 82(3), 300–308.

Labay, V., Weichert, R. M., Makishima, T., & Griffith, A. J. (2010). Topology of transmembrane channel-like gene 1 protein. *Biochemistry*, 49(39), 8592–8598.

Lelli, A., Asai, Y., Forge, A., Holt, J. R., & Géléoc, G. S. G. (2009). Tonotopic gradient in the developmental acquisition of sensory transduction in outer hair cells of the mouse cochlea. *Journal of Neurophysiology, 101*(6), 2961-2973.

Lelli, A., Kazmierczak, P., Kawashima, Y., Müller, U., & Holt, J. R. (2010). Development and regeneration of sensory transduction in auditory hair cells requires functional interaction between cadherin-23 and protocadherin-15. *Journal of Neuroscience*, 30(34), 11259–11269.

Leone, P., Shera, D., McPhee, S. W. J., Francis, J. S., Kolodny, E. H., Bilaniuk, L. T., et al. (2012). Long-term follow-up after gene therapy for canavan disease. *Science Translational Medicine*, 4(165), 165ra163.

Liberman, M. C. (1980). Morphological differences among radial afferent fibers in the cat cochlea: an electron-microscopic study of serial sections. *Hearing Research*, 3(1), 45–63.

Liberman, M. C., Gao, J., He, D. Z. Z., Wu, X., Jia, S., & Zuo, J. (2002). Prestin is required for electromotility of the outer hair cell and for the cochlear amplifier. *Nature*, 419(6904), 300–304.

Liu, Y., Okada, T., Sheykholeslami, K., Shimazaki, K., Nomoto, T., Muramatsu, S.-I., et al. (2005). Specific and efficient transduction of Cochlear inner hair cells with recombinant adeno-associated virus type 3 vector. *Molecular Therapy*, 12(4), 725–733.

Liu, Y., Okada, T., Nomoto, T., Ke, X., Kume, A., Ozawa, K., & Xiao, S. (2007). Promoter effects of adeno-associated viral vector for transgene expression in the cochlea in vivo. *Experimental & Molecular Medicine*, 39(2), 170–175.

Long, C., McAnally, J. R., Shelton, J. M., Mireault, A. A., Bassel-Duby, R., & Olson, E. N. (2014). Prevention of muscular dystrophy in mice by CRISPR/Cas9-mediated editing of germline DNA. *Science*, 345(6201), 1184–1188.

Lu, X.J., Xue, H.Y., Ke, Z.kK, Chen, J.L., & Ji, L.J. (2015). CRISPR-Cas9: a new and promising player in gene therapy. *Journal of Medical Genetics*, 52(5), 289–296.

Luebke, A. E., Foster, P. K., Muller, C. D., & Peel, A. L. (2001). Cochlear Function and Transgene Expressionin the Guinea Pig Cochlea, Using Adenovirus and Adeno-Associated Virus Directed Gene Transfer. *Human Gene Therapy*, 12(7), 773–781.

Lumpkin, E. A., Marquis, R. E., & Hudspeth, A. J. (1997). The selectivity of the hair cell's mechanoelectrical-transduction channel promotes Ca2+ flux at low Ca2+ concentrations. *PNAS,* 94(20), 10997-11002.

Maeda, Y., Fukushima, K., Nishizaki, K., & Smith, R. J. H. (2005). In vitro and in vivo suppression of GJB2 expression by RNA interference. *Human Molecular Genetics*, 14(12), 1641–1650.

Maeda, R., Kindt, K. S., Mo, W., Morgan, C. P., Erickson, T., Zhao, H., Clemens-Grishama, R., Barr-Gillespie, P.G., & Nicolson, T. (2014). Tip-link protein protocadherin 15 interacts with transmembrane channel-like proteins TMC1 and TMC2. *PNAS*, 111(35), 12907–12912.

Maison, S. F., Liu, X.-P., Vetter, D. E., Eatock, R. A., Nathanson, N. M., Wess, J., & Liberman, M. C. (2010). Muscarinic signaling in the cochlea: presynaptic and

postsynaptic effects on efferent feedback and afferent excitability. *Journal of Neuroscience*, 30(19), 6751–6762.

Mali, P., Esvelt, K. M., Church, G. M. (2013) Cas9 as a versatile tool for engineering biology. *Nature Methods*, 10, 957–963.

Manno, C. S., Pierce, G. F., Arruda, V. R., Glader, B., Ragni, M., Rasko, J. J., et al. (2006). Successful transduction of liver in hemophilia by AAV-Factor IX and limitations imposed by the host immune response. *Nature Medicine*, 12(3), 342–347.

Marcotti, W., & Kros, C. J. (1999). Developmental expression of the potassium current IK,n contributes to maturation of mouse outer hair cells. *The Journal of Physiology,* 520 Pt 3, 653-660.

Marcotti, W., Erven, A., Johnson, S. L., Steel, K. P., & Kros, C. J. (2006). Tmc1 is necessary for normal functional maturation and survival of inner and outer hair cells in the mouse cochlea. *Journal of Physiology*, 574(Pt 3), 677–698.

McCarty, D. M., Monahan, P. E., & Samulski, R. J. (2001). Self-complementary recombinant adeno-associated virus (scAAV) vectors promote efficient transduction independently of DNA synthesis. *Gene Therapy*, 8(16), 1248–1254.

Meyers, J. R., MacDonald, R. B., Duggan, A., Lenzi, D., Standaert, D. G., Corwin, J. T., & Corey, D. P. (2003). Lighting up the senses: FM1-43 loading of sensory cells through nonselective ion channels. *Journal of Neuroscience*, 23(10), 4054–4065.

Mietzsch, M., Broecker, F., Reinhardt, A., Seeberger, P. H., & Heilbronn, R. (2014). Differential adeno-associated virus serotype-specific interaction patterns with synthetic heparins and other glycans. *Journal of Virology*, 88(5), 2991–3003.

Mingozzi, F., Anguela, X. M., Pavani, G., Chen, Y., Davidson, R. J., Hui, D. J., et al. (2013). Overcoming preexisting humoral immunity to AAV using capsid decoys. *Science Translational Medicine*, 5(194), 194ra92.

Mitchell, R. E., & Karchmer, M. A. (2004). Chasing the mythical ten percent: Parental hearing status of deaf and hard of hearing students in the United States. *Sign Language Studies*, 4(2), 138–163.

Molinier-Frenkel, V., Lengagne, R., Gaden, F., Hong, S.-S., Choppin, J., Gahery-Ségard, H., et al. (2002). Adenovirus hexon protein is a potent adjuvant for activation of a cellular immune response. *Journal of Virology*, 76(1), 127–135.

Mutai, H., Mann, S., & Heller, S. (2005). Identification of chicken transmembrane channel-like (TMC) genes: expression analysis in the cochlea. *Neuroscience*, 132(4), 1115–1122.

Nakanishi, H., Kurima, K., Kawashima, Y., & Griffith, A. J. (2014). Mutations of TMC1 cause deafness by disrupting mechanoelectrical transduction. *Auris, Nasus, Larynx*, 41(5), 399–408.

Nenov, A. P., Norris, C., & Bobbin, R. P. (1997). Outwardly rectifying currents in guinea pig outer hair cells. *Hearing Research, 105*(1-2), 146-158.

Nin, F., Hibino, H., Doi, K., Suzuki, T., Hisa, Y., & Kurachi, Y. (2008). The endocochlear potential depends on two K+ diffusion potentials and an electrical barrier in the stria vascularis of the inner ear. *PNAS*, 105(5), 1751–1756.

Quint, E., & Steel, K. P. (2003). Use of mouse genetics for studying inner ear development. *Current Topics in Developmental Biology*, 57, 45–83.

Pan, B., Waguespack, J., Schnee, M. E., LeBlanc, C., & Ricci, A. J. (2012). Permeation properties of the hair cell mechanotransducer channel provide insight into its molecular structure. *Journal of Neurophysiology*, 107(9), 2408–2420.

Pan, B., Géléoc, G. S., Asai, Y., Horwitz, G. C., Kurima, K., Ishikawa, K., et al. (2013). TMC1 and TMC2 are components of the mechanotransduction channel in hair cells of the mammalian inner ear. *Neuron*, 79(3), 504–515.

Pandya, A., Arnos, K. S., Xia, X. J., Welch, K. O., Blanton, S. H., Friedman, T. B., et al. (2003). Frequency and distribution of GJB2 (connexin 26) and GJB6 (connexin 30) mutations in a large North American repository of deaf probands. *Genetics in Medicine*, 5(4), 295–303.

Powel, Cynthia M., Berg, Jonathan S., Bailey, Donald B. (2014) NC NEXUS: North Carolina Newborn Exome Sequencing for Universal Screening Project. American Association of Public Health Laboratories Newborn Screening and Genetic Testing Symposium. http://www.aphl.org/conferences/proceedings/Pages/2014-Newborn-Screening-and-Genetic-Testing-Symposium.aspx#sthash.a8mDqI2f.dpuf

Raphael, Y., Frisancho, J. C., & Roessler, B. J. (1996). Adenoviral-mediated gene transfer into guinea pig cochlear cells in vivo. *Neuroscience Letters*, 207(2), 137–141.

Raper, S. E., Chirmule, N., Lee, F. S., Wivel, N. A., Bagg, A., Gao, G.P., et al. (2003). Fatal systemic inflammatory response syndrome in a ornithine transcarbamylase deficient patient following adenoviral gene transfer. *Molecular Genetics and Metabolism*, 80(1-2), 148–158.

Rhode, W. S., & Geisler, C. D. (1967). Model of the displacement between opposing points on the tectorial membrane and reticular lamina. *The Journal of the Acoustical Society of America, 42*(1), 185-190.

Ricci, A. J., Crawford, A. C., & Fettiplace, R. (2000). Active hair bundle motion linked to fast transducer adaptation in auditory hair cells. *Journal of Neuroscience*, 20(19), 7131–7142.

Ricci, A. J., Crawford, A. C., & Fettiplace, R. (2003). Tonotopic variation in the conductance of the hair cell mechanotransducer channel. *Neuron, 40*(5), 983-990.

Richard, C., Fayad, J. N., Doherty, J., & Linthicum, F. H. (2012). Round window versus cochleostomy technique in cochlear implantation: histologic findings. *Otology & Neurotology*, 33(7), 1181–1187.

Rivière, C., Danos, O., & Douar, A. M. (2006). Long-term expression and repeated administration of AAV type 1, 2 and 5 vectors in skeletal muscle of immunocompetent adult mice. *Gene Therapy*, 13(17), 1300–1308.

Rogers, G. L., Martino, A. T., Aslanidi, G. V., Jayandharan, G. R., Srivastava, A., & Herzog, R. W. (2011). Innate Immune Responses to AAV Vectors. *Frontiers in Microbiology*, 2, 194.

Ryan, A., & Dallos, P. (1975). Effect of absence of cochlear outer hair cells on behavioural auditory threshold. *Nature*, 253(5486), 44–46.

Sacheli, R., Delacroix, L., Vandenackerveken, P., Nguyen, L., & Malgrange, B. (2013). Gene transfer in inner ear cells: a challenging race. *Gene Therapy*, 20(3), 237–247.

Safieddine, S., & Wenthold, R. J. (1999). SNARE complex at the ribbon synapses of cochlear hair cells: analysis of synaptic vesicle- and synaptic membrane-associated proteins. *European Journal of Neuroscience*, 11(3), 803–812.

Samulski, R. J., Srivastava, A., Berns, K. I., & Muzyczka, N. (1983). Rescue of adeno-associated virus from recombinant plasmids: gene correction within the terminal repeats of AAV. *Cell*, 33(1), 135–143.

Samulski, R. J., Chang, L. S., & Shenk, T. (1987). A recombinant plasmid from which an infectious adeno-associated virus genome can be excised in vitro and its use to study viral replication. *Journal of Virology*, 61(10), 3096–3101.

Seal, R. P., Akil, O., Yi, E., Weber, C. M., Grant, L., Yoo, J., et al. (2008). Sensorineural deafness and seizures in mice lacking vesicular glutamate transporter 3. *Neuron*, 57(2), 263–275.

Senften, M., Schwander, M., Kazmierczak, P., Lillo, C., Shin, J.-B., Hasson, T., et al. (2006). Physical and functional interaction between protocadherin 15 and myosin VIIa in mechanosensory hair cells. *Journal of Neuroscience*, 26(7), 2060–2071.

Shearer, A. E., DeLuca, A. P., Hildebrand, M. S., Taylor, K. R., Gurrola, J., Scherer, S., et al. (2010). Comprehensive genetic testing for hereditary hearing loss using massively parallel sequencing. *PNAS*, 107(49), 21104–21109.

Sheffield, A. M., Gubbels, S. P., Hildebrand, M. S., Newton, S. S., Chiorini, J. A., Di Pasquale, G., & Smith, R. J. (2011). Viral vector tropism for supporting cells in the developing murine cochlea. *Hearing Research*, 277(1), 28–36.

Shibata, S. B., Di Pasquale, G., Cortez, S. R., Chiorini, J. A., & Raphael, Y. (2009). Gene transfer using bovine adeno-associated virus in the guinea pig cochlea. *Gene Therapy*, 16(8), 990–997.

Shotwell, S. L., Jacobs, R., & Hudspeth, A. J. (1981). Directional sensitivity of individual vertebrate hair cells to controlled deflection of their hair bundles. *Annals of the New York Academy of Sciences, 374*, 1-10.

Shu, X., Lev-Ram, V., Deerinck, T. J., Qi, Y., Ramko, E. B., Davidson, M. W., et al. (2011). A genetically encoded tag for correlated light and electron microscopy of intact cells, tissues, and organisms. *PLoS Biology*, 9(4), e1001041.

Siemens, J., Lillo, C., Dumont, R. A., Reynolds, A., Williams, D. S., Gillespie, P. G., & Müller, U. (2004). Cadherin 23 is a component of the tip link in hair-cell stereocilia. *Nature*, 428(6986), 950–955.

Sirmaci, A., Duman, D., Oztürkmen-Akay, H., Erbek, S., Incesulu, A., Oztürk-Hişmi, B., et al. (2009). Mutations in TMC1 contribute significantly to nonsyndromic autosomal recessive sensorineural hearing loss: a report of five novel mutations. *International Journal of Pediatric Otorhinolaryngology*, 73(5), 699–705.

Smith, C. A., Lowry, O. H., & Wu, M.-L. (1954). The Electrolytes of the Labyrinthine Fluids. *The Laryngoscope*, 64(3), 141-153.

Söllner, C., Rauch, G.-J., Siemens, J., Geisler, R., Schuster, S. C., Müller, U., et al. (2004). Mutations in cadherin 23 affect tip links in zebrafish sensory hair cells. *Nature*, 428(6986), 955–959.

Spicer, S. S., & Schulte, B. A. (1996). The fine structure of spiral ligament cells relates to ion return to the stria and varies with place-frequency. *Hearing Research, 100*(1-2), 80-100.

Stauffer, E. A., & Holt, J. R. (2007). Sensory transduction and adaptation in inner and outer hair cells of the mouse auditory system. *Journal of Neurophysiology*, 98(6), 3360–3369.

Stone, I. M., Lurie, D. I., Kelley, M. W., & Poulsen, D. J. (2005). Adeno-associated virus-mediated gene transfer to hair cells and support cells of the murine cochlea. *Molecular Therapy*, 11(6), 843–848.

Thomas, C. E., Ehrhardt, A., & Kay, M. A. (2003). Progress and problems with the use of viral vectors for gene therapy. *Nature Reviews Genetics*, 4(5), 346–358.

Tucci, D., Merson, M. H., & Wilson, B. S. (2010). A summary of the literature on global hearing impairment: current status and priorities for action. *Otology and Neurotology*, 31(1), 31–41.

Van Camp G, Smith RJH. Hereditary Hearing Loss Homepage. URL: http://hereditaryhearingloss.org

Vreugde, S., Erven, A., Kros, C. J., Marcotti, W., Fuchs, H., Kurima, K., et al. (2002). Beethoven, a mouse model for dominant, progressive hearing loss DFNA36. *Nature Genetics*, 30(3), 257–258.

Wang, Y., Sun, Y., Chang, Q., Ahmad, S., Zhou, B., Kim, Y., et al. (2013). Early postnatal virus inoculation into the scala media achieved extensive expression of exogenous green fluorescent protein in the inner ear and preserved auditory brainstem response thresholds. *The Journal of Gene Medicine*, 15(3-4), 123–133.

Wangemann, P. (2002). K+ cycling and the endocochlear potential. *Hearing Research*, 165(1-2), 1–9.

Wangemann, P., Itza, E. M., Albrecht, B., Wu, T., Jabba, S. V., Maganti, R. J., et al. (2004). Loss of KCNJ10 protein expression abolishes endocochlear potential and causes deafness in Pendred syndrome mouse model. *BMC Medicine*, 2, 30.

Watchko, J., O'Day, T., Wang, B., Zhou, L., Tang, Y., Li, J., & Xiao, X. (2002). Adeno-associated virus vector-mediated minidystrophin gene therapy improves dystrophic muscle contractile function in mdx mice. *Human Gene Therapy*, 13(12), 1451–1460.

Weisz, C., Glowatzki, E., & Fuchs, P. (2009). The postsynaptic function of type II cochlear afferents. *Nature*, 461(7267), 1126–1129.

Willott, James F. Handbook of Mouse Auditory Research: From Behavior to Molecular Biology. CRC Press. 2001.

Wilson, J. M. (2009). Lessons learned from the gene therapy trial for ornithine transcarbamylase deficiency. *Molecular Genetics and Metabolism*, 96(4), 151–157.

Xia, L., Yin, S., & Wang, J. (2012). Inner ear gene transfection in neonatal mice using adeno-associated viral vector: a comparison of two approaches. *PloS One*, 7(8), e43218.

Xiao, X., Li, J., & Samulski, R. J. (1996). Efficient long-term gene transfer into muscle tissue of immunocompetent mice by adeno-associated virus vector. *Journal of Virology*, 70(11), 8098–8108.

Xiao, W., Chirmule, N., Berta, S. C., McCullough, B., Gao, G., & Wilson, J. M. (1999). Gene therapy vectors based on adeno-associated virus type 1. *Journal of Virology*, 73(5), 3994–4003.

Xiong, W., Grillet, N., Elledge, H. M., Wagner, T. F. J., Zhao, B., Johnson, K. R., Kazmierczak, P. & Müller, U. (2012). TMHS Is an Integral Component of the Mechanotransduction Machinery of Cochlear Hair Cells. *Cell*, 151(6), 1283–1295.

Yu, Q., Wang, Y., Chang, Q., Wang, J., Gong, S., Li, H., & Lin, X. (2014). Virally expressed connexin26 restores gap junction function in the cochlea of conditional Gjb2 knockout mice. *Gene Therapy*, 21(1), 71–80.

Zhao, Y., Wang, D., Zong, L., Zhao, F., Guan, L., Zhang, P., et al. (2014). A novel DFNA36 mutation in TMC1 orthologous to the Beethoven (Bth) mouse associated with autosomal dominant hearing loss in a Chinese family. *PloS One*, 9(5), e97064.

Zhao, B., Wu, Z., Grillet, N., Yan, L., Xiong, W., Harkins-Perry, S., & Müller, U. (2014). TMIE is an essential component of the mechanotransduction machinery of cochlear hair cells. *Neuron*, 84(5), 954–967.

Zincarelli, C., Soltys, S., Rengo, G., & Rabinowitz, J. E. (2008). Analysis of AAV serotypes 1-9 mediated gene expression and tropism in mice after systemic injection. *Molecular Therapy*, 16(6), 1073–1080.

Zolotukhin, S., Potter, M., Zolotukhin, I., Sakai, Y., Loiler, S., Fraites, T. J., et al. (2002). Production and purification of serotype 1, 2, and 5 recombinant adeno-associated viral vectors. *Methods*, 28(2), 158–167.